(2)

HgCdTe SURFACE STUDY PROGRAM

Jerry A. Wilson
Santa Barbara Research Center
75 Coromar Drive
Goleta, California 93117

W.E. Spicer, Joel Silberman,
and Per Morgen
Stanford Electronics Laboratories
Stanford, California 94305

September 1982

FINAL TECHNICAL REPORT

Contract No. MDA-903-80-C-0496

The views, opinions, and findings contained in this report are those of the authors and should not be construed as an official Department of Defense position, policy, or decision, unless so designated by other official documentation

Prepared for:
DARPA
1400 Wilson Blvd
Arlington, Virginia 22209
Attention: Dr. Richard A. Reynolds
Material Science Division

UNCLASSIFIED

SECURITY CLASSIFICATION OF THIS PAGE (When Data Entered)

REPORT DOCUMENTATION PAGE	READ INSTRUCTIONS BEFORE COMPLETING FORM
1. REPORT NUMBER	2. GOVT ACCESSION NO. AD-A132071 / 3. RECIPIENT'S CATALOG NUMBER
4. TITLE (and Subtitle) HgCdTe Surface Study Program	5. TYPE OF REPORT & PERIOD COVERED Final Technical Report September 1982
	6. PERFORMING ORG. REPORT NUMBER 83-1069
7. AUTHOR(s) Jerry A. Wilson, Joel Silberman, Per Morgen and W.E. Spicer	8. CONTRACT OR GRANT NUMBER(s) MDA-903-80-C-0496 AO 3485
9. PERFORMING ORGANIZATION NAME AND ADDRESS SBRC, 75 Coromar Drive, Goleta, CA 93117; Stanford Electronics Laboratories, Stanford, CA 94305	10. PROGRAM ELEMENT, PROJECT, TASK AREA & WORK UNIT NUMBERS
11. CONTROLLING OFFICE NAME AND ADDRESS Defense Advanced Research Project Administration, 1400 Wilson Blvd, Arlington, VA 22209	12. REPORT DATE September 1982 13. NUMBER OF PAGES 62
14. MONITORING AGENCY NAME & ADDRESS (if different from Controlling Office) Night Vision and Electro-Optics Laboratory, NVEOL-RD, Fort Belvoir, VA 22060	15. SECURITY CLASS. (of this report) Unclassified 15a. DECLASSIFICATION/DOWNGRADING SCHEDULE
16. DISTRIBUTION STATEMENT (of this Report) APPROVED FOR PUBLIC RELEASE DISTRIBUTION UNLIMITED	
17. DISTRIBUTION STATEMENT (of the abstract entered in Block 20, if different from Report)	
18. SUPPLEMENTARY NOTES	
19. KEY WORDS (Continue on reverse side if necessary and identify by block number) HgCdTe, CdTe, HgTe, photoemission spectroscopy, electronic structure, interface states, DLTS, alloy bonding, capacitance voltage	

20. ABSTRACT (Continue on reverse side if necessary and identify by block number)

This report presents the conclusions of a two-year study of the surface of HgCdTe conducted jointly by Santa Barbara Research Center and Stanford University.

Photoemission spectroscopy (PES) of HgCdTe cleaved in UHV has indicated a surface which is very stable against Hg loss. The surface has shown a tendency to type-convert (p to n) due to defects in the surface region stressed by →

DD FORM 1 JAN 73 1473 EDITION OF 1 NOV 65 IS OBSOLETE

UNCLASSIFIED

SECURITY CLASSIFICATION OF THIS PAGE (When Data Entered)

cleaving. Type conversion has been confirmed by independent electrolytic electro-reflectance (EER) measurements.

Photoemission has also been used to probe the bulk band structure and indicates a fundamental difference in bonding of Cd and Hg in the lattice. A breakdown of the virtual crystal approximation is noted and an improved computation for the alloy is discussed.

Oxygen chemistry has been studied using PES; results show the undamaged surface is inert to unexcited molecular oxygen. Oxidation proceeds with exposure to excited oxygen and is preceded by a loss of Hg from the surface. The oxide formed does not contain Hg. Differences in oxidation between HgTe and HgCdTe indicate Cd plays a role in the oxidation.

Auger electron spectroscopy coupled with ion sputtering (AES-ion profiling) has been used to study the composition of the interface with thin natural oxides, anodic oxides and deposited PHOTOX™ SiO_2. The thin natural oxide is a Te-rich oxide. A small amount of Hg has been detected in the anodic oxide which is composed principally of Te and Cd in a complex oxide. The interface with deposited SiO_2 is formed of a thin region (on the order of 20Å) composed principally of Te, Si, and O, resulting from the reduction of the Te-oxide by silane.

Structure of the interface has been measured with capacitance-voltage (C-V) and deep level transient spectroscopy (DLTS) using metal-oxide-semiconductor (MIS) structures. This has shown that electrical properties are determined by prepassivation surface treatments through their effects on the oxidation chemistry of the surface. These treatments also affect bulk properties to depths of hundreds of Angstroms.

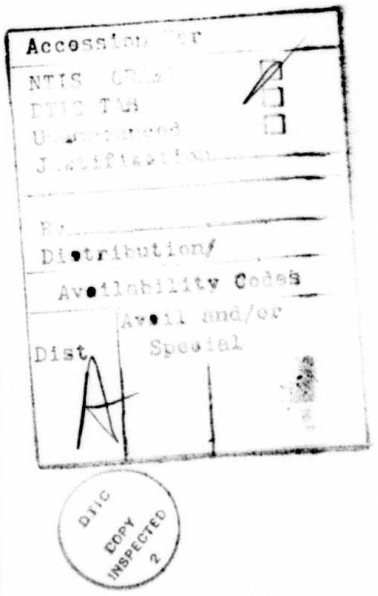

SUMMARY

This report presents the results of a two-year cooperative effort between SBRC and Stanford University to study the surface and surface region of HgCdTe. Tasks were followed which focused on four areas: (1) study of the atomically clean surface produced by cleaving HgCdTe in ultra-high vacuum (UHV); (2) study of the oxygen chemistry of this surface, particularly the role played by defects; (3) composition studies of natural oxides, anodic oxides, and deposited SiO_2; and (4) study of the electrical properties of passivated interfaces. Principal results are outlined below.

1. It was established that the surface is very sensitive to both surface and bulk defects, and that the surface must be understood in the context of bulk damage.
   - established the inherent stability of "undamaged" HgCdTe surfaces at room temperature (RT), Hg vapor pressure less than 10^{-10} Torr.
   - established that Hg vapor pressure above HgCdTe is very sensitive to surface damage and crystal quality.
   - working with Professor Paul Raccah, University of Illinois at Chicago circle, it was established that cleaved surfaces were much less damaged than any polished surfaces provided by various DOD vendors.
   - using PES, it was established that cleaving converts p- to n-type in the surface.
   - HgCdTe was found to be the first semiconductor alloy in which the virtual crystal approximation breaks down using PES. This is well understood and was confirmed theoretically, working with Arden Sher of SRI and A.B. Chen of Auburn University. This also helps explain mechanical weakness of HgCdTe in terms of the nature of metal-Te bonds. Breakdown of virtual crystal approximation and reduction of bandgap to zero with increased Hg were found to be two aspects of the same phenomena. Finally, because of the characteristic changing of bonding with composition, an increase in materials stability problems is to be expected as one goes from 3 to 5 μm and 8 to 12 μm detectors.
2. Using PES, it was established that HgCdTe does not react with O_2 in sharp contrast to Si and III-V semiconductors. Oxygen excited by an ion gauge in direct line of sight with HgCdTe will form an oxide on HgCdTe, and it appears that Hg must be removed by gas exposure, TeO_2 is the preferred oxide.
3. Established the capability of the Stanford sputter-Auger technique to determine chemical depth profile of passivated HgCdTe. Effects of preferential sputtering and chemical shifts, were identified and calibrated. Analysis showed the anodic oxide is composed of a complex Cd and Te oxide with less than 1% Hg; the natural oxide produced during MIS processing is a Te-rich oxide.

4. The interface and interface region was studied using an MIS structure made with PHOTOX™ SiO_2 on HgCdTe. Using DLTS we have seen that pre-passivation surface treatments affect bulk electronic structure. Using C-V and AES we have shown that these treatments strongly affect interface electrical properties by controlling pre-SiO_2 deposition oxide growth. The best performance is seen in devices made by depositing SiO_2 on HgCdTe with a layer of Te oxide.

CONTENTS

ILLUSTRATIONS

INTRODUCTION

The purpose of this two-year study was to characterize surface states, effects of overlayers and surface treatments, and their expression in an interface structure. This is aimed at developing a fundamental understanding of how to passivate HgCdTe devices. Significant progress toward that end has been achieved and is summarized in this report. However, investigation of the fundamental problem of passivation has revealed a subtler nature encompassing many supposedly separate effects, all of which must be considered to account for the alloy's unique bulk and surface behavior. Of principal importance is the intimate connection between bulk and surface effects. This means the surface cannot be treated without altering bulk properties which, in turn, alter interface activity. The connection arises due to the ease of inducing native defects, particularly removing Hg from the Lattice which becomes highy mobile and the resulting alteration of electrical and chemical properties. It also became clear during this study that bulk properties and their defect structures are not significantly better understood than surface effects. This has necessitated a reexamination of ideas underlying bulk band structure and bonding. This has formed a major portion of the experimental effort, particularly at Stanford, as well as guiding the formation of very successful collaborations with other groups (Dr. A. Sher at SRI, Prof. A.B. Chen at Auburn University, and Prof. P.M. Raccah at the University of Illinois).

The work at SBRC has concentrated on studies of interfaces, passivations and the role played by native defects in these systems, both in their effects on surface treatment and interface electrical properties and is presented in Section 1, while Section 2 is devoted to a discussion of surface structure, surface oxidation, and bulk bonding, work done principally at Stanford University.

Section 1

INTERFACE STRUCTURE

The growing demand for high-density infrared detector arrays using HgCdTe has placed increasing pressure on existing abilities to produce these high-performance devices. In many cases, device performance is affected and even limited by the behavior of the surface. Understanding surface properties will be increasingly critical as device size is reduced in future generations. A HgCdTe surface presents a special problem because one of the alloy components, Hg, is much less strongly bonded than the others. Also, the bonding becomes weaker as Hg content increases.[1] This leads to a number of important effects which impact surface properties. The two of immediate importance are the ease with which defects are induced, principally Hg vacancies, and local alterations in stoichiometry.[2] Both have strong effects on electronic structure and oxide formation, which together determine the effectiveness of surface passivation.

A great deal of work has been done on the anodic oxide interface and techniques for growing other oxide layers with slightly different properties.[3-4] These interfaces are quite promising except for a consistently large fixed charge density which renders them useless as a passivation in many applications.[5] Alternate materials have also been studied which promise lower charge densities along with slightly better interfaces; principal among these has been low-temperature CVD SiO_2.[6] We have determined that this type of material also relies on a native oxide layer for its properties.[7]

SAMPLE PREPARATION

For these studies we prepared metal insulator semiconductor (MIS) devices on wafers of bulk-grown (horizontal zone melt) $Hg_{1-x}Cd_xTe$ with x in the range of 0.3. These wafers were isothermally annealed in Hg vapor, resulting in an n-type surface at with $N_D \approx 1 \times 10^{15}$ cm^{-3}. This donor level is determined by the concentration of residual impurities in the HgCdTe whose exact identity is unknown. The wafers were processed using a two-step treatment, the first being a chemo-mechanical polish with bromine in dimethylformamide (DMF) followed by a solvent cleaning process; toluene, acetone, methanol and isopropanol sequentially sprayed. Next a light spray etch with 1/16% bromine in ethylene-glycol is applied, again followed by a solvent cleaning. Surface conditions are monitored after each step with a monochromatic ellipsometer operating at 6328Å.

Devices were fabricated on these surfaces by application of low-temperature CVD SiO_2 by the patented PHOTOX™ (Patent No. 4,371,587) process to a thickness of 1500Å. These depositions were done as soon after surface preparation as possible, less than 15 minutes. The surface is nearly static at this stage; however, a few hours exposure to air can increase the native oxide thickness by up to ~10Å. Metal contacts are formed on the HgCdTe substrate by application of In using a small soldering iron, and to the SiO_2 by evaporation through a shadow mask of 400Å of Ti followed by 6000Å of Au. The resulting capacitance is about 60 pF with an area of 2.04×10^{-3} cm^2.

The anodized interfaces used for comparison were made in a solution of 10% 1 normal KOH in glycerine and water. Voltage is stepped in increments to a final value which determines the film thickness. A standard thickness of 1100Å (voltage = 22V) was used, which produces devices with capacitance of about 200 pF and with high enough resistivity to acquire quasi-static C-V data.

The interface electronic structure was measured using the capacitance-voltage (C-V) technique with data taken at 1 MHz using a PAR 410 capacitance meter, and dc using an electrometer. Currents measured are typically in the range of 10^{-11} ampere.

Composition of the interface, as well as the wafer surface prior to the SiO_2, was measured using AES in conjunction with ion milling. The milling was done using 1 keV Ne^+; the primary electron energy for AES was in the 4.5 keV to 5 keV range.

EXPERIMENTAL RESULTS

The ellipsometer is capable of measuring the thickness (t) and index of refraction (n) for overlayers on the wafer surface. This is done by recording changes in the amplitude and phase of the polarization components parallel and perpendicular to the surface. Two parameters are calculated, Δ and ψ, where $\Delta = 360-P_1-P_2$ and $\psi = \frac{180 - A_1 + A_2}{2}$; A and P are the ellipsometer analyzer and polarizer settings required to obtain a null; these in turn can be reduced to give n and t. In the case of very thin layers on the order of 10Å, it becomes very difficult to interpret the data in a manner which allows us to identify the composition. Measurements made after the chemical polish show Δ in the range of 147 to 148, which we take as a clean, uncoated surface. After the spray etch, Δ has typically lowered by several degrees, indicating accumulation of some surface layer. Due to the simplicity of the treatment, the most likely

candidates are an oxide layer, a bromide layer, or some combination. Thicknesses of the overlayer vary from wafer to wafer, but generally fall in the range of 10Å to 20Å.

Capacitance measurements of the finished MIS devices show near ideal behavior. Figure 1 shows capacitance data taken quasistatically and at 1 MHz (dashed curves), compared to a theoretically predicted curve (solid line) derived by considering the effects of the semiconductor space charge region only. When the experimental curves show low hysteresis (<0.2V when ramped -5V to +5V) and are undistorted, indicating little or no surface potential nonuniformity, any differences with the "ideal" curve can be considered to be due to contributions from interface states. Figure 2 shows surface state densities derived from the curves of Figure 1. Two curves of the surface state density of a device made with anodic oxide are shown for comparison. The anodic oxide density of states has been derived by two different techniques from the same data, the upper curve by comparing the quasistatic and high-frequency curves and the lower from quasistatic and theoretical curves. The former is valid from midgap to accumulation region. The difference is taken as a measure of the uncertainty of the N_{SS} curve. The local maxima and a subsequent dropoff of these curves at their ends are not considered reflective of the real N_{SS} structure. These curves show a number of interesting points. First, they completely span an interval that corresponds to the expected energy gap for this temperature (77K) and composition, indicating no Fermi energy pinning at the interface. Also, the curves are smoothly "U" shaped for both types of interfaces; that is, they are free of sharp structures indicating no high densities of discrete interface states. In fact, the principal differences between the two types of interfaces are that the SiO_2 N_{SS} values are consistently lower than those of the anodic oxide and the SiO_2 lacks the large positive fixed charge seen in the other. This difference is repeatedly seen provided the bulk crystal is consistent. A comparison of C-V results of the best interface achieved with each type of dielectric is shown in Table 1.

By pulsing the MIS device into deep depletion and measuring capacitance during the return to steady state, it is possible to determine the rates at which minority carriers are generated at or near the surface. An example for SiO_2 on HgCdTe at 77K with zero field of view is shown in Figure 3. The bias was stepped from -3 to -4V. The storage time, defined as the time for 90% recovery of the capacitance, is 1400 sec (23 min). Applying the Zerbst analysis method, [8-9] we obtain the plot of surface recombination velocity s shown in Figure 4.

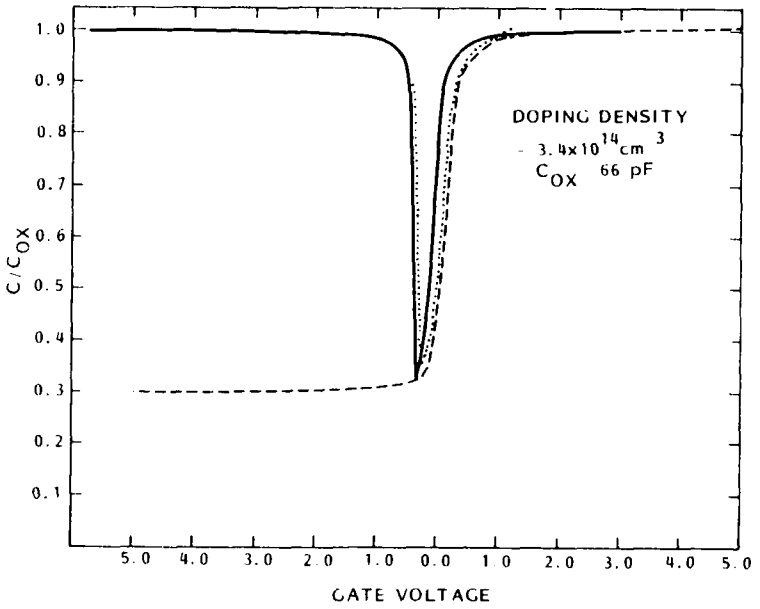

Figure 1. High Frequency (1 MHz) and Quasistatic Capacitance Curves of SiO_2 on $Hg_{0.7}Cd_{0.3}Te$. Theoretical curve calculated from effects of space charge region only in series with oxide capacitance is shown as solid line.

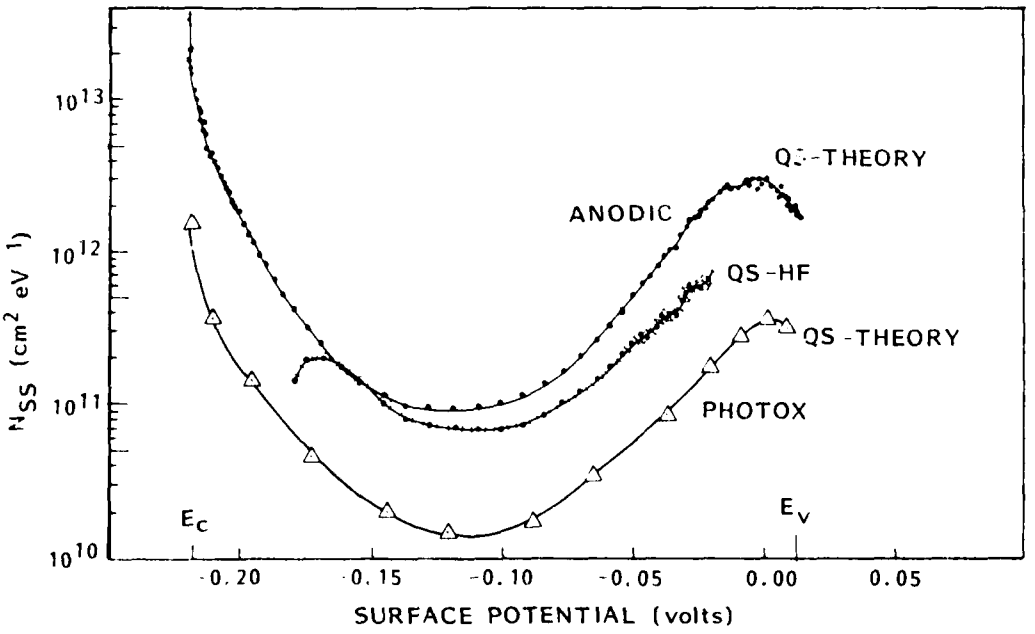

Figure 2. Surface State Density (N_{SS}) for PHOTOX™ and Anodic Oxide Interface with $Hg_{0.7}Cd_{0.3}Te$. Anodic curves calculated by two different methods from the same data. PHOTOX™ curve used method which gave higher anodic curve.

Table 1. Comparison of CV Results

	ANODIC OXIDE	SiO_2
FLATBAND VOLTAGE (charges/area)	-2.0V (1×10^{12} cm^{-2})	-0.4V ± 0.5F ($<3\times10^{10}$ cm^{-2})
HYSTERESIS	0.5V	<0.2V
SURFACE STATE DENSITY N_{SS} (minimum)	1×10^{11} cm^{-2} eV^{-1}	1.4×10^{10} cm^{-2} eV^{-1}
STORAGE TIME	85 sec	1.4×10^{3} sec
SURFACE RECOMBINATION VELOCITY	1.6×10^{2} cm sec^{-1}	1×10^{-2} cm sec^{-1}

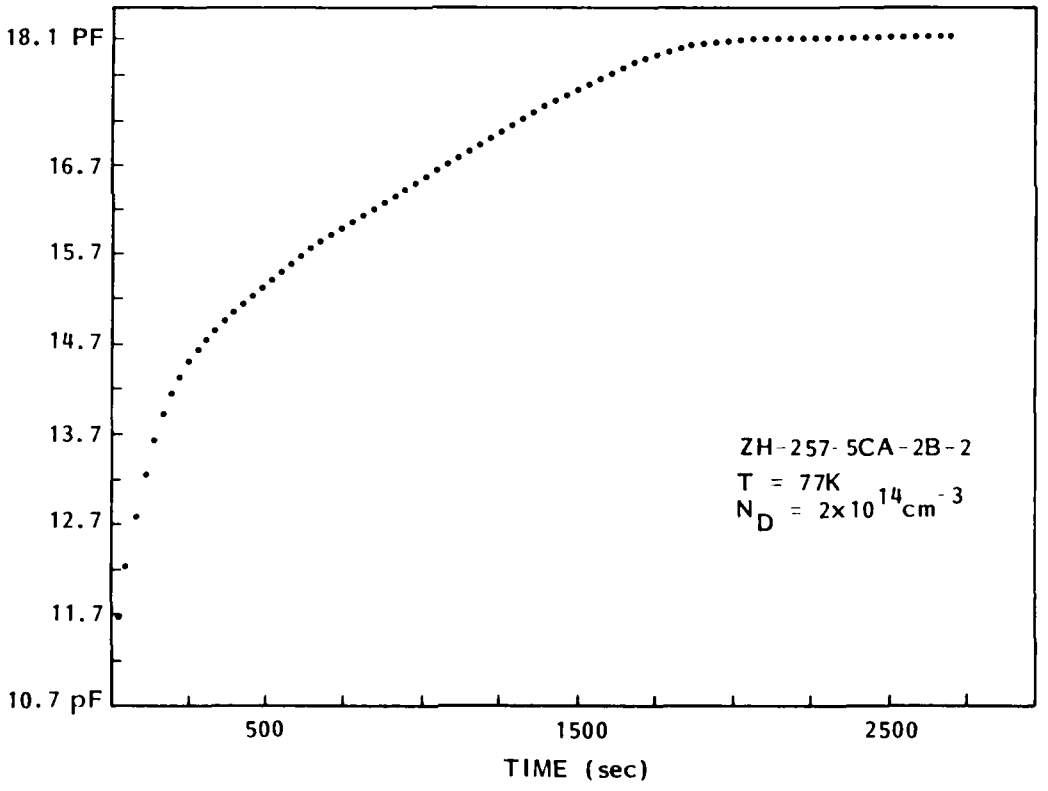

Figure 3. Capacitance Transient Following Deep Depletion Step for MIS Device with photochemical SiO_2 on $Hg_{0.7}Cd_{0.3}Te$ at 77K in Shielded Dewar

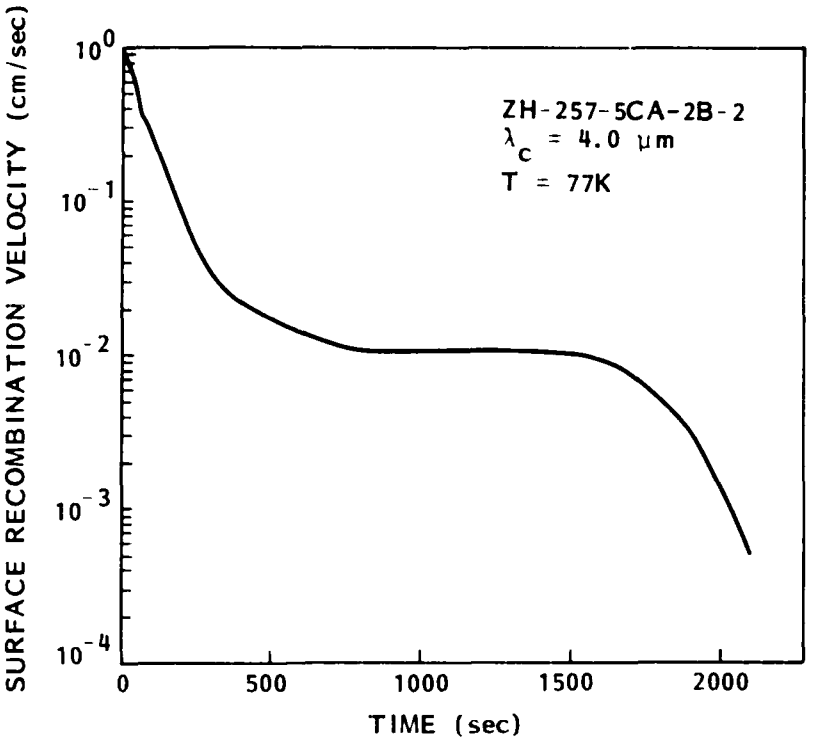

Figure 4. Time-Dependent Surface Recombination Velocity Derived from the Curve of Figure 3; Rolloff Beyond 1500 sec is an Artifact

Initially, s appears to be 1 cm sec^{-1}, but it is probably higher because the start of the transient is not resolved on this time scale. The plateau at 10^{-2} cm sec^{-1} represents the screened condition, which would pertain to diode surfaces passivated with this SiO_2.

In an effort to examine an interface made on a clean (oxide free) HgCdTe surface, the usual preparation was followed by an HF etch. This is known to remove oxides of HgCdTe and to leave the surface with a high Δ. The photochemical deposition process is not considered likely to re-oxidize the surface, as the silane is known to reduce these native oxides[10]; thus, an oxide-free surface prior to deposition is likely to remain so. Capacitance measurements of these interfaces show strikingly different structures, as illustrated in Figure 5. The quasistatic curve shows structure indicative of a high density of discrete surface states near the valence band maximum (VBM). Calculation of surface potential versus gate bias indicates a narrowing of the effective energy gap by the states at 0.07 eV above VBM. The presence of the native oxide overlayer on the surface prior to SiO_2 deposition seems to benefit the eventual

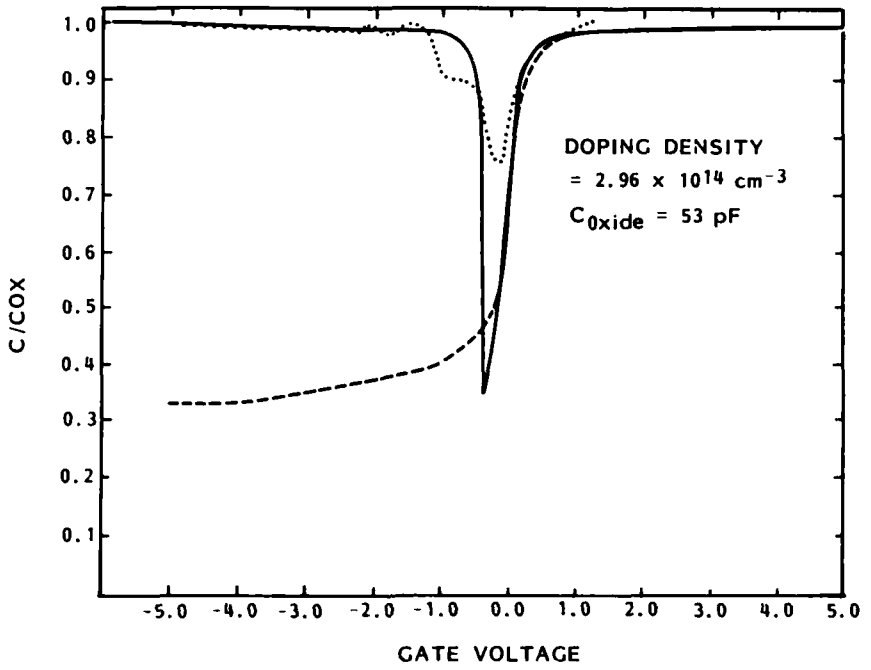

Figure 5. High Frequency and Quasistatic Capacitance (Dashed) of SiO_2 on $Hg_{0.7}Cd_{0.3}Te$ Treated with HF to Remove Native Oxide, Compared to Theoretical Curve (Solid)

interface properties, as judged by the degradation caused by its removal. It should also be mentioned that the possibility that the HF has induced some other form of surface defect in addition to removing the oxide has not been completely ruled out.

In order to identify the exact nature of this overlayer, samples were measured using AES. The spectra obtained are dominated by the overlapping O and Te signals between 480 eV and 510 eV. As shown in Figure 6, the signals from Hg (76 eV) and Cd (376 eV) are smaller in comparison to the Te than expected for a clean stoichiometric surface. This is consistent with the existence of a Te-rich oxide layer through which the underlying Hg and Cd signals are seen. The escape depths for these lines are estimated to be on the order of 25Å in the semiconductor, but is expected to be longer in the oxide; thus, it is difficult to quantify the overlayer thickness from AES amplitudes. Some surface contamination is indicated by the S and C lines; these are probably deposited during the AES measurement.

Results of the onset of ion milling during the AES measurements indicate the surface nature of the contaminants. The S, C, and O signals all decrease

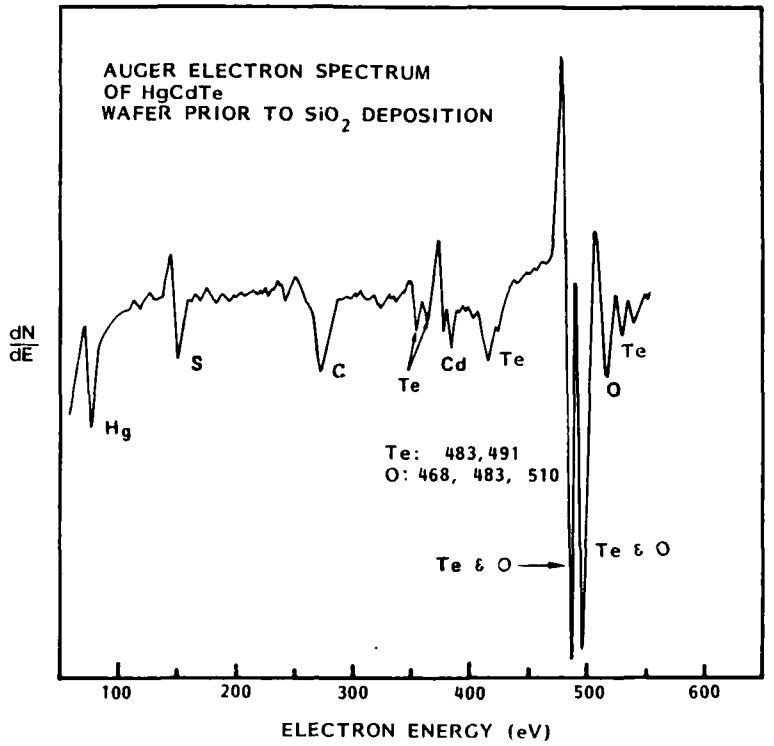

Figure 6. Auger Electron Spectrum (AES) of $Hg_{0.7}Cd_{0.3}Te$ Wafer Prior to SiO_2 Deposition

rapidly as material is removed, as shown in Figure 7. Here, peak-to-peak heights for selected lines are shown as signal amplitude versus fluence (time integral of the flux). Ion milling began at zero fluence. Though all three drop quickly to zero, S and C decrease significantly more quickly, implying a thin overlayer on the oxide. The oxygen signal's decrease is slightly more gradual and corresponds to the increase in that of Cd and Hg. The continuing transient behavior of the Hg signal is caused by the mobility of Hg in the subsurface region, which in turn is due to ion damage and has been discussed in previous work.[11]

The Te signal is essentially unchanged by the initiation of milling and removal of the oxide layer. We see a count rate for Te in the oxide approximately equivalent to that in the HgCdTe, as expected for a layer composed primarily of Te-oxide.

These results, combined with the ellipsometric and capacitance data, lead us to conclude that the Te-rich native oxide grows to a depth of about 20Å on the HgCdTe surface as a result of our preparation technique. In addition, the

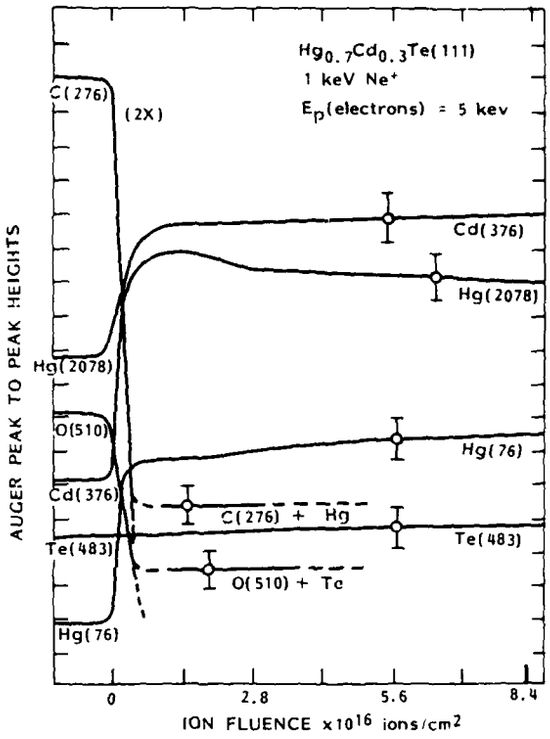

Figure 7. Effect of Ion Milling on Peak-to-Peak AES Signals for Selected Elements Seen in Spectrum of Figure 6

presence of this oxide layer prior to SiO_2 deposition is beneficial to producing well-behaved interfaces.

To decide what role this oxide plays in the final interface, measurements were made of the interface again using ion milling and AES. A depth profile of the interface region, which has been corrected for the change in escape depth with electron energy,[12] is shown in Figure 8. The Hg line at 76 eV was not profiled, as it conflicts with the main Si line. The Si profiles shown are from smaller peaks.

The interface is taken as the point where the intensity is 50% of its maximum. The uncertainty in the 50% point of the larger Si signal, due to the small peak seen before the interface region, is indicated by the crosshatched region. The Si, Cd, O, and the superimposed Te and O lines, all show 50% points in this region. A second Te line at 31 eV shows a half-height point 20Å below the other Te. From our earlier measurement of anodic oxides on HgCdTe we have seen that this Te line represents the nonoxidized Te of the substrate.[13]

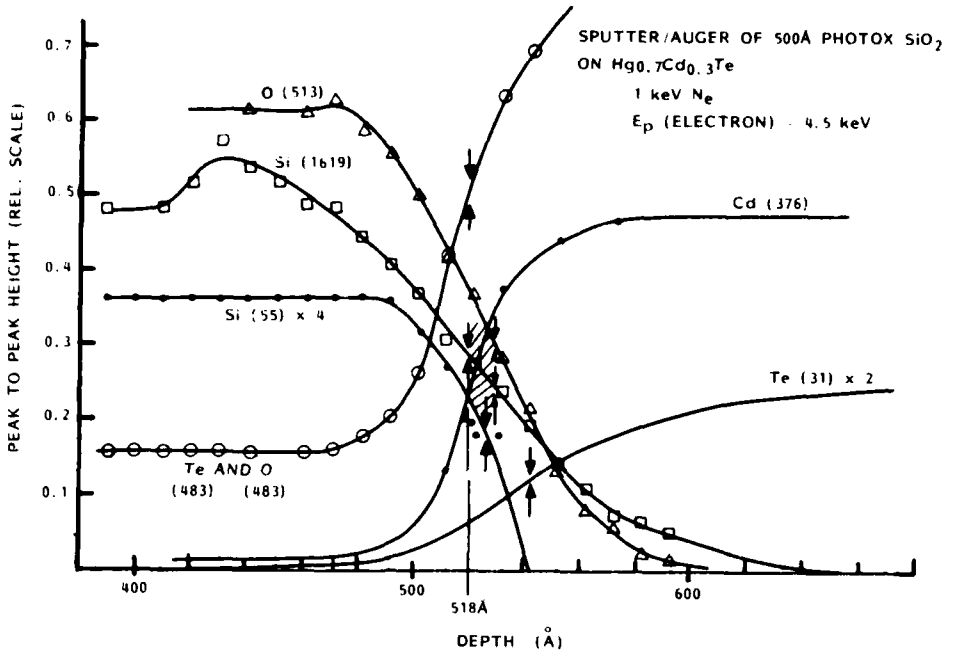

Figure 8. Depth Profile of Interface Region of SiO_2 on $Hg_{0.7}Cd_{0.3}Te$ Obtained by Simultaneous Ion Milling and AES. Signal amplitudes have been corrected for the variation in escape depth with electron energy

We also do not see any line shifts indicative of oxidized Te. We interpret this to indicate that the initial thin Te oxide layer has been substantially reduced, leaving an interfacial layer of Si, Te, and O between the applied SiO_2 and HgCdTe.

INVESTIGATION OF THE INTERFACE REGION IN n-TYPE HgCdTe

The capacitance technique is very interface sensitive and allows us to determine directly the surface state density (N_{SS}) as well as other properties of the interface region, such as fixed charge density (flat band shift) and carrier concentration profiles[14]. The DLTS process is employed to characterize traps in the interface region, since it is less biased toward surface states. Distortions of bulk properties due to surface treatments have been reported which extend hundreds of angstroms below the surface.[15] These changes affect carrier concentration, trap activity, stoichiometry, and even electrical type. Properties of the passivation layer itself are not the focus of this study and are covered extensively elsewhere.[16-18] We are focusing on the semiconductor side of the interface.

In a separate set of measurements on devices similar to those of Table 1, in the previous section, the region below the interface was examined using Deep Level Transient Spectroscopy (DLTS). The data are shown in Figure 9. The spectra of both types of interfaces (anodic and SiO_2) are similar in their major structure in that they are dominated by the same large peak corresponding to an electron trap. The large peak is seen to be asymmetrically broadened indicating a possible field dependence to the activation energy. An Arrhenius plot of the DLTS data gives $E_T = E_C - 0.02$ eV. Correction for a field effect yields an energy of $\sim E_C - 0.07$ eV or about 1/3 the gap energy in this material. Bulk trap levels at 1/2 E_g and E_C - 1/4 E_g have been previously reported.[19]

Depth profile data taken of the SiO_2 interface are shown in Figure 10. These results are consistent with two types of distributions: a distribution of interface states near the valence band, or a bulk trap level near the conduction band which is depleted near the interface. As the interpretation of interface states giving rise to this signal is inconsistent with the activation energy and does not comply with N_{SS} derived from C-V data, we conclude that we

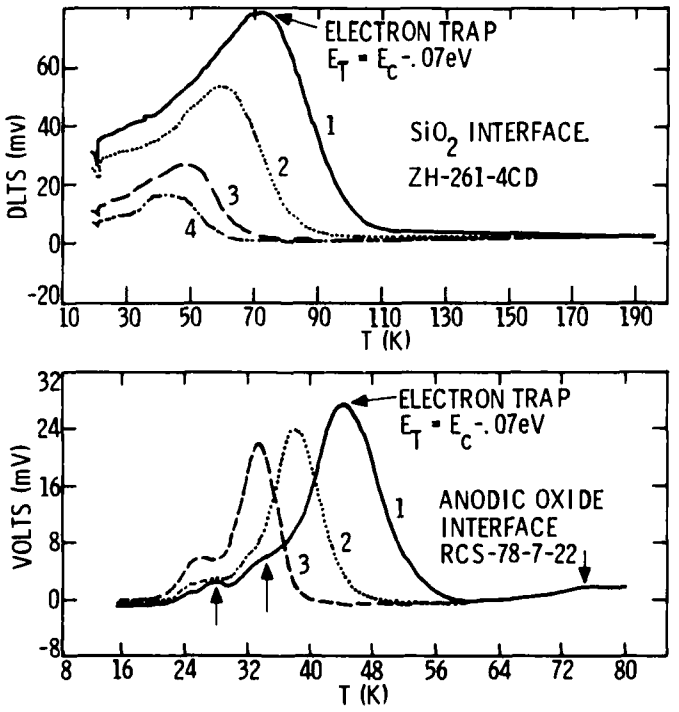

Figure 9. Comparison of DLTS Spectra for Anodic Oxide and SiO_2 Interfaces. Both spectra are dominated by an electron trap with $E_A \approx 1/3\ E_g$ (0.07 eV)

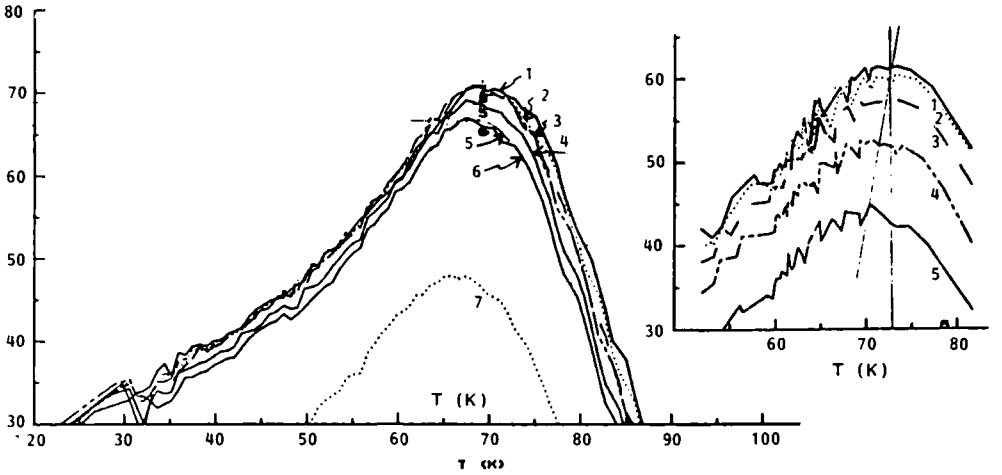

CURVE #	t_1 (ms)	t_1^* (ms)	t_w (..s)	V_p(v) /OFFSET
1	0.50	1.00	900.00	4.99 / -4.99
2	0.50	1.00	900.00	3.00 / 4.99
3	0.50	1.00	900.00	1.00 / 4.99
4	0.50	1.00	900.00	0.00 / -4.99
5	0.50	1.00	900.00	-2.50 / 4.99
6	0.50	1.00	900.00	-3.50 / 4.99
7	0.50	1.00	900.00	-4.50 / 4.99

V_p(v) /OFFSET
-3.50 / -4.99
3.75 / -4.99
-4.00 / -4.99
4.25 / -4.99
-4.50 / -4.99

Figure 10. DLTS Spectra Taken of SiO_2 Interface. The rate window is held constant while pulse height is varied to provide depth profile information.

are seeing the effects of bulk traps. Based on this interpretation, a relative concentration is derived and plotted in Figure 11.

Mechanical action on HgCdTe, such as that involved in chemical polishing, has been seen to cause substitutional Hg to be depleted in the surface region. Electro-reflectance measurements have monitored these effects up to 100Å deep.[20] This distortion toward a Hg-poor stoichiometric ratio may have the effect of altering the deep trap due to the Hg vacancy. The Hg concentration has been shown to strongly affect the Hg binding energy so that a decrease in Hg concentration increases the strength of the Hg binding in the lattice and may alter the trap level.[21]

Hg depletion over these depths has also been detected by Morgen, et al., on anodic interfaces using sputter-Auger. The altered stoichiometry was attributed solely to preanodization processing.[22] It is clear that the details of surface preparation play a key roll in surface region stoichiometry, oxide formation and interface electronic structure, all of which contribute to a properly passivated interface.

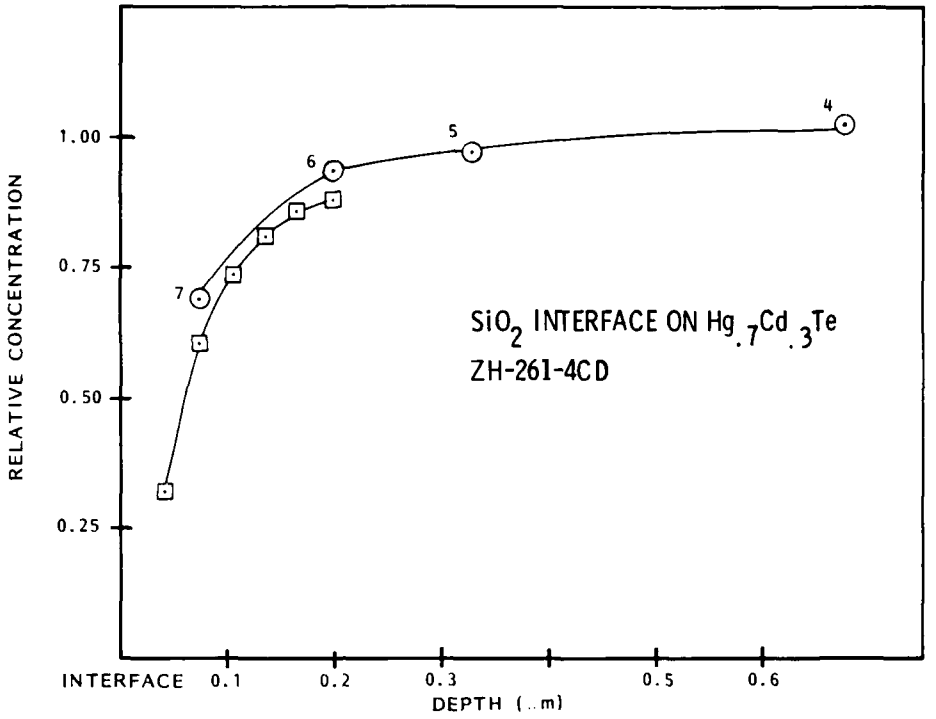

Figure 11. Relative Depth Profile of the Bulk Trap Derived from DLTS Data of Figure 9

CONCLUSIONS

It is strongly evident at this point that the most promising form of passivation of HgCdTe is a thin native oxide grown on the surface prior to deposition of a chemically inert insulating layer such as PHOTOX™ SiO_2. Devices with a layer of Te-rich oxide have produced very promising results. In these cases, the actual interface properties are determined by the bonding between a region of reduced native oxide mixed with Si and the surface of the HgCdTe distorted to some degree by the surface treatment.

The interface property with the greatest impact on device performance (e.g., photodiodes and monolithic CCDs) is fixed charge which, if large enough, can cause severe band bending to strong accumulation or strong inversion and degrade performance in a variety of ways: increasing 1/f noise; increased generation current; and recombined carriers with the associated signal loss, to name a few. The amount of fixed charge typicaly seen in interfaces made with SiO_2 deposited on oxidized HgCdTe has been measured at 3×10^{10} cm^{-2} compared with 1×10^{12} cm^{-2} for typical anodic oxide layers. The composition of these

oxides is significantly different due to the difference in method used to grow the oxide and does not appear in either case to result in the most stable equilibrium composition of $CdTeO_3$.[23] The thin native oxide is a Te-rich layer which grows to a thickness of less than 20Å and produces interfaces which perform better, not only with respect to fixed charge but surface state density (N_{SS}), hysteresis (V_{HYST}), and storage time (τ_{STO}), than do anodics. Surface state densities lower than 1×10^{10} eV^{-1} cm^{-2} have been produced.

In these cases, we are seeing limitations set to a large extent by properties of the HgCdTe surface; i.e., the passivation is not the limiting case. We come to this conclusion by noting trends in N_{SS} and τ_{STO} which are seen to correlate to ingot number and in a given ingot to wafer location. Of the types of materials used, those grown by the horizontal zone melt technique have produced the best results and are the only ones reported here. This material is highly pure with background donor levels in the low 10^{14} cm^{-3} and occasionally mid 10^{13} cm^{-3} regions. The actual parameter limiting storage time is not currently identified, however. It also appears that the limits to τ_{STO} and N_{SS} are to some extent independent of each other; i.e., a low N_{SS} does not guarantee a long τ_{STO}.

As indicated above, surface treatments also alter bulk properties in the region near the surface. Stoichiometry is altered to some depth and bulk trap activity is changed. Bulk traps near the surface can be expected to be altered due to very close proximity of the surface for any material. However, there appears to be an additional effect in HgCdTe. The dominant bulk trap seen (by DLTS) in the interface region of devices formed with anodic oxide and PHOTOX™ SiO_2 is that associated with the Hg vacancy. Depth profiling of this trap near an SiO_2 interface shows a decrease in activity as the interface is approached over a larger distance than ordinarily expected.

It may be possible to improve interface properties further by growing thicker oxides composed of Hg-free $CdTeO_3$ before deposition of SiO_2. The $CdTeO_3$ is the most stable room temperature oxide form, while growing a thicker layer can consume much of the distorted stoichiometry of the surface region, thus ensuring bonding to a more defect-free region of the semiconductor. Use of a thick native oxide may, however, reintroduce the large flat band shifts seen with the thick oxides but avoided with the current SiO_2 deposition scheme. In any event, the overlayer of SiO_2 is still likely to be necessary due to the wide range of chemicals in which the native oxides are soluble.

Section 2
SURFACE STRUCTURE, SURFACE OXIDATION, AND BULK BONDING

INTRODUCTION

Control of surface and interface electrical properties remains a critical issue in advanced HgCdTe technology. The approach taken in this study has been to apply surface science techniques to the study of surfaces prepared in a well-controlled manner (e.g., by cleaving in vacuum) and "real" surfaces and interfaces. These results will then be correlated with characterizations of interface properties performed by SBRC. The feedback loop so configured - study of fundamental properties on materials and interfaces supplied by SBRC - and characterization of interfaces formed in processes modified to include the Stanford results, should allow rapid control and optimization of the technological development necessary to HgCdTe devices. The success of this program is reflected in the strides in understanding discussed in the following section. It must be emphasized that progress in research at Stanford depended critically on the participation of SBRC, and we acknowledge their invaluable contribution.

Understanding the electronic structure of HgCdTe has proved to be an essential key to beginning to understand many of the difficult materials problems associated with the alloy. While exploration of this topic was initially undertaken to provide baseline information for study of the surface electronic structure, the unusual features of the bulk bonding have merited continued attention. The results of our investigations, experimental evidence and theoretical confirmation of a breakdown of the virtual crystal approximation and differences in the bonding of Cd and Hg in the lattice, are discussed in the papers comprising Sections 2.4, 2.7, 2.8, and 2.9. These papers also discuss the link between the difference in strength of Hg-Te and Cd-Te bonds and properties such as ease of dislocation formation and high Hg mobility of the lattice. A general conclusion suggested by this work is that similar materials difficulties may be encountered in other alloy systems which exhibit the range of bandgap tunability found in HgCdTe.

The role of defects in controlling interface properties is well documented in other materials (Section 2.3). In HgCdTe, defects often determine the conductivity of the bulk of the material. In addition, these defects can be highly mobile. Two aspects of these issues formed the focus of a portion of

the surface studies on HgCdTe: Hg loss from the cleaved surface (Sections 2.1 and 2.6), and the inversion at the surface formed by cleaving p-type material in vacuum (Section 2.10). Based on this and related work, it is apparent that an intercommunication unique to this material (and not previously observed in any other material) exists between surface and bulk due to the rapid transport of defects. Before material processing can be controlled on a scientific basis, the subtle interplay of bulk and structure defects must be understood.

In addition to the surface properties related to Hg migration, the oxygen chemistry of the alloy surface was also examined. Adequate passivation of the alloy surface remains a critical requirement. The "demands" of passivation increase as more advanced devices are developed. By studying the oxidation of the alloy, a detailed understanding of the electronic structure of the interface can be formed for subsequent optimization of passivation processes. Because of the inertness of the (110) surface to dry oxygen in the molecular ground state, activated oxygen was used to study the uptake. The use of activated oxygen may permit more direct insight into processes such as plasma anodization or photochemical SiO_2 deposition (where atomic oxygen is used) in addition to increasing the oxygen uptake. The results of these studies are given in Sections 2.1 and 2.2.

Finally, the surface sensitivity of our techniques has been used to examine surfaces and interfaces of technological importance through the use of AES combined with inert gas ion sputtering. This technique requires further calibration before its full potential can be utilized (Section 2.5.). AES was used to examine wafer surfaces following pre-oxidation preparation and to profile the chemical composition of the anodic oxide-semiconductor interface (Sections 2.2 and 2.5).

Conclusions regarding the topics outlined above can be found in the papers in Section 2; Section 3 includes some general results of the surface study program.

Journal of Crystal Growth 56 (1982) 493–497
North-holland Publishing Company

2.1

STABILITY OF AN ATOMICALLY CLEAN $Hg_{1-x}Cd_xTe$ SURFACE IN VACUUM AND UNDER O_2 EXPOSURE

P. MORGEN *, J. SILBERMAN **, I. LANDAU and W.E. SPICER ***
Stanford Electronics Laboratories, Stanford University, Stanford, California 94305, USA

and

J.A. WILSON
Santa Barbara Research Center, Goleta, California 93017, USA

We report studies of the stability of single crystal surfaces of $Hg_{1-x}Cd_xTe$ with respect to loss of Hg. Ultraviolet photoemission spectroscopy (UPS) and X-ray-induced photoemission (XPS) were used to monitor the electronic structure and atomic composition of a cleaved surface under ultrahigh vacuum (UHV) ($p \simeq 5 \times 10^{-10}$ Torr) and under oxygen exposures. These experiments showed the surface to be remarkably stable in UHV for extended periods of time at room temperature. However, changes in the surface concentrations can be induced during exposure to excited oxygen or during ion bombardment. The importance and relevance of these findings to the question of the stability of the material are discussed.

1. Introduction

Studies of mechanical and electronic properties of crystalline $Hg_{1-x}Cd_xTe$ are required to assess the potential and quality of the material for application in infrared-sensitive devices [1]. A relatively large number of such studies are reported in the literature [2]. However, until recently, studies of surface properties of the material, and the effects of different surface treatments, have not been published. At present, several groups are engaged in this type of research [3–7]. The oxidation and passivation of the surface has been studied with XPS [3] and with XPS combined with ion sputtering for the purpose of cleaning the surface [5]. It has been reported that Hg leaves the surface very easily during ion bombardment, during heating, and even at room temperature. In the past, various attempts have been made to determine the equilibrium vapor pressure of Hg above $Hg_{1-x}Cd_xTe$ [8,9]. For temperatures slightly above room temperature (100°C), equilibrium vapor pressures of the order of 10^{-6} Torr to several orders of magnitude higher have been reported. Type conversion of n-type material was found to occur [9] for samples stored in air for several years at room temperature and explained as a loss of Hg [8] from the surface due to chemical decomposition.

The present work deals with some of the questions raised by the previously published results on $Hg_{1-x}Cd_xTe$ surfaces. To study the possible loss of Hg from a clean $Hg_{1-x}Cd_xTe$ surface in UHV, we use photoemission techniques [10] which sample the outermost layers of the material [11]. We have investigated (110) cleaved surfaces of p-type material of $x = 0.31$ grown by the recrystallization technique. In particular, the stability of clean surfaces produced by cleavage at a pressure of 5×10^{-10} Torr was examined. Exposure of the clean surface to oxygen was also studied with UPS and XPS. Finally, in a different type of experiment, crystalline wafers with (111) surfaces were subjected to bombardment with Ne^+ ions. These wafers had initially been cleaned by etching in Br/MeOH and then left in the ambient atmosphere for weeks. Auger electron spectroscopy (AES) was performed on these surfaces to detect changes in composition resulting from the ion bombardment.

Our results at present indicate that the cleaved surface is remarkably stable at room temperature. No

* On leave from Odense University, Denmark.
** National Science Foundation predoctoral fellow.
*** Stanford Ascherman Professor of Engineering.

0022-0248/82/0000-0000/$02.75

adsorption is detected for molecular oxygen. Only excited oxygen reacts with the surface to start formation of a native oxide layer. Ion bombardment induces an inhomogeneous concentration of Hg through the surface and subsurface regions. This is most likely caused by preferential sputtering coupled with effects of a high mobility of Hg in the disrupted lattice.

2. Experimental

Ultraviolet light from a He discharge lamp with monochromator (to eliminate satellite lines) and Al Kα X-rays were used for excitation of the $Hg_{1-x}Cd_xTe$ samples. The electrons emitted due to the incident photons were collected and analyzed for energy in a double-pass cylindrical mirror electron spectrometer. The resolution during analysis may be varied to assure optimum discrimination in the measured distributions. In UPS, the experimental resolution was 0.1 eV, as compared to 1.0 eV in XPS.

Samples in the form of 1.5 cm long square rods of $Hg_{0.69}Cd_{0.31}Te$ were introduced into the ultrahigh vacuum after bakeout of the system. A cleaving mechanism inside the chamber allowed cleaves to be made perpendicular to the long ⟨110⟩ axis of the rod. The cleaves were normally smooth but showed some curvature and large areas of terraces. A stainless-steel plate was mounted in the system in electrical contact with the $Hg_{1-x}Cd_xTe$ samples. Evaporation of Au on the plate could be carried out in situ. The spectrum of photoemitted electrons from this Au sample shows a well-defined Fermi edge, which serves to identify the position of the Fermi level [13] for the $Hg_{1-x}Cd_xTe$ samples when measured under identical conditions.

The oxygen exposures were carried out in situ by admitting spectroscopically pure oxygen to the vacuum chamber with the ion pumps switched off.

A commercial system (Varian) with a 10 keV electron gun and a high-resolution cylindrical mirror analyzer was used for the ion bombardment AES measurements. The Ne^+ ions were produced in the ion gun after backfilling the system with Ne to 5×10^{-5} Torr. Gettering and cryopumping at liquid nitrogen temperature assures a low ($\sim 10^{-9}$ Torr) background pressure of reactive gases during the experiments.

3. Results

The spectrum of electrons photoemitted from a cleaved $Hg_{0.69}Cd_{0.31}Te$ (110) surface at a photon energy, $h\nu$, of 21.2 eV is shown as spectrum a in fig. 1. At this photon energy, several layers of the material are sampled. Similar experiments were carried out at $h\nu = 40.8$ eV, in which a more shallow sampling depth is expected. No significant differences were noted between the two sets of experiments for the results reported here. However, more work at 40.8 eV and other photon energies is under way; so, for the present, we shall concentrate on the results obtained at 21.2 eV. The spectrum (a in fig. 1) displays the valence band at 0 to 6 eV below the upper edge of

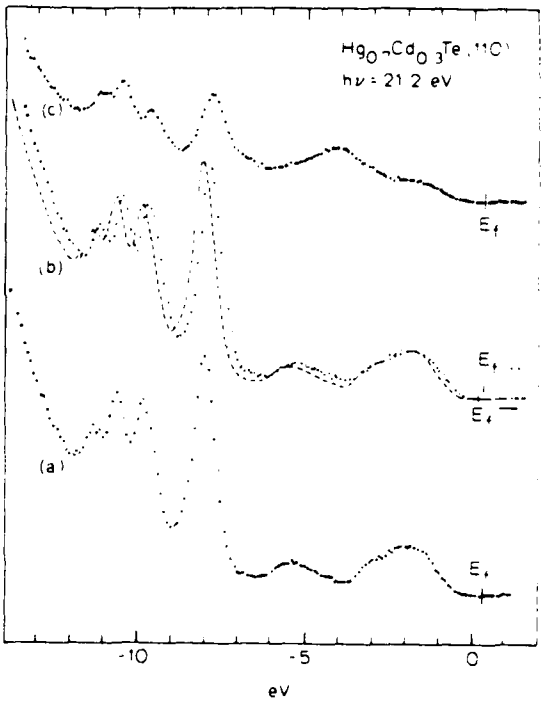

Fig. 1. Photoemission at 21.2 eV. (a) Just after cleavage. (b) 120 h later and after exposure to 4×10^{13} L of oxygen. Dotted curve is the same spectrum as in (a). (c) After exposure to 4.2×10^8 L of excited oxygen (produced by an ion gauge). All spectra normalized to the height of the Cd ($4d_{5/2}$) peak at -10.5 eV in (a). The valence band emission occurs from 0 to -6 eV. In sequence, towards more negative energies, the core lines are: Hg ($5d_{5/2}$), Hg ($5d_{3/2}$), Cd ($4d_{5/2}$), Cd ($4d_{3/2}$). More negative energies in the figure correspond to higher binding energies.

emission and, more than 6 eV below the edge, Hg 5d and Cd 4d levels. Thus, we are able to monitor the relative concentrations of Hg and Cd at the surface (estimated accuracy 1 at%), looking at the relative intensities of the Hg and Cd peaks. The position of E_F, the Fermi level at the surface, suggests conversion of type (p to n) at the cleaved surface, but further studies will be done to confirm this finding.

Spectrum (b) in fig. 1 was recorded 120 h after the cleave (a) and after an oxygen exposure of 4×10^{13} L ($1\ L = 10^{-6}$ Torr s). All spectra in fig. 1 have been normalized to the height of the Cd ($4d_{5/2}$) peak. The areas of the Cd (4d) and the Hg (5d) peaks are identical to within 1% in the two experiments in (a) and (b), and the features of the valence band are unchanged. Thus, from the lack of decomposition (i.e., Hg loss), we estimate the Hg vapor pressure to be below 10^{-12} Torr.

Significantly higher pressures ($\geq 10^{-10}$ Torr) were implied to explain the findings in refs. [8] and [9].

In fig. 1, spectrum (c), we see the effect of exposure to 4.2×10^{8} L of oxygen in the presence of an ion gauge [13]. An oxygen-induced structure at 4.1 eV below the edge of the valence band is clearly developing. At the same time, the Hg (5d) peaks decrease relative to the Cd (4d) peaks. Changes in the relative concentrations of Hg, Cd, and Te are also detected from XPS, although the changes observed, deduced from the intensities of various core lines which sample different depths, differ slightly. This could indicate an inhomogeneous composition of the surface region of the sample due to the interaction with excited oxygen. More work is needed, however, to elaborate on these observations.

The results of the ion bombardment/AES measurements are shown in fig. 2. This figure shows, in arbitrary units, the peak-to-peak heights of the (derivative) Auger signals from several different constituents of the sample. With increasing doses of Ne^+ ions, material is removed from the sample due to sputtering. Thus, from the figure, we see how surface oxygen and carbon are removed during the initial stage of the bombardment. The oxide layer was probably formed during etching of the samples in Br/MeOH [3]. From a similar experiment with layers of anodic oxides, we know the sputtering rate in the oxide. The oxide found on the surface in the present experiment is less than 20 Å thick.

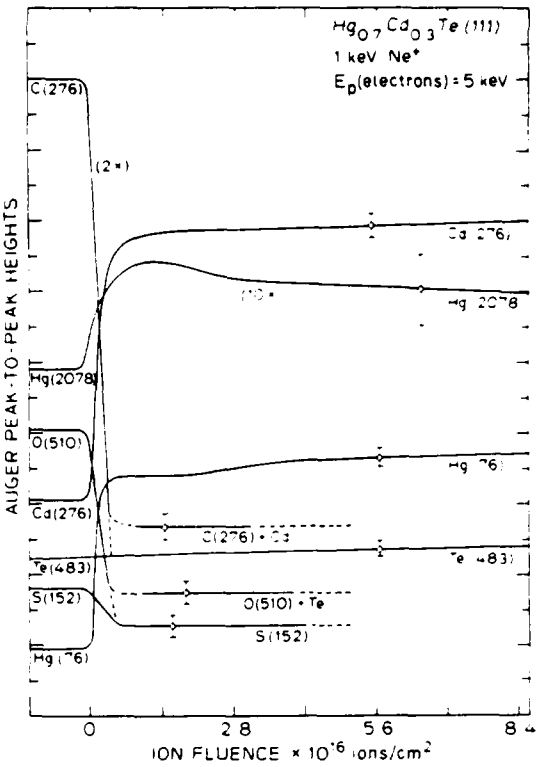

Fig. 2. Sputter/Auger measurements. Auger signals (peak-to-peak heights) are plotted as functions of total dose (fluence) of ions. The C (276) and O (510) signals coincide with Cd and Te signals, respectively. Thus, below a certain level, the real concentrations of C and O are inaccessible. The Hg (2078) signal is recorded at 10× higher sensitivity than the other signals.

During the ion bombardment, the concentrations of the different constituents change as indicated by the corresponding Auger signals. The analysis of the corresponding atomic concentrations and their spatial variation as sampled with this technique is complicated and will not be presented here. However, one important observation will be mentioned. The lowest (76 eV) and the highest (2078 eV) Hg Auger lines show different tendencies during prolonged bombardment times. They sample rather different depths below the surface because of their different average mean free paths in the sample (5 and 25 Å). Separate experiments have been performed to confirm the findings of fig. 2. The ion bombardment experiment

Table 1
Concentrations (Auger peak-to-peak heights) of $Hg_{1-x}Cd_xTe$ samples before sputtering and after 10 min sputtering; only Hg, Cd, and Te signals given

$Hg_{0.7}Cd_{0.3}Te$				
	Hg(76)	Hg(2078)	Cd(376)	Te(483)
Before	0.16	0.29	0.16	1.00 [a]
After	0.26	0.26	0.34	1.00 [a]
$Hg_{0.8}Cd_{0.2}Te$				
	Hg(76)	Hg(2078)	Cd(376)	Te(483)
Before	0.13	0.37	0.13	1.00 [a]
After	0.31	0.31	0.29	1.00 [a]

[a] Auger signals normalized to Te(483) signal.

was repeated, and the Auger signals were determined before and 10 min ($\sim 2.8 \times 10^{16}$ ions/cm^2) after the start of the bombardment. The resulting signals are given in table 1. It is seen that the concentration of Hg as measured by the 76 eV line increases strongly while the 2078 eV signal indicates a decrease. Thus, an obvious explanation of this finding would be that the ion bombardment changes the concentration gradient of Hg. At the moment, studies, at a range of ion energies, of several different multicomponent systems including $Hg_{1-x}Cd_xTe$ samples are undertaken. The purpose is to determine what degree of inhomogeneity can be expected due to preferential sputtering [14]. It is felt at present that the effects observed for Hg in $Hg_{0.7}Cd_{0.3}Te$ (and in $Hg_{0.8}Cd_{0.2}Te$) would indicate a high degree of preferential sputtering [4,5] and diffusional transport of Hg to the surface during the ion bombardment.

4. Discussion and summary

The stability of crystalline $Hg_{1-x}Cd_xTe$ has been tested by looking at surfaces of the material subjected to different mechanical, chemical, and radiative effects in UHV. At room temperature, cleavage and exposure to oxygen was examined. After cleaving p-type material, no instability of the surface was detected for extended periods of time in ultrahigh vacuum, and a limit of 10^{-13} Torr was placed on the Hg vapor pressure above the surface. This is considerably lower than previously reported [4,8,9]. We suggest that surface perfection, i.e., lack of mechanical damage to the surface, is critical in reducing the vapor pressure. Further experiments will be devoted to study this.

The surface produced by cleavage in UHV was highly inert to oxygen. A similar conclusion was reached for sputtered surfaces [5]. However, during exposure to oxygen excited by an ion gauge, oxidation and changes in stoichiometry were detected. Ion bombardment of $Hg_{1-x}Cd_xTe$ is a process which results in an inhomogeneous surface region. Previous experiments [4,5] have not discovered this effect but reported a net depletion of Hg over a somewhat intermediate sampling depth. The concerns about the stability of the system [4] during certain conditions of surface preparation (scraping and ion bombardment) seem warranted, as suggested by the present findings. For other types of surface preparations, our experiments indicate an excellent stability of the material. However, at this preliminary stage of investigations of surface properties of $Hg_{1-x}Cd_xTe$, direct comparisons between results obtained by different groups may easily lead to premature conclusions. Thus, we do not yet have enough published data to illustrate how important the different crystal preparation methods are for the properties we are investigating here. Such studies are presently being carried out in several laboratories, and the results should soon be available.

Acknowledgments

This project is supported by DARPA, Contract No. MDA 903-90-C-0496. One of the authors (P.M.) acknowledge Odense University, Denmark, and the Danish Natural Science Research Council for granting and financing a leave of absence. The hospitality and support of Stanford University extended to him is gratefully acknowledged.

References

[1] D. Long and J.L. Schmit, in: Semiconductors and Semimetals, Vol. 5, Eds. R.K. Willardson and A.C. Beer

(Academic Press, New York, 1970);
T.C. Harman, in: Physics and Chemistry of II–VI Compounds, Eds. M. Aven and J.S. Prener (North-Holland, Amsterdam, 1967);
T.C. Harman and I. Melngailis, in: Applied Solid State Science, Vol. 4, Ed. R. Wolfe (Academic Press, New York, 1974).

[2] See, e.g., R. Dornhaus and G. Nimtz, The Properties and Applications of the $Hg_{1-x}Cd_xTe$ Alloy System, Springer Tracts in Modern Physics, Vol. 78 (Springer, Berlin, 1976).

[3] S.P. Kowalczyk and J.T. Cheung, J. Vacuum Sci. Technol., in press.

[4] H.M. Nitz, O. Ganschow, U. Kaiser, L. Wiedemann and A. Benninghoven, Surface Sci. 104 (1981) 365.

[5] U. Solzbach and H.J. Richter, Surface Sci. 97 (1980) 191.

[6] G. Davis, T.S. Sun, S.P. Buchner and N.E. Byer, Abstracts, PCSI 8, Williamsburg, Virginia, 1981;
G. Davis, T.S. Sun, S.P. Buchner and N.E. Beyer, J. J. Vacuum Sci. Technol., to be published;
T.S. Sun, S.P. Buchner and N.E. Byer, J. Vacuum Sci. Technol. 17 (1980) 1067.

[7] B.A. Orlowski, Polish Academy of Sciences, Warsaw, Poland, private communication.

[8] W.F.H. Micklethwaite and R.F. Redden, Appl. Phys. Letters 36 (1980) 379.

[9] G. Nimtz, B. Schlicht and R. Dornhaus, Appl. Phys. Letters 34 (1979) 490.

[10] W.E. Spicer, Bulk and Surface Ultraviolet Photoemission Spectroscopy, in: Optical Properties of Solids, Ed. B.O. Seraphin (North-Holland, Amsterdam, 1976).

[11] I. Lindau and W.E. Spicer, J. Electron. Spectrosc. Related Phenomena 3 (1974) 409, and references therein.

[12] P. Skeath, I. Lindau, P.W. Chye, C.Y. Su and W.E. Spicer, J. Vacuum Sci. Technol. 16 (1979) 1143.

[13] P. Pianetta, I. Lindau, C.M. Garner and W.E. Spicer, Phys. Rev. B18 (1978) 2792.

[14] H.F. Winters and J.W. Coburn, Appl. Phys. Letters 28 (1976) 176.

OXIDATION OF $Hg_{1-x}Cd_xTe$ STUDIED WITH SURFACE SENSITIVE TECHNIQUES

by

P. MORGEN, J. A. SILBERMAN, I. LINDAU, W. E. SPICER, AND J. A. WILSON

Reprinted from: Vol. 11, Number 4, July, 1982

Journal of ELECTRONIC MATERIALS

A Publication of The Metallurgical Society of AIME

22

Journal of Electronic Materials, Vol. 11, No. 4, 1982

2.2

OXIDATION OF $Hg_{1-x}Cd_xTe$ STUDIED WITH SURFACE SENSITIVE TECHNIQUES

P. Morgen,* J. A. Silberman,** I. Lindau, W. E. Spicer,† and J. A. Wilson††

Solid State Electronics Laboratory
Department of Electrical Engineering
Stanford University
Stanford, California 94305

(Received August 27, 1981; revised February 18, 1982)

We report the use of surface sensitive electron spectroscopies to monitor the initial steps of formation of a native oxide on atomically clean cleaved $Hg_{1-x}Cd_xTe$ single crystal surfaces in ultrahigh vacuum (UHV). Here the oxide is formed by oxygen excited by the presence of an operating ion gauge. During the reaction, the composition of the surface region of the substrate was found to change, with a net loss of Hg from the surface. Parallel studies of the compositions of thick anodic oxides using sputter profiling techniques showed only small amounts of Hg in the anodic oxides.

Key words: $Hg_{1-x}Cd_xTe$, dry oxidation, anodic oxidation.

---

*On leave from Odense University, Denmark.

**National Science Foundation Predoctoral Fellow.

†Stanford W. Ascherman Professor of Engineering.

††Santa Barbara Research Center, Goleta, California 93017.

0361-5235/82/1104-0597$3.00

Introduction

The performance of $Hg_{1-x}Cd_xTe$ [(Hg,Cd)Te] infrared devices depends critically on surface passivation. It has been suggested to use an oxide layer covering the semiconductor substrate for this purpose (1-4). However, studies of anodic oxide-(Hg,Cd)Te MOS structures (1,5,6) have indicated problems with charge trapping in the oxide layer. These studies did not address questions about the growth mechanisms and their influence on the microscopic properties of the interface. For a better understanding of the semiconductor-insulator interface, and of possible growth mechanisms, we have studied the initial steps of the oxidation process as well as the composition of thick oxide layers with techniques which are surface sensitive on an atomical scale. These include X-ray and Ultraviolet Photoemission Spectroscopy (XPS, UPS) with HeI light and synchrotron radiation (7) and sputter profiling/AES (Auger Electron Spectroscopy) measurements. The oxidation of (Hg,Cd)Te has earlier been studied with XPS (2,3). It was reported that oxidation of clean surfaces had to include some kind of excitation, as by chemical reactions with oxidizing agents (2) or by excitation of oxygen with light (3). After a detectable quantity of oxide had been formed with oxidizing agents, its composition was found to be Te rich by XPS (2). Other studies have reported mixed oxides of all three constituents to form during dry- (3), wet- (3), and anodic (4) oxidation. It was suggested from sputter profiling and XPS (4) that the anodic process had left the substrate depleted of Hg 150 to 200 Å below the interface.

The present results are obtained with single crystals of composition $x = 0.2$ and $x = 0.3$. To produce atomically clean surfaces, we cleave the crystals in ultrahigh vacuum, exposing a (110) surface. We have found that this method produces stable surfaces with the same concentration as in the bulk (8,9). These surfaces are practically inert to molecular oxygen (8) but react with excited oxygen. In one set of experiments, exposure to 10^4 L of O_2 (1 Langmiur = 10^{-6} torr-sec) excited by an operating ionization gauge (the guage was not in line of sight with the sample) resulted in a slight change in the band bending at the surface. At 10^6 L of O and higher, (excited by the guage) oxidized Te at the surface is detected as well as a

significant loss of Hg. At the higher exposures of excited O_2, a clearly distinguishable oxygen derived feature is also observed in the valence band region of the spectra. For comparison, exposures of 4×10^{13} L of O_2 without excitation did not show any measurable effects on core lines or valence band structure (8).

From the present results, we are led to conclude that excited oxygen interacts with the (Hg,Cd)Te surface in a complicated manner, involving the volatilization of Hg.

The present sputter profiling/AES results for thick oxides are in qualitative agreement with results reported earlier (3,4,10) for the composition of such oxides. All the studies show that there is very little Hg in the oxide. With the higher depth resolution obtained using AES instead of XPS, we find interface widths of less than 50 Å. Hg depletion of the substrate is not observed in the present case.

Experimental Methods

All photoemission experiments were carried out in ultrahigh vacuum (UHV), with background pressures between 4×10^{-11} torr and 2×10^{-10} torr. For the XPS measurements K_α X-rays of Al or Mg were produced with water cooled anodes situated close to the sample. A differentially pumped He-discharge lamp with monochromator was used for the UPS measurements and set for operation at 21.2 eV (HeI) (11). Photons of energy $h\nu = 110$ eV were obtained in experiments at the 4° beam line at the Stanford Synchrotron Radiation Laboratory. Crystals were transferred into the measuring chamber after pump down and bakeout to a pressure $<10^{-10}$ torr. Here they could be cleaved in situ and positioned in front of the electron spectrometer where they were illuminated at an incident angle of 75° with respect to the (110) axis. This axis was coincident with the axis of rotation of the spectrometer, which was a double-pass cylindrical mirror analyzer with retarding grids. The oxygen gas was of research grade purity and contained in a glass flask brazed to a stainless steel leak valve. Exposures were measured with a cold cathode discharge gauge in order not to have any additional sources of excitation of the gas. Exposures of 10^4 L and 10^6 L were performed at 10^{-5} and 10^{-3} torr, respectively. For excitation of the

oxygen a standard nude ionization gauge was switched on during exposure and operated at 0.4 mA emission current. While the gauge was not in line of sight of the samples, at the higher pressures, excited species could reach the sample by a series of collisions with only other gas molecules.

The position of the Fermi energy of the sample was obtained by measuring the high energy cut-off (Fermi level) of the energy distribution of electrons from a Au sample in contact with the (Hg,Cd)Te samples (12). The Au sample was a freshly prepared film evaporated in situ onto a stainless steel substrate.

The cleavable samples were p-type bars of x = 0.2 and 0.31 material grown by solid state recrystallization at the Santa Barbara Research Center. Because of their large extent, 6 × 6 × 10 mm, these samples were not annealed after growth. CdTe samples were obtained from II-VI Compounds, Inc.

The sputter profiling measurements were performed on 500 and 1000 Å thick anodic oxides grown on wafers of x = 0.2 and 0.3 material. Anodization was performed in a solution of 0.1 N KOH and glycerine with a platinum counter electrode. A separate commercial UHV system (Varian) was used for the sputter-Auger measurements. For this system, a number of samples could be loaded simultaneously and analyzed in sequence. This system was not baked and had a background pressure of 1×10^{-9} torr. Sputtering was performed with a beam of 1 keV Ne^+ ions. The ions were produced and accelerated in an ion gun after the chamber had been back filled with Ne gas to a pressure of 5×10^{-5} torr. Pumping of active gases with a Ti-getter pump and a liquid nitrogen cooled cryoshield kept the residual gas pressure below 10^{-8} torr during sputtering. The Auger transitions were excited by a 5 keV electron beam from an electron gun coaxial with the axis of the analyzer, which in this case was a single stage cylindrical mirror analyzer. The 1 μA beam was incident at 30° to the sample normal and scanned over a 0.04 mm^2 area. Spectra were recorded in the dN/dE mode; a multiplexer with several channels registered the peak-to-peak heights for the various Auger lines.

Experimental Results

The effect of exposure of a $Hg_{0.7}Cd_{0.3}Te$ (110) surface to molecular oxygen (8) is illustrated in Figure 1 (b), the dashed curve. By comparison with the spectrum of the clean surface (a), which is also shown as the dotted curve in (b), it is seen that the present exposure, 4×10^{13} L does not lead to any changes in the intensities of the Hg 5d and Cd 4d core lines or of the valence band emission (8). The upper spectrum (c) in Figure 1 was recorded after a 4.2×10^8 L exposure in the presence of the activated ion

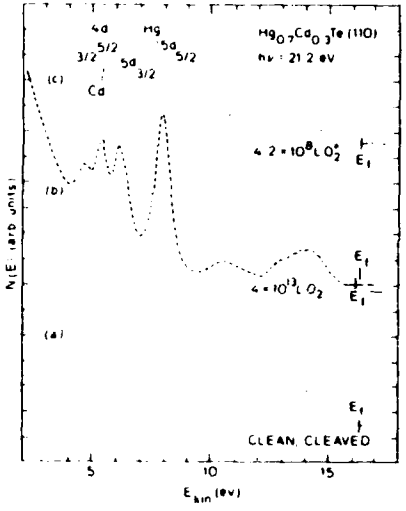

Fig. 1. Photoemission spectra of (p-type) $Hg_{0.7}Cd_{0.3}Te$ (110) at hυ = 21.2 eV (HeI). (a) Cleaved, (b) after 4×10^{13} L of molecular O_2, dashed curve. The dotted spectrum is the same as in (a) but displaced slightly for clarity. (c) Recorded after 4.2×10^8 L of excited oxygen. All spectra have been normalized to the height of the Cd $4d_{5/2}$ in (a). The valence band emission occurs from 16 to 9 eV kinetic energy. The assignment of the other lines in the spectrum is indicated in the figure.

gauge. The heights of the Cd $4d_{5/2}$ peaks above the baseline have been normalized in all three cases; we therefore see that, in the case of excited oxygen, the intensity of the Hg 5d lines is significantly reduced relative to the Cd emission. Because of the overlap of the Cd $4d_{5/2}$ and Hg $5d_{3/2}$ peaks, the reduction in Hg core line intensity produces a change in the appearance of the Cd lines as well. Features in the valence band emission at 12 eV in Figure 1 (c) also indicate the presence of bound oxygen (8). Using XPS, the relative concentrations of all elements in the sample can be measured. In Table I, we list the relative concentrations, as deduced from known photoionization cross sections (13) and electron escape depths (14) and analyzer characteristics for the ground state and excited oxygen exposures shown in Figure 1, plus an intermediate exposure to escited oxygen. Because no change was detected in the UPS spectra between the clean surface and the surface exposed to 4×10^{13} L ground state oxygen, the concentrations in the latter case are taken to represent

Table I. Relative Concentrations* of $Hg_{0.7}Cd_{0.3}Te$ Surface During Oxygen Exposure, from XPS

Core line	$4x10^{13}$ L O_2	$3x10^{6}$ L O_2**	$4.2x10^{8}$ L O_2**
Hg $5d_{5/2}$	0.63	0.55	0.53
Cd $4d_{5/2}$	0.35	0.38	0.41
Te $4d_{5/2}$	1.00	1.00	1.00†

*Cation concentrations are relative to the Te signal and have not been prorated to total 100%.

**Oxygen exposure performed with the operating ionization gauge as an excitation source.

†Sum of oxidized and unoxidized components.

the clean surface as well. The XPS data confirm the loss of Hg observed in the UPS spectra and indicate an increase in the Cd concentration. The XPS measurement samples 20 to 30 Å below the surface, whereas the spectra in Figure 1 are more surface sensitive (13).

In a separate experiment, oxidation was studied with the surface sensitivity afforded by synchrotron radiation. Looking at the Hg 5d, Cd 4d, and Te 4d core lines at photon energies around 110 eV permits the highest possible degree of surface sensitivity with electron escape depths for these lines below 10 Å. In Figure 2, we show the results of exposure of a $Hg_{0.8}Cd_{0.2}Te$ (110) surface to 10^4 and 10^6 L of O_2 with the ion gauge on. The exposure conditions deviate from the experiment shown in Figure 1. The main difference is in ion gauge filament current (0.4 mA in this case versus 9 mA in the previous 10^6 L exposure), but

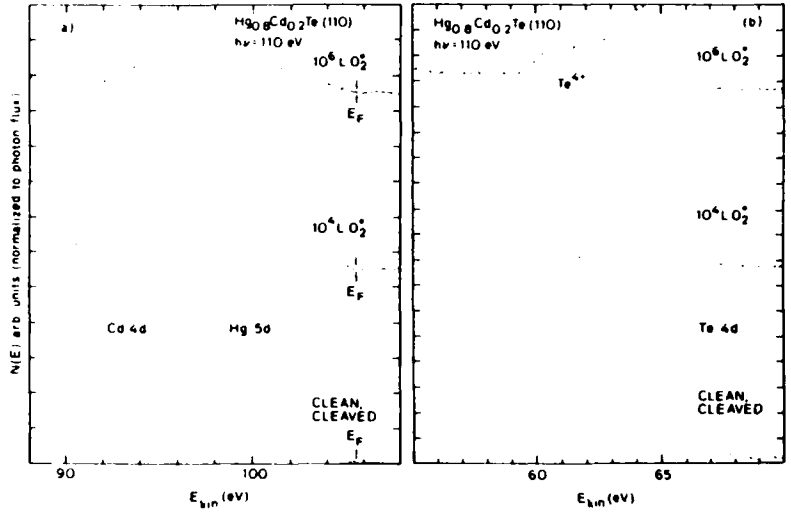

Fig. 2. a. Photoemission spectra of (p-type) $Hg_{0.8}Cd_{0.2}Te$ (110) at hν = 110 eV. (a) Cleaved, (b) after 10^4 L of excited O_2, (c) after 10^6 L of excited O_2. Emission from the valence band, Hg 5d and Cd 4d core levels. The spectra are normalized to the photon flux. b. Te 4d core lines for surfaces as in a. Note Te^{4+}

pressures and exposure times were also different. Thus, the rate of production of excited oxygen is probably different in the two experiments. At 10^4 L, a 0.1 eV shift of positions of all peaks toward lower binding energies (higher kinetic energies) is observed, indicating a change in band bending. For the higher exposure, 10^6 L, the Hg 5d emission decreases relative to the Te emission (Table II) and an oxygen induced structure appears in the valence band region, as seen in Fig. 2a around 101 eV kinetic energy or at 4 eV below the valence band edge. At the 10^6 L, the Te lines are strongly affected with various oxidation states present including Te^{4+}, as evidenced by its chemical shift of 3.5 eV (15). For this exposure, the Cd signal again appears to increase relative to the Te concentration (Table II), as observed previously (8).

Table II. Relative Core Line Intensities* at $h\nu$ = 110 eV, Excited Oxygen Exposures

	Core line(s)	Clean	10^4 L O_2**	10^6 L O_2**
CdTe	Te	1.0	1.0	1.0
	Cd	0.17	0.17	0.18
$Hg_{0.8}Cd_{0.2}Te$	Te	1.0	1.0	1.0
	Cd	0.030	0.030	0.034
	Hg	0.16	0.16	0.064

*Te intensity is integral of all Te components. Cd and Hg values are sum of spin-orbit split components determined by visually fitting Lorenzian lines with Gaussian broadening to the measured curve.

**Oxygen exposures in presence of operating ionization guage.

A sample of CdTe was also studied, as shown in Figure 3. In this case, oxidized Te (Te^{4+}) is again apparent. For the 10^6 L exposure, the O 2p emission is again seen in the valence band region near 101 eV, and a weaker oxygen peak is evident about 2.5 eV lower; the lower feature may be obscured in the case of the alloy by the Hg 5d emission. While the Cd emission is reduced after the 10^6 L exposure, so is that of Te; the relative Cd concentration thus remains the same (Table II). The shifts in position observed at 10^6 L for both the Cd 4d and unoxidized Te 4d core lines are in the direction of lower binding energies with respect to the position of the Fermi level at the surface with similar shifts of about 0.4 eV. Such uniform shifts are due to a change in band bending at the surface with the Fermi level now 0.4 eV closer to the valence band maximum. We associate this with defect levels formed in the CdTe surface region (16).

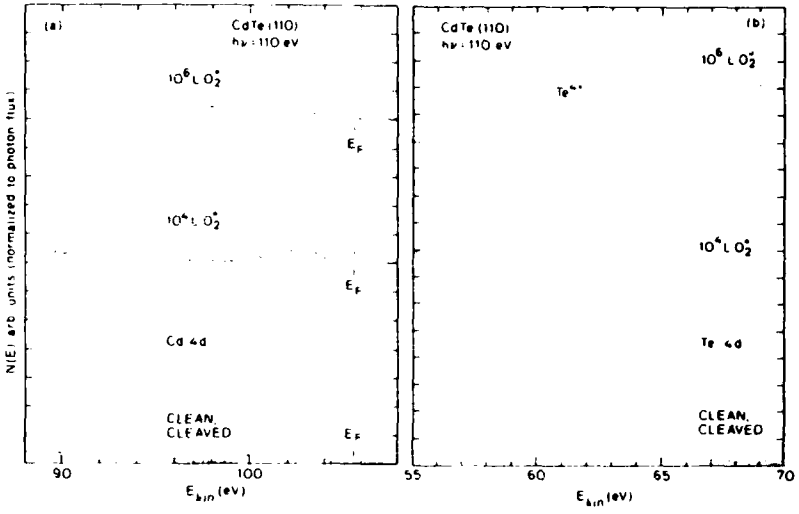

Fig. 3. a. Photoemission spectra of (n-type) CdTe (110) at $h\nu$ = 110 eV. (a) Cleaved, (b) after 10^4 L of excited O_2, (c) after 10^6 L of excited O_2. Emission from the valence band and Cd 4d core levels. Normalized to photon flux. b. Te 4d core lines for surfaces as in a. Note Te^{4+}.

The oxidation experiments for both x = 0.31 and x=0.2 material both demonstrate that Hg is lost during the exposure to excited oxygen. From the present results, the first steps in the oxidation process are seen as a change in band bending. The later stages of oxidation further lead to oxidation of Te.

Auger Electron Spectroscopy (AES) was used to obtain the depth profile of anodic oxides. While effects of the electron beam on composition have been reported (10,17) we observe the Auger peak-to-peak heights to be constant in time, indicating electron beam damage did not occur. The beam current used (10) or the surface preparation (17) may contribute to the difference in stability observed; additional study is required, however, to determine accurately the factors which promote electron beam damage.

In Figure 4 we present data from a sputter profiling experiment with an anodic oxide sample. The concentration profiles of the various elements show some variation near the surface of the oxide and near the oxide-semiconductor

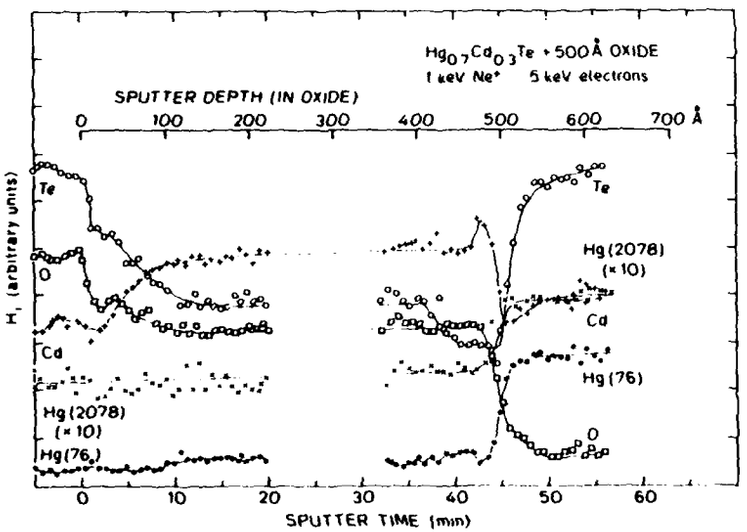

Fig. 4. Sputter profile of a 500 Å anodic oxide film on $Hg_{0.7}Cd_{0.3}Te$.

interface. Such variations are caused primarily by real changes of concentration but are probably somewhat aggravated due to effects of preferential sputtering and ion knock-on (18). More work is required to quantify the extent of these effects on the profiles. Since the profiles flatten in the oxide, it is reasonable to assume that the bulk oxide is homogeneous. During the interrupted part of the profiles in the oxide, high resolution Auger spectra were recorded of all the transitions used in the analysis. After profiling past the interface, another set of high resolution spectra were recorded. From these spectra, the composition of the oxide and the substrate past the interface were derived by means of reference spectra and appropriate corrections for analyzer transmission and electron escape depth (19). The oxide on both x = 0.2 and x = 0.3 samples was found to be 52% O, 19% Te, 25% Cd, and 4% Hg. While a depletion of Hg in the substrate beyond the interface was reported previously (20), comparison of recent profiles to carefully prepared standards as well as extensive sputtering past the interface indicates the anodized samples are not Hg deficient as a result of anodization.

Discussion

The experimental evidence presented here shows that excited oxygen interacts with (Hg,Cd)Te surfaces in a complicated manner. The measurements of Figures 1 and 2 indicate that Hg is released from the surface in the process and not retained in the oxide. The data collected in Table I for the experiments shown in Figure 1 indicate that the amount of Hg lost might be partially compensated for by an increase of the Cd concentration. The more surface sensitive results (Table II) obtained with synchrotron radiation indicate similar behavior. The Te 4d core line spectra recorded at 110 eV show a component shifted by 3.5 eV for both CdTe and (Hg,Cd)Te. The chemically shifted line is consistent with the formation of TeO_2 or $CdTeO_3$ (3,4). For the two sets of experiments shown in Figures 1-3, the amount of oxygen picked up for similar exposures (10^6 L) are not the same due to a difference in the exposure conditions, as explained earlier.

Solzbach and Richter have studied the oxidation of sputter cleaned surfaces of $Hg_{0.8}Cd_{0.2}Te$ with XPS (3). Even such surfaces were found to be inert to molecular oxygen. For ex-

cited oxygen (ozone) they observed oxidation of Te and suggest an oxide of TeO_2 and $CdTeO_3$; they did not detect the presence of any Hg in the oxide. These surfaces were depleted of Hg from the outset due to the effects of the sputter cleaning of the surfaces prior to oxidation. The present results of XPS and UPS studies of the oxidation give clear evidence that Hg is released upon oxidation.

Our present profiling results agree with those of the previous investigations (2-4,10) in that there is only a small percentage of Hg in the oxide. Difficulties in applying the sputter/AES technique remain and must be resolved to make the profiling process more quantitative. Preferential sputtering of Hg observed in (Hg,Cd)Te (3,17), for example, makes the calculation of the Hg content strongly dependent on the electron escape depth characteristic of the transition used due to the inhomogeneous distribution with depth of the Hg.

A Hg depletion in the substrate resulting from anodic oxidation was earlier reported by Sun et al (4) using sputter profiling/XPS. For the samples studied we find no depletion in the substrate. Differences in the details of the anodic process may account for the difference in the two results. The present results indicate rather sharp interfaces (~50 Å) at both 500 and 1000 Å thicknesses (Figure 4).

Conclusion

The present experiments demonstrate that excited oxygen interacts with (Hg,Cd)Te surfaces causing the release of Hg and the oxidation of Te. From experiments with thick anodic oxides we find that loss of Hg from the substrate below the oxide does not take place for the anodization process used, but that little Hg is retained in the oxide.

Acknowledgments

This project is supported by DARPA, contract no. MDA 903-80-C-0496. One of the authors (PM) acknowledges support from the Danish Natural Research Council. He is grateful to Stanford University for support and hospitality. Part of this work was carried out at the Stanford Synchrotron Radiation Laboratory, which is supported by the National Science Foundation through the Division of Materials Research in cooperation with the Department of Energy.

References

1. J. D. Langan, Ph.D. dissertation, University of California, Santa Barbara (1979).

2. S. P. Kowalczyk and J. T. Cheung, J. Vac. Sci. Tech. 18, 944 (1981).

3. U. Solzbach and H. J. Richter, Surf. Sci. 97, 191 (1980).

4. G. Davis, T. S. Sun, S. P. Buchner, and N. E. Byer, J. Vac. Sci. Tech. 19, 472 (1981).

5. B. K. Janousek, J. J. Daugherty, and R. B. Schoolar, paper presented at the SPIE meeting, Washington, April 1981.

6. Y. Nemirovsky and J. Kidron, Solid State Electr. 22, 831 (1979); Y. Nemirovsky and E. Finkman, J. Electrochem. Soc. 126, 768 (1979).

7. W. E. Spicer, Bulk and Surface Ultraviolet Photoemission Spectroscopy, in Optical Properties of Solids, ed. by B. O. Seraphin (North Holland Publ., Amsterdam, 1976).

8. P. Morgen, J. Silberman, I. Lindau, W. E. Spicer, and J. A. Wilson, J. Cryst. Growth 56, 493 (1982).

9. J. A. Silberman, P. Morgen, I. Lindau, W. E. Spicer, and J. A. Wilson, presented at the U.S. Workshop on the Physics and Chemistry of HgCdTe, Minneapolis, Mn, Oct. 28-30, 1981.

10. T. S. Sun, S. P. Buchner, and N. E. Byer, J. Vac. Sci. Tech. 17, 1067 (1980).

11. K. Y. Yu, Ph.D. dissertation, Stanford University (1976); J. N. Miller, Ph.D. dissertation, Stanford University (1979).

12. P. Pianetta, I. Lindau, C. M. Garner, and W. E. Spicer, Phys. Rev. B17, 2792 (1978).

13. J. H. Scofield, University of California Radiation Laboratory Report (1973).

14. For CdTe: J. Szajman, R. C. G. Leckey, J. Liesegang, and J. G. Jenkin, J. electr. Spectrosc. Rel. Phen. 20, 323 (1980); I. Lindau and W. E. Spicer, J. Electr. Spectrosc. Rel. Phen. 3, 409 (1974), and references therein.

15. R. G. Musket, Surf. Sci. 74, 437 (1978).

16. W. E. Spicer, J. A. Silberman, P. Morgen, and I. Lindau, presented at the U.S. Workshop on the Physics and Chemistry of HgCdTe, Minneapolis, Mn., Oct. 28-30, 1981; W. E. Spicer, I. Lindau, P. Skeath, and C. Y. Su, J. Vac. Sci. Tech. 17, 1019 (1980).

17. H. M. Nitz, O. Ganschow, V. Kaiser, L. Wiedmann, and A. Benninghoven, Surf. Sci. 104, 365 (1981).

18. See, e.g., H. F. Winters and J. W. Coburn, Appl. Phys. Lett. 28, 176 (1976).

19. L. E. Davis, N. C. McDonald, P. W. Palmberg, G. E. Riach, and R. E. Weber, Handbook of Auger Electron Spectroscopy, published by Physical Electronics Industries, Inc. (1972).

20. Results reported at the Electronic Materials Conference, Santa Barbara, Ca., June 24-26, 1981.

2.3

Surface and interfaces of HgCdTe. What can we learn from 3-5's? What is unique with HgCdTe?

W. E. Spicer,[a] J. A. Silberman,[b] P. Morgen,[c] and I. Lindau

Department of Electrical Engineering, Stanford University, Stanford, California 94305

J. A. Wilson

Santa Barbara Research Center, Goleta, California 93017

(Received 18 December 1981; accepted 12 February 1982)

Fundamental studies of the surfaces and interfaces of HgCdTe are in their infancy. Major developments have been made in the understanding of the free surfaces of closely related 3-5 compound semiconductors and, making use of this knowledge, on the mechanism of formation of Schottky barriers and MOS (or MIS) interface states on the 3-5 materials. Thus, the 3-5 work provides an important starting point for the HgCdTe work. For 3-5's, a unified defect model has been developed which explains both the Schottky barrier formation and the source of the MOS interface states. This work is briefly reviewed and related to HgCdTe surface and interface phenomena. Based on this and a wide range of practical work plus the early results of fundamental work on HgCdTe it is clear that defects also play an important role at HgCdTe interfaces. However, in all previous work it has appeared that the interface may not be so strongly coupled to defects in the bulk (i.e. to defects, dislocations, etc. in the bulk); this does not appear to be the case for HgCdTe where the "intercommunication" between the surface and bulk makes it essential to treat the surface in the context of bulk interactions and imperfections.

PACS numbers: 73.20.Cw, 73.20.Hb, 73.30. + y, 73.40.Lq

I. THE FREE SURFACES OF COMPOUND SEMICONDUCTORS

A. Introduction

Strong fundamental studies of the surface and interfaces of $Hg_{1-x}Cd_xTe$ have just been started. Early reports of such work appear in these Proceedings. These represent the continuation of a revolution that has occurred in our understanding of the electronic structure of semiconductors in general and the 3-5 compound semiconductors in particular during recent years. The work on the 3-5's provides an invaluable framework for consideration of $Hg_{1-x}Cd_xTe$. Thus, it will be our objective in this paper to provide that framework and, as much as possible, to relate it to $Hg_{1-x}Cd_xTe$. Since all of our present knowledge indicates that the surfaces of the 2-6's are similar to those of the 3-5's (provided that bandgaps are similar), we will concentrate on the 3-5's. Note that GaAs and CdTe have almost identical bandgaps.

In less than a decade, monumental breakthroughs have been made in the understanding of both the free surfaces of compound semiconductors (principally 3-5's) and of the mechanism of formation of: 1) Schottky barriers and 2) oxide-semiconductor interface states.[1] Preceding this work by a few years was the first direct observation (by photoemission spectroscopy, PS) of the filled surface states on Si.[2]

Experimental work preceding[3] and following[4] the Si work established a very surprising result—that there were no surface states in the bandgap of GaAs (except for those due to structural defects at or near the surface). As we will describe in the following paragraphs, the intrinsic surface states (i.e., those associated with the "broken bonds" of an otherwise perfect surface) are moved out of the bandgap region by the rearrangement of the surface atoms. Recent work by Duke, *et al.*,[5] shows that the rearrangement on CdTe is essentially identical to that of GaAs. As we will show, new results from Silberman *et al.*[6] establish that the intrinsic surface states are swept out of the bandgap of that material. Thus, it is important that we understand the mechanism going on at the surface of GaAs and other 3-5's in order to gain insight into the surfaces of HgCdTe.

Fortunately, the theory of surface electronic structure[7] has kept well abreast of the advance in experiment. Methods have been developed which can calculate the electronic structure taking into account the rearrangement of the surface atoms. Thus a powerful self-consistent approach has been developed for determining the electronic and lattice structure of solids. The electronic structure can be determined experimentally. Through LEED measurements and their analysis, surface lattice structure determination can be made. Using the surface lattice parameters, surface electronic structure calculations can be made[8] and compared to very detailed experimental[9] results on the surface electronic structure. (Calculations can be made a function of surface lattice parameters to check the sensitivity of these parameters.) The agreement between experimental electronic structure and theory is strikingly good. Thus, one gains confidence in our ability to determine surface electronic and lattice structure.

B. GaAs (110): A detailed example

In the above we have attempted to give some overall background. In this section, we will get much more specific concerning the compound semiconductor surface which is best

 0022-5355/82/050149-05$01.00

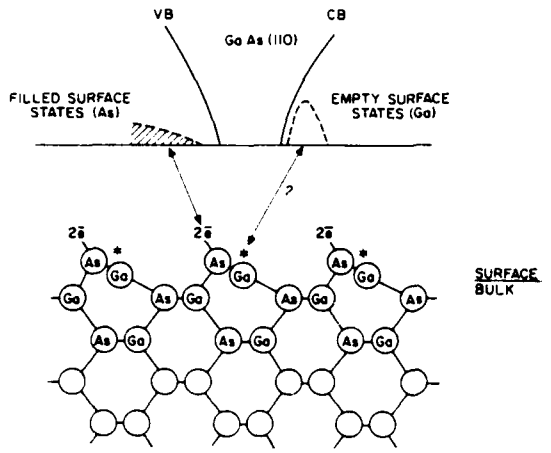

FIG. 1. A schematic drawing of the lattice and electronic structure of the GaAs (110) face after rearrangement (relaxation). The As surface atoms have taken up a p^3 bonding arrangement (with two electrons in a $4s^2$ filled state), while the Ga has gone from the bulk sp^3 to a sp^2 arrangement. Since the p^3 bond angles are more acute than the bulk sp^3 bonds, the As moves outward; conversely, the Ga moves inward. The movements are large (large fractions of an angstrom). This rearrangement moves the filled and empty surface states out of the bandgap. However, since the surface lattice is no longer lattice matched to the bulk, there is strong strain at the surface (*marks the location of empty surface state).

understood—the GaAs (110).[10] These results seem to be typical of all faces of the 3-5's and of the smaller bandgap 2-6's such as CdTe and $Hg_xCd_{1-x}Te$. The one exception is GaP, where due to its large bandgap, the empty surface states are not moved entirely out of the bandgap.[10] In Fig. 1, we summarize these GaAs (110) results by schematically showing both the atomic and electronic rearrangement. A fact of prime importance is the realization that rearrangements of atoms, electrons, and electronic states are inextricability interwoven. (Perhaps the most comfortable and familiar bulk analogy is the Jahn-Teller effect.) On the surface of GaAs and most 3-5's the atoms and electrons rearrange themselves so that the filled surface states move to lower energy below the valence band maximum (VBM) and the empty states to higher energy above the conduction band minimum (CBM). Because the column 3 and 5 elements can dehybridize toward their atomic configuration with 3 and 5 valence electrons, respectively, the electronic rearrangements for the 3-5's can take place much more ideally than for Si. Thus, the surface states are swept completely out of the bandgap. Ga with three valence electrons moves toward a sp^2 (graphite-like) bonding scheme with its three neighbors. In contrast, the As surface atom goes toward a p^3 bonding configuration with the two remaining valence electrons in a s^2 filled nonbonding orbital. The p^3 bond angle is more acute than the bulk sp^3 covalent bond, thus moving the As atom outward. In contrast, the sp^2 Ga bond is almost planar pulling the Ga inward[11,12] (see Fig. 1). Note that there are no "dangling" bonds in the classical sense. The As "s^2" electrons are available for bonding; however, if the "s^2" arrangement is thus changed the surface will rearrange at this point, inducing additional strain.[12]

In the past a very elementary picture of the interrelation of intrinsic surface and bulk states has been popular. The bulk electronic and lattice structure was thought to extend right up to the vacuum-semiconductor interface and then surface electronic states were added in the bandgap at the surface. The inadequacies of this are now apparent. The lattice structure generally changes as we move to the surface. It is unlikely that these changes are completely restricted to the last layer of the semiconductor.[11] The large atomic rearrangements must lead to large changes in the electronic structure associated with the surface. Thus, our older models (and even that of Fig. 1 insofar as it is interpreted in those terms) must be abandoned and we must think in terms of a lattice and thus electronic structure which are unique to the surface region. This is reflected in recent theoretical work which calculates the local density of states layer by layer as one moves from the surface into the bulk.[7]

The rearranged surface atoms are not lattice matched to the bulk crystal. This results in distortion of the bulk lattice for at least one additional layer of atoms beneath the surface. Because of lattice mismatch, a large stress field can be expected in the outmost surface layers. The difference in crystal structure within the surface unit cell should produce a surface lattice vibrational structure different from the bulk. This will be important in explaining the interaction of adsorbates on the surface.

A key concept which has been brought into focus by the removal of surface states from the bandgap region (Fig. 1) is the distinction between intrinsic and extrinsic surface states. Intrinsic refers to the states characteristic of the perfect (albeit rearranged) surface. In contrast, the extrinsic states are those due to defects, either structural or impurity-related, at or near the surface. The extrinsic bulk states are of such importance because they dominate the electrical and thus the practical applications of semiconductors.

Although we have concentrated on the discussion of the GaAs (110) face, it should be emphasized that studies of the other principle surfaces of GaAs—the (100) and (111)—give similar results, i.e., the intrinsic surface states are removed from the semiconductor bandgap.[1]

C. Clean cleaved CdTe and $Hg_{1-x}Cd_xTe$ (110) faces

It is now useful to present PS data from CdTe. This is done in Fig. 2. The results are identical to those from GaAs in that there is no evidence for surfaces states in the bandgap. Thus, it appears that it is similar to GaAs in that the intrinsic surface states have been moved out of the bandgap by surface reconstruction. This is not unexpected since the surface lattice reconstruction for the CdTe (110) is so similar to that for GaAs (110).[5] Based on the 3-5 results one would expect the same result for other CdTe crystal faces and for all crystal faces of the HgCdTe crystals. Although much more work must be done before this is definitively established, the HgCdTe work done to date (see, e.g., Silberman *et al.* in these Proceedings) indicates this to be the case. It is very important to recognize that, just as for GaAs, the reconstructed HgCdTe surfaces are expected to be strongly stressed. Because of the possible weakness of the Hg-Te bond this may be of particular importance.

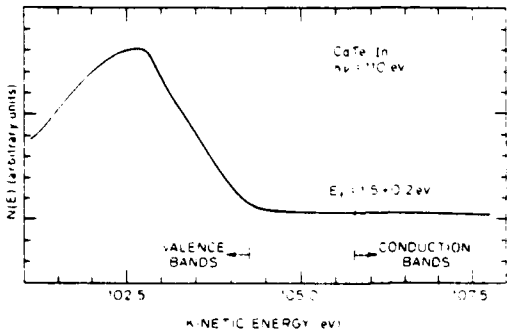

FIG. 2. Upper 3 eV of CdTe valence band emission at 110 eV photon energy and location at the Fermi level. As is the case for GaAs and in contrast to that of Si (see Ref. 2), emission from filled surface states in the bandgap is not observed. It is likely that, as in the 3-5's, surface lattice rearrangement has swept the surface states out of the gap. The CdTe sample was indium doped in-type at a level greater than $10^{17}/cm^3$

However, rather than going directly into a discussion of the problems of $Hg_{1-x}Cd_xTe$ device interfaces, we should once again build a foundation making use of the fundamental understanding which has been achieved on the formation of Schottky barriers and the semiconductor-oxide interface states by studying the 3-5's.[1]

II. 3-5 INTERFACES: KEY ROLE OF DEFECTS

Until recently, the approach to understanding Schottky barriers was to assume an ideal planar junction between the semiconductor and metal. The interaction between the metal and semiconductor was then considered within the framework of that configuration and in order to attempt to understand the mechanism of Schottky barrier formation. However, new experimental techniques have been developed in recent years which have allowed the formation of the Schottky barrier to be examined on an atomic basis. Synchrotron radiation sources[13] such as that at the Stanford Synchrotron Radiation Laboratory (SSRL) provide a continuous source of radiation extending from the visible to the hard x-ray region ($6 \lesssim h\nu \lesssim 10^4$eV). Monochromators are used to proved tunable monochromatic sources of radiation for PS and other types of experiments.[11] Using this source and PS for $10 \lesssim h\nu \lesssim 300$eV, the electronic structure—particularly the surface position of the Fermi level—could be followed as various metals (or oxygen) were deposited on the surface.[1] In addition, the chemistry and spatial location of the semiconductor atoms could be followed by studying the intensity and positions of the core levels[1] (e.g., the Ga and As 3d levels).

Of extreme importance to this work is the ability to restrict the depth of material studied to the last one or two atomic layers; thus, it is truly a surface sensitive technique. This is helped by the use of synchrotron radiation.[1] Again, it is very important that the foreign atoms be placed on the surface in very small quantities. Thus, the changes in surface electronic structure, chemistry, and "intermingling" of atoms can be followed as foreign atoms are added almost in an "atom by atom" way. (We are beginning to apply these techniques to $Hg_{1-x}Cd_xTe$. Some results will be reported in these Proceedings[6] but we expect much more progress in the coming year.) Thus, for the first time, Schottky barrier and 3-5:oxide formation was followed on a microscopic basis (e.g., PS) rather than the macroscopic basis (e.g., using I-V or C-V measurements) used previously.

The results of the application of such techniques to the 3-5's are now well documented in the literature. They forced a complete reevaluation of the concepts of the interfaces involved in these systems and the mechanism of Schottky barrier formation. The key results[1] are as follows:

1) The interface cannot be considered ideal with an abrupt transition between the semiconductor and metal—considerable intermixing takes place between the semiconductor and metal in Schottky barrier formation.

2) The Schottky barrier height is determined by defect states induced in the semiconductor at or near the surface by the deposition of the metal.

3) The same defects were formed on deposition of oxygen—forming the semiconductor-oxide interface states—as were formed at the metal-semiconductor interface.

4) As a result of 3) and 4), a Unified Model has been developed[1] explaining both Schottky barrier and 3-5 oxide interface states based on the defect formation.

As an illustration of these results, we present, in Fig. 3, the defect levels which were found to control the interface characteristics (Schottky, MOS, or MIS) of n- and p-type GaAs, InP, and GaSb.[1] The accuracy of energy location is ± 0.1 eV.

One of the key considerations in this work was to make sure that these results correlated in a reasonable way with the results on actual device Schottky barrier and MOS or MIS structures. Such data is available for GaAs and InP. For example, GaAs barrier heights correspond to Fermi level pinning near midgap so that, for example, the barrier height is near midgap for metals on n-type GaAs as would be

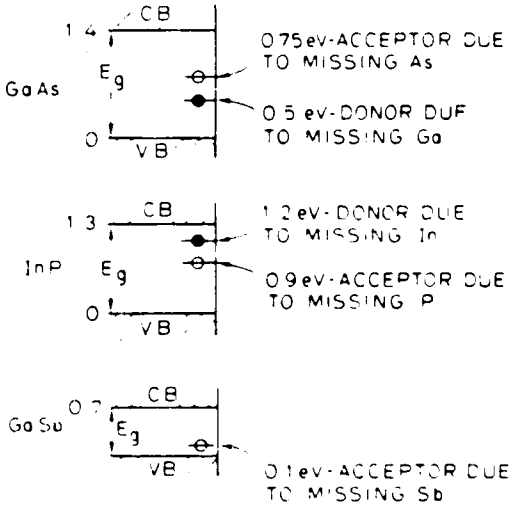

FIG. 3. Unified model for interface states and Schottky barriers. The defect energy levels induced by overlayers on GaAs, InP, and GaSb. The position in energy and donor or acceptor nature of the defect is shown as well as a suggestion as to the missing atom responsible for the defect.

expected from Fig. 3. For n-type InP, the Schottky barrier height is either about 0.1 or 0.4 eV depending on the surface treatment of the InP and/or the metal.[14] This is again in agreement with the results of Fig. 3. For MOS or MIS structures, agreement is again obtained.[14] (It should be recognized that, for all MIS structures formed to date, there is a thin oxide layer between the semiconductor and insulator.)

III. INTERFACES OF HgCdTe

A. Introduction

To place this section in perspective, it should be noted that until recently attempts to passivate 3-5 surface were completely dominated by an empirical approach. This proved both extremely expensive and unsuccessful in so far as producing, for example, GaAs MOS's. The fundamental understanding recently obtained is visibly helping to guide development of practical device structures in a more economic and profitable way.[1,14]

Processes to passivate HgCdTe also have been developed empirically. Notable successes have been attained in photoconductive and other devices. However, more advanced device structures will be more demanding and there is a clear need for more fundamental understanding. We will always have to include empirical methods in our practical techniques. But would not we be well advised to learn as much as possible about the basic phenomena taking place and use this knowledge as much as possible to guide us in the right paths and reduce the costs of purely empirical approaches?

The fundamental 3-5 results mentioned above leading to the Unified Defect Model involved many years of work extending over more than a decade. They have been emphasized in the hope that we all can draw on them in attempting to understand and conquer the HgCdTe interface problems in the most timely and economical manner possible. If we draw on the knowledge gained in the 3-5 studies, this process can be strongly accelerated. If it does not prove to be applicable, then our task will be much more difficult.

The indications to date suggest that there are strong similarities between the 3-5's and $Hg_{1-x}Cd_xTe$ and that defect levels quite possibly dominate the interface between HgCdTe and the passivating overlayers. However, we would be ill advised to simply try to carry over the 3-5 experience in total to the HgCdTe system. Rather, we must identify the similarities and differences between these two material systems and then carefully attempt to choose the most profitable experiments to understand the HgCdTe interface system. Let us next briefly examine some of the similarities and differences between HgCdTe and the 3-5's.

B. Differences between 3-5 and HgCdTe surfaces and interfaces

The most striking difference between the 3-5's and HgCdTe is the relative instability of Hg in the HgCdTe lattice. The Hg-Te bond energy is at least 30% less than the Cd-Te bond energy. No such large differences in bond energies exist for the 3-5's.

Although the difference in Hg and Cd bond energies is a bulk property, it is also critical to the understanding of surfaces and interfaces for two reasons: 1) It will be reflected by a difference in the Hg and Cd bonding at the surface (and, thus, in the interface chemistry), and 2) in the production of defects (e.g., Hg defects, vacancies, and interstitials, and dislocations along which the interstitials may move easily to the surface) not only in the surface regions but also in the bulk where they may migrate easily to the surface. Thus, we cannot restrict our interest to the surface region, as has been the case with the 3-5's. We must also understand the critical features of bulk lattice bonding, its effect on bulk defect production, and the transportation of certain of these defects to the surface. Rather surprising and most encouraging, the work reported in these Proceedings by Silberman *et al.*[6] and by Chen and Sher[15] show that this bonding difference is reflected in the band structure and the energy of the core levels (as detected by PS). Thus, we have new and powerful tools to study the bonding. Most interestingly, it appears that 1) the bond difference is due to the ionization energy of the valence (s^2) electron levels of Hg being 1.5 eV larger than the ionization energy of the corresponding valence levels (also s^2) of Cd (this can be understood in terms of the larger positive nuclear charge of Hg as compared to Cd), and 2) this difference is also reflected in the change of band structure near the bandgap with increasing Hg content. In fact, it appears possible that this difference in bond energy is a *necessary condition* for any semiconductor system whose bandgap drops from a large value to zero as the composition is changed. Therefore, it is likely that the difficulties associated with the bond difference cannot simply be eliminated by going to a new alloy system.

The importance of the bonding of Hg in the HgCdTe lattice is illustrated by early work using the new tools of surface science to study the rate of Hg loss from clean HgCdTe surfaces in ultrahigh vacuum. Nitz *et al.*[16] found massive loss of Hg from scraped surfaces with depletion of Hg up to microns in depth after many hours in vacuum. However, Silberman *et al.*,[6,17] using cleaved surfaces, found negligible loss of Hg under comparable time and pressure conditions, as did Faurie *et al.*,[18] using n-type HgCdTe formed by MBE. Nitz *et al.*[16] also found large diffusion coefficients for Hg and Cd at room temperature (10^{-13} cm^2/sec). We would like to suggest (although it remains to be definitively proven) that the Hg loss and large diffusion coefficients of Nitz *et al.*[16] reflect the effect of imperfections (for example, dislocations) extending from the surface far beneath it. This is important because it suggests that bulk defects which extend up to the surface can have first-order effects on HgCdTe surfaces and interfaces—an effect which has not appeared in the 3-5's. It also emphasizes the need to understand the "bulk" as well as the surface in HgCdTe.

In the 3-5's, an important consideration is that both theory and experiment indicate that the defect levels disappear into the conduction (acceptor levels) or valence (donors) bands as the band gap decreases.[19,20] However, it is generally believed that excess Hg creates n-type HgCdTe whereas a deficit of Hg produces p-type material for all alloy compositions of the semiconductor. This suggests that defect levels associated with the surface may not disappear into the valence or conduction band with decreasing bandgap as in the

case of the 3-5's.

Another difference between the 3-5's and HgCdTe is their reactivity with O_2 in the ground state.[21] Such oxygen has a very small sticking coefficient on the GaAs cleavage (110) surface (about 10^{-9});[21] however, it is so small that it cannot be measured on HgCdTe (less than about 10^{-13}).[6,17] However, if the GaAs is exposed to oxygen excited by an ion gauge (located in a remote position so as to decrease the probability of oxygen atoms or ions striking the GaAs surface), the sticking probability can be increased by orders of magnitude and a very complex chemistry takes place at the GaAs surface.[21] If excited oxygen is used in the same way with HgCdTe, it appears that Hg leaves the surface and then the oxygen chemically reacts with the excess Te left behind.[6,17]

One conclusion drawn early in the fundamental studies[22] of the 3-5's was that, because of the complex oxygen chemistry, it was best not to attempt to grow a thick native oxide but to minimize the amount of native oxide and deposit an external oxide, e.g., SiO_2 as gently as possible to passify the surface. It is important to ask whether this may not also be the case for HgCdTe—at least for some demanding device structures.

IV. CONCLUSIONS

It is strongly argued that fundamental understanding of HgCdTe surfaces and interfaces can have a large return in advancing device technology. The recently gained fundamental understanding of 3-5 surfaces and interfaces form an important framework for HgCdTe work. However, certain strong differences between the 3-5's and HgCdTe must be identified and taken into account. Examples of such differences are given above. The most important single difference is that the HgCdTe interface and bulk properties cannot be treated as two separate entities as people have tried to do for the 3-5's, Si, and other semiconductors; rather, the strong effect of bulk imperfections and rapid communications of defects between bulk and surface must be properly taken into account. This is, principally, a result of the "weak" Hg–Te bond.

ACKNOWLEDGMENTS

Stimulating discussions with W. Harrison and A. Sher are gratefully acknowledged. Work supported by DARPA. Contract No. MDA 903-80-C-496. Part of the work was done at the Stanford Synchrotron Radiation Laboratory, which is supported by the NSF through the Division of Materials Research in cooperation with the Department of Energy.

[a] Stanford W. Ascherman Professor of Engineering.
[b] National Science Foundation Predoctoral Fellow
[c] On leave from Odense University, Denmark (partially supported by the Danish Natural Science Research Council)

[1] W. E. Spicer, P. Skeath, C. Y. Su, and I. Lindau, in J. Phys. Soc. Jpn **49**, Suppl. A, 1079 (1980) and references therein; W. E. Spicer, I. Lindau, P. Skeath, C. Y. Su, and P. Chye, Phys. Rev. Lett. **44**, 420 (1980).
[2] L. F. Wagner and W. E. Spicer, Phys. Rev. Lett. **28**, 1381 (1972); D. E. Eastman and W. D. Grobman, Phys. Rev. Lett. **28**, 1378 (1972).
[3] J. van Laar and J. J. Scheer, Surf. Sci. **8**, 342 (1967).
[4] W. E. Spicer, I. Lindau, P. E. Gregory, C. M. Garner, P. Pianetta, and P. W. Chye, J. Vac. Sci. Technol. **13**, 780 (1976); ibid. W. Gudat and D. E. Eastman, 831; ibid. J. van Laar and A. Huijser, 769.
[5] C. B. Duke, A. Paton, W. K. Ford, A. Kahn, and G. Scott, Phys. Rev. B **24**, 3310 (1981).
[6] J. A. Silberman, P. Morgen, I. Lindau, W. E. Spicer, and J. Wilson, J. Vac. Sci. Technol. this issue.
[7] D. J. Chadi, in J. Phys. Soc. Jpn **49**, Suppl. A, 1035; ibid. M. L. Cohen, 13 and references therein.
[8] D. J. Chadi, J. Vac. Sci. Technol. **15**, 1244 (1978).
[9] A. Huijser, J. van Laar, and T. L. van Rooy, Phys. Lett. **65A**, 337 (1978).
[10] An excellent view of these developments can be obtained from the Proceedings of the Physics of Compound Semiconductor Interfaces, published as J. Vac. Sci. Technol. **13**, (4) (1976); **14**, (4) (1977); **15**, (4) (1978); **16**, (4) (1979); and **18**, (5) (1980); in view of this, the number of individual references will be drastically limited.
[11] S. Y. Tong, A. R. Lubinsky, B. J. Mrstik, and M. A. Van Hove, Phys. Rev. B **17**, 3303 (1978); R. J. Meyer, C. B. Duke, A. Paton, E. Kahn, E. So, J. L. Jeh, and P. Mark, Phys. Rev. B **19**, 5194 (1979).
[12] J. Barton, W. Goddard, III, and T. McGill, J. Vac. Sci. Technol. **16**, 1178 (1979) and references therein.
[13] H. Winick and S. Doniach, (editors), *Synchrotron Radiation Research*, (Plenum, New York, 1980).
[14] W. E. Spicer, I. Lindau, P. Skeath, and C. Y. Su, J. Vac. Sci. Technol. **17**, 1019 (1980).
[15] An-Ban Chen and A. Sher, J. Vac. Sci. Technol. This issue.
[16] H. M. Nitz, O. Ganschow, V. Kaiser, L. Wiedmann, and A. Benninghoven, Surf. Sci. **104**, 365 (1981).
[17] P. Morgen, J. Silberman, I. Lindau, W. E. Spicer, and J. Wilson, J. Crys. Growth (in press); also see J. Vac. Sci. Technol. These Proceedings.
[18] J. P. Faurie, J. Vac. Sci. Technol. this issue.
[19] H. H. Wieder, Appl. Phys. Lett. **38**, 170 (1981).
[20] M. S. Daw and D. L. Smith, Appl. Phys. Lett. **36**, 690 (1980).
[21] P. Pianetta, I. Lindau, C. M. Garner, and W. E. Spicer, Phys. Rev. **18**, 2792 (1978).
[22] W. E. Spicer, P. Pianetta, I. Lindau, and P. W. Chye, J. Vac. Sci. Technol. **14**, 885 (1978).

2.4

UPS study of the electronic structure of $Hg_{1-x}Cd_xTe$: Breakdown of the virtual crystal approximation

J. A. Silberman,[a] P. Morgen,[b] I. Lindau, and W. E. Spicer[c]

Stanford Electronics Laboratory, Stanford University, Stanford, California 94305

J. A. Wilson

Santa Barbara Research Center, Goleta, California 93017

(Received 18 December 1981; accepted 10 February 1982)

Ultraviolet photoemission spectroscopy (UPS) with photon energies between 7 and 30 eV has been used to probe the electronic structure of cleaved (110) single-crystal $Hg_{1-x}Cd_xTe$ ($x = 0.2$, 0.31, 0.39, and 1.0). Structure in the emission from the upper valence bands (within ~3.5 eV of the valence band maximum) is qualitatively similar for the compositions studied and exhibits band-structure-related dispersion with photon energy. Features arising from the lower lying, mainly metal *s*-electron derived states (-4 to -6 eV) correlate separately with Hg and Cd. Thus the UPS spectra give evidence of differences in the contributions of the two cations to the electronic structure and the breakdown of the virtual crystal approximation in the valence states lying about 5 eV below the valence band maximum.

PACS numbers: 71.25.Tn, 79.60.Eq

I. INTRODUCTION

Knowledge of the electronic structure of $Hg_{1-x}Cd_xTe$ is important in understanding the bulk and surface properties of the alloy. While transport properties suggest one picture of the electronic structure, phenomena related to structural properties suggest another. The high mobility in narrow gap alloys, for example, indicates highly nonlocalized electron wave functions characteristic of a periodic rather than a random lattice for states near the band edge. The relative ease of forming a Hg vancancy[1] on the other hand, suggests that the bonding differs for Hg and Cd and that the electronic structure may reflect the difference in potential of the Hg and Cd sites in the cation sublattice. Because photoemission spectroscopy examines the complete valence band, it has the potential for identifying valence regions reflecting localized and highly nonlocalized valence states, as will be shown.

While important differences exist in the details of the band structure[2] of CdTe and HgTe, particularly at $k = 0$ (the band gap in CdTe is 1.5 eV; HgTe is a semimetal with inverted band order at $k = 0$[2]), ultraviolet photoemission spectroscopy (UPS) studies of these compounds have shown the valence band emission for these two materials to be similar.[3,4] The band of states contributing to the bottom of the valence bands occurs at about 0.8 eV higher binding energy in HgTe, however, resulting in a greater total valence bandwidth. To our knowledge, no systematic determination of the compositional dependence of the electronic structure in $Hg_{1-x}Cd_xTe$ alloys has been reported, and it is of interest to examine the relationship of the alloy electronic structure to that of its pseudobinary constituents.

To investigate the electronic structure of $Hg_{1-x}Cd_xTe$, we have used UPS with photon energies from 7 to 30 eV to examine single-crystal alloys of three compositions. The upper, mainly *p*-like valence states[5] within ~3.5 eV of the valence band maximum (VBM) were found to be bandlike and qualitatively similar for all compositions studied. The lower-lying states near 5 eV below the VBM, which are principally metal *s*-electron derived but contains 40% cation *p*-character,[5] are more localized and distinctly reflect Hg or Cd parentage. Thus the UPS data document differences in the contributions of the two cations to the electronic structure of the alloy. Additional evidence suggests that these differences in cation bonding increase with increasing Hg content.

Our results will be presented in greater detail following a description of the experimental procedure employed and are then discussed in light of a recent theoretical calculation of the electronic structure.

II. EXPERIMENTAL

Single-crystal samples of $Hg_{1-x}Cd_xTe$ of composition $x = 0.2$, 0.31, and 0.39, grown by solid-state crystallization (Santa Barbara Research Center) and a sample of CdTe[6] were introduced into the vacuum chamber through an air interlock. In this way, heating the samples during the preparation of the chamber was avoided. Clean surfaces for study were prepared by cleaving the samples along a (110) face in vacuum ($p < 10^{-10}$ Torr). Light from a synchrotron source was incident on the cleaved surface at a 75° angle to the surface normal and was largely *p*-polarized. A double pass cylindrical mirror electron spectrometer with symmetry axis along the sample normal performed the energy analysis of the emitted electrons. Electron energy distributions curves were recorded for photon energies ranging from 7 to 30 eV. The energy resolution in the spectra obtained is believed to be better than 0.2 eV.

No evidence for loss of Hg from the surface was obtained during the course of the measurements,[7] and traces of carbon or oxygen contamination were not apparent in x-ray photoemission data.

 0022-5355/82/050142-04$01.00

III. RESULTS

Using UPS to probe $Hg_{1-x}Cd_xTe$ samples of different compositions provides insight into the contribution of each constituent to the electronic structure of the alloy. Measured electron energy distributions show emission from the valence states in the alloy as well as the Hg 5*d* and Cd 4*d* levels just below the valence bands. Both valence electron emission and core lines exhibit compositional variation.

The details of the x dependence of emission from the valence states for the four samples are given in Fig. 1 for $h\nu = 17$ eV. The broad feature extending to ~ 3.5 eV below the valence band maximum (VBM) corresponds to emission from the largely *p*-like upper valence states in the alloy; structure between -4 and -6 eV aries from the lower valence states, which are mainly cation *s*-electron derived.[5] The upper, *p*-like bands are qualitatively similar for all compositions; broad parks near -1.8 and -3.0 eV and a weak shoulder around -1.0 eV are seen in each curve. In the samples containing Hg, however, this region of states is somewhat wider and the features occur further from the VBM.

The cation *s*-derived states exhibit a much stronger and systematic variation with composition. As can be seen in Fig. 1, these valence states in the alloy produce emission to a lower energy than in CdTe. The energy of this contribution, -5.4 eV for the $x = 0.2$ sample, compares well with the peak in the principally *s*-like band in spectra of HgTe[3,4] confirming that the states of this energy are of Hg origin. As the Cd content is increased from $x = 0.2$, a feature around -4.6 eV grows in intensity giving a broad peak for $x = 0.39$ that we suggest is made up of Hg (~ -5.4 eV) and Cd (~ -4.6 eV) related components. The correlation of the intensity near -4.6 eV with x is evidence that it is Cd derived. Thus states of distinctly Hg or Cd origin are observed, indicating that differences in the cation–Te bonds exist. The vertical lines in Fig. 1 serve to highlight the x variation of the Cd and Hg contributions; the exact energy of these states, however, may vary from that indicated by the lines in the figure.

The photon energy dependence of the valence electron emission is presented for $h\nu$ between 12 and 17 eV for $Hg_{0.8}Cd_{0.2}Te$ and CdTe in Fig. 2. As noted, the *p*-like upper bands show similar structure. Peaks in the emission from this region are observed to shift in binding energy as a function of photon energy. This dispersion is a result of *k*-conserving transition occuring between bandlike states.[6] The dispersion is somewhat more extensive in the alloys than in CdTe, but in all cases follows a similar pattern. For the lower lying, *s*-like states, dispersion is not apparent, indicating that these states are more localized. Localization is consistent with the distinctly Hg or Cd origin of these levels.

Differences in the cation bonding apparent in the separate metal *s*-electron contributions to the valence electronic structure are also observed in the variation in binding energy of the cation *d* levels which lie just below the valence bands. Figure 3, showing spectra recorded at 21 eV, details the location of these core levels relative to the VBM for the four samples studied. The peaks at -7.9 and -9.6 eV arise from the spin-orbit split Hg 5*d* levels, while the Cd 4*d* lines appear around -10.4 eV and are split by 0.6 eV. Apparent in Fig. 3 is a shift of 0.2 eV to higher binding energy for the Cd *d* levels in going from CdTe to the $x = 0.39$ alloy. The Cd

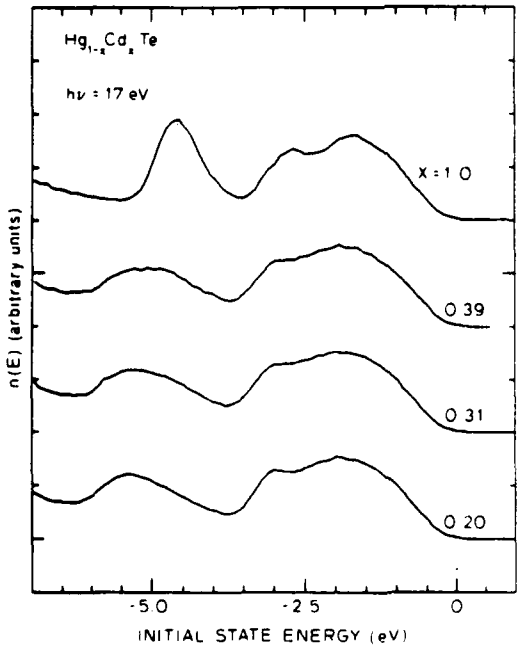

FIG. 1. UPS Spectra at 17 eV show features of distinctly Hg (−5.4 eV) and Cd (−4.6 eV) origin.

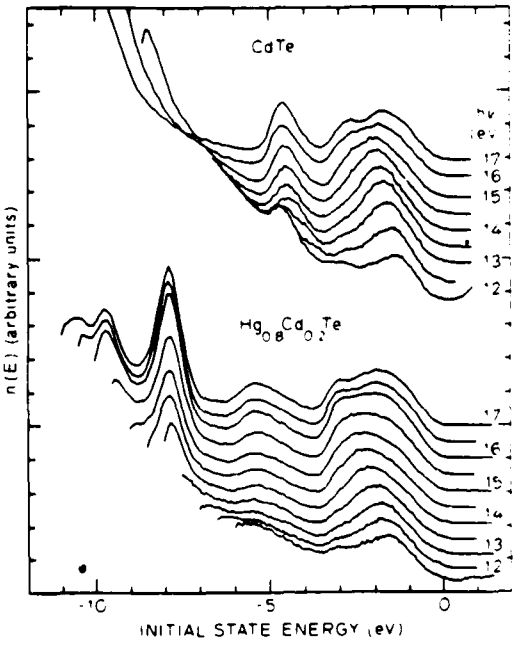

FIG. 2. Photon energy dependence of valence electronic structure of $Hg_{1-x}Cd_xTe$. Dispersion is observed in the upper states while the lower states (−4 to −6 eV) appear stationary.

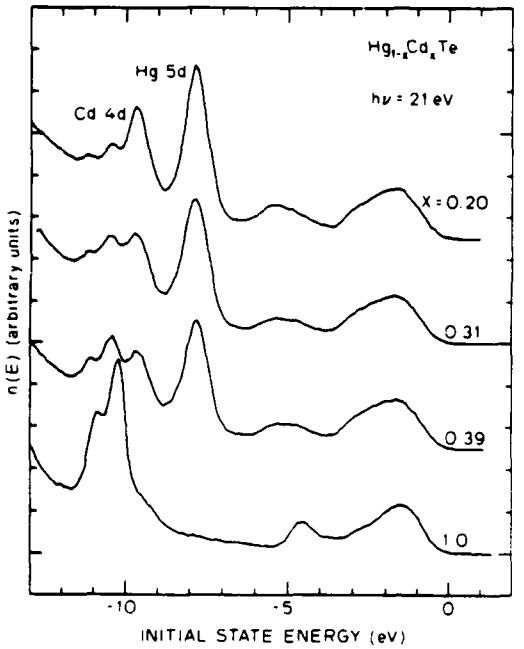

FIG. 3. Comparison of valence band and cation core level emission for the four samples studied. Note the shift in the Cd 4*d* lines with the addition of Hg.

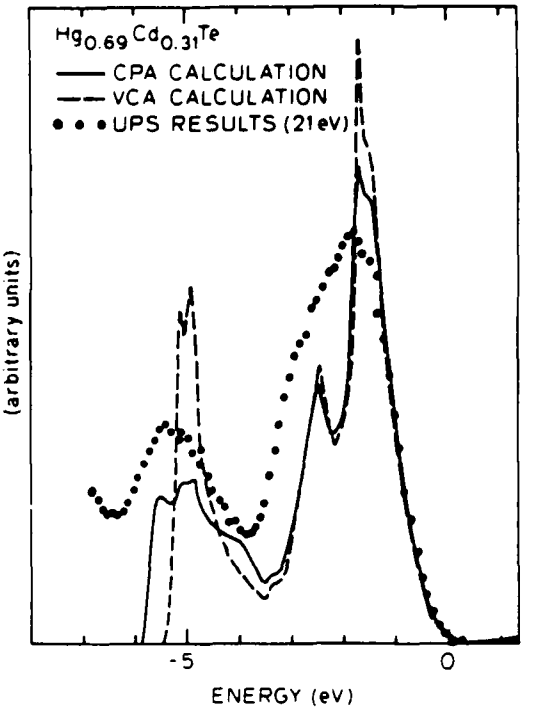

FIG. 4. Calculated valence density of states (Chen and Sher, private communication) in the CPA (solid) and virtual crystal case (dashed) plotted with the measured electron distribution (dotted) at 21 eV. All curves are for $Hg_{0.69}Cd_{0.31}Te$.

and Hg contributions to the bonding, therefore, vary as the average composition changes.

IV. DISCUSSION

The UPS results document differences in the cation–Te bonds which appear predominantly in the cation *s*-derived electronic structure. This can be understood at least qualitatively by considering atomic Hg and Cd. The valence *s* electrons in Hg are bound 1.4 eV more strongly than those of Cd while the *p*-state energies are nearly equal. The difference in Hg and Cd potentials seen by an *s* electron in the atomic states remains in the alloy, resulting in distinct cation contributions to the measured electron emission. As in the atomic case, the Hg-derived states in the alloy are more tightly bound. The shift in binding energy observed for the Cd 4*d* levels with the addition of Hg likely reflects the relative ease of involving the more loosely bound Cd valence electrons in bond formation. The direction of the shift suggests that Cd becomes more ironic when it has Hg next-nearest neighbors. As the Cd content decreases, therefore, the Cd bond strength should increase.

Theoretical calculations of the band structure of $Hg_{1-x}Cd_xTe$[2] have been performed within the framework of the virtual crystal approximation (VCA), in which the random alloy is treated as a periodic lattice by replacing the cation potentials by a compositionally weighted average of the potentials of Hg and Cd. In this way, Hg–Te and Cd–Te interactions are indistinguishable. In view of the UPS results, this approach appears unjustified over the full extent of the valence electronic structure, although it may be applicable for the upper valence states.

A recent calculation by Chen and Sher[9] for $Hg_{1-x}Cd_xTe$ has been performed using the coherent potential approximation (CPA). This treatment takes into account the difference in cation potentials in evaluating the alloy electronic structure. The density of states thus obtained is quite similar to the virtual crystal case for the upper *p*-like bands, but it exhibits important differences in the mainly *s*-derived region when compared to the virtual crystal results. In the virtual crystal case, the peak in the density of states in the mainly *s*-like band for an $x = 0.31$ alloy remains sharp and occurs at an energy intermediate to those of the corresponding peak in HgTe and CdTe. The CPA result,[9] which is reproduced in Fig. 4, exhibits instead three broad features separated by roughly $\frac{1}{4}$ eV. The lowest and highest peaks correspond to the Hg and Cd *s*-electron contributions respectively, while the intermediate peak has cation *p* character and shifts to a lower binding energy as the Cd content increases.[5] Also plotted on the same scale in Fig. 4 is the electron distribution obtained by UPS at $h\nu = 21$ eV. Overall, structure in CPA density of states is reproduced in the measured distribution. In particular, good correspondence is obtained for the Hg and Cd related features in the lower group of states. Thus the apparent increase with increasing x in the emission at -4.6 eV in the measured distribution (see Fig. 1) results from a reduction in the Hg component (-5.4 eV), a shift toward the VBM of the *p*-derived component due to the higher Cd

content, and an increased contribution from the states of Cd *s* origin. The virtual crystal results,[9] also included in Fig. 4, do not fit the data appreciably in this region. Both methods accurately predict the features observed within roughly 2 eV of the VBM. That the VCA and coherent potential results show such close agreement in the *p*-like states is not surprising given the highly bandlike nature observed for these states in the photon energy dependence of emission from this region. Both calculations underestimate the width of the bands, a trend in comparing theory and experiment observed in other systems as well.[8]

V. CONCLUSIONS

UPS studies of the electronic structure of $Hg_{1-x}Cd_xTe$ over a range of photon energies provide evidence of differences in the bonding of Hg and Cd. These differences are most apparent in the separate contributions of the cations to the mainly *s*-derived states in the valence electronic structure. The shift in binding energy of the Cd 4*d* levels indicates that these differences vary somewhat with composition.

The states above -3.5 eV appear to be bandlike, suggesting that the VCA is applicable in this region. To accurately calculate the electronic structure of the alloy, however, differences in the Cd and Hg potentials must be accounted for, as seen in the good agreement between the CPA calculation and the UPS results.

ACKNOWLEDGMENTS

The authors gratefully acknowledge valuable discussions with Professor W. A. Harrison. This work was supported by DARPA Contract No. MDA-903-80-C496. Work was performed at the Standford Synchrotron Radiation Laboratory, which is supported by the NSF through the Division of Materials Research in cooperation with the Department of Energy.

[a] National Science Foundation predoctoral fellow
[b] Permanent address: Fysisk Institut, Odense University, Campusvej 55, DK-5230, Odense M, Denmark
[c] Stanford W. Ascherman Professor of Engineering
[1] H. R. Vydyanath, presented at the U.S. Workshop on the Physics and Chemistry of Mercury Cadmium Telluride, Minneapolis, MN, Oct. 28–30, 1981
[2] See portions of R. Dornhaus and G. Nimtz, in *Springer Tracts in Modern Physics, Vol. 78* (Springer, Berlin, 1976); and references therein
[3] N. J. Shevchik, J. Tejeda, M. Cardona, and D. W. Langer, Phys. Status Solidi B **59**, 81 (1973)
[4] L. Ley, R. A. Pollak, F. R. McFeely, S. D. Kowalczyk, and D. A. Shirley, Phys. Rev. B **9**, 600 (1974).
[5] A. Sher (private communication)
[6] The CdTe was supplied by II-VI Compounds, Inc.
[7] J. A. Silberman, P. Morgen, I. Lindau, W. E. Spicer, and J. A. Wilson, these proceedings
[8] W. E. Spicer, in *Optical Properties of Solids—New Developments*, edited by B. O. Seraphim (North-Holland, Amsterdam, 1976).
[9] An-Ban Chen and A. Sher, these proceedings.

2.5

AES sputter profiles of anodic oxide films on (Hg, Cd)Te

P. Morgen,[a] J. A. Silberman,[b] I. Lindau, and W. E. Spicer[c]

Stanford Electronics Laboratories, Stanford University, Stanford, California 94305

J. A. Wilson

Santa Barbara Research Center, Goleta, California 93017

(Received 23 December 1981; accepted 16 February 1982)

Sputter profiling with Auger electron spectroscopy has been used to determine the depth profiles of Hg, Cd, Te, and O in anodic oxides on (Hg, Cd)Te in an effort to monitor the composition of the oxides and the properties of the oxide-semiconductor interface. The measurements are straightforward, but the analysis and extraction of atomic concentration profiles are complicated due to nonstoichiometric erosion of the base material and possibly of the oxide. Conclusions from this and earlier investigations about the composition of the semiconductor past the interface are still dependent on a more basal understanding of the effects of low energy ion bombardment on (Hg, Cd)Te.

PACS numbers: 68.60. + q, 79.20.Fv, 79.20.Nc

I. INTRODUCTION

In a number of recent studies of (Hg, Cd)Te and anodic oxide layers on this material, ion bombardment techniques have been used.[1–4] It emerges as a firm conclusion of all these reports that preferential ejection of Hg takes place. It has also been reported that even low doses of electrons induce desorption of Hg from the surface regions of (Hg,Cd)Te samples,[1,3] and that consequently only x-ray or ultraviolet photoemission spectroscopy (XPS or UPS) would be suitable tools for the evaluation of surface atomic compositions of the material. Thus concentration profiles have so far mainly been obtained with XPS during bombardment with noble gas ions.[1] For reasons detailed in Ref. 1, such profiles appear with a low spatial resolution which would preclude the observation of details of the interfacial properties. In contrast, using Auger electron spectroscopy (AES) one would be able to obtain a significantly better spatial resolution and to resolve structure in the concentration profiles only limited by the sampling depths of the Auger lines and artifacts induced by the ion bombardment. The latter include surface roughness, preferential sputtering, radiation (sputter) induced diffusion and recoil implantation.[5,6]

In view of the depth resolution available using sputter AES profiling, a program to understand the sputtering process and apply the technique to depth profiles of anodic oxides has been undertaken. The experimental results include concentration profiles for (Hg, Cd)Te and anodic oxide layers obtained with AES during ion bombardment with Ne^+ ions of 1.0-keV energy. The data contributes to an understanding of some of the effects of the ion beam, especially preferential sputtering and radiation induced diffusion, which act to alter the composition of the material over the range of the ion beam in the target. Comments can also be made about the use of AES signals to determine the atomic concentrations. It appears, finally, that not all of the discrepancies between presently available reports can be resolved. As the most obvious reason for this we suggest that material from different sources may be of dissimilar quality with respect to the amount of free Hg and other defects as well as processing technique.

II. BACKGROUND

The theoretical description of ion beam induced erosion from multi-component samples is presently under development[6] but far from complete. Some qualitative features are already predictable, however, without resorting to a detailed theory,[5] and we shall make use of the most simplified concepts as they seem relevant for our purposes.

An important concept is the inverse proportionality expected between the relative sputter yields and the surface binding energies.[6] Thus measurements of relative sputter yields could contribute to the understanding of the binding of Hg, Cd, and Te in the lattice.

The main conclusion of a recent summary of the experimental situation[5] is that clearcut cases of preferential sputtering are hard to find, but combinations of radiation enhanced diffusion and recoil implantation seem to be the rule. Thus in the present context we will assume that these are the

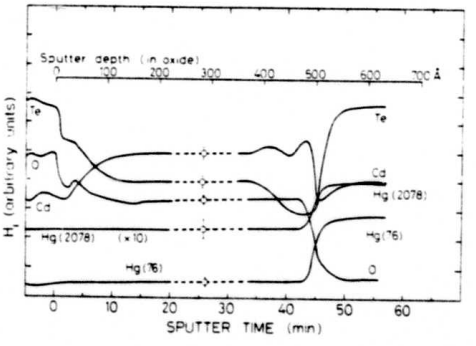

FIG. 1. AES signals (peak-to-peak heights) during ion bombardment of a 500-Å anodic oxide on $Hg_{0.7}Cd_{0.3}Te$. During the period with flat profiles, a high-resolution scan of the AES lines was recorded for quantification. 1 keV, Ne^+, 5 keV electrons.

 0022-5355/82/050161-03$01.00

effects we have to look for when analyzing the observed concentration profiles. For more details the reader is referred to Refs. 5 and 6.

III. EXPERIMENTAL

The experiments were carried out in a commercial ultrahigh vacuum system (Varian) with a single pass cylindrical mirror analyzer, 10-keV integral electron gun, and a 3-keV ion gun.

The experimental results and procedures are illustrated in Fig. 1. This figure presents the observed AES signals (peak-to-peak height of the Auger line in a dN/dE spectrum) for an anodic oxide of 500 Å. A profile of an etched, air exposed (lightly oxidized) (Hg, Cd)Te sample is shown in Fig. 2.

Effects of the electron beam were evaluated prior to sputtering by monitoring the AES signals under different irradiation conditions. Thus a narrowly focused beam with a high current was indeed found to induce desorption and decomposition of the surface. However, scanning the beam spot across an area of approximately $200 \times 200\mu$ and reducing the current to $1\,\mu$A was sufficient to obtain constant signals over periods of the order of half hours. This condition was always ascertained before initiating the ion bombardment. Thus for the present results, no effects are encountered of the electron beam on the concentration profiles.

The ion beam profile was extended to erode an area much wider than that sampled by the electron beam to insure the Auger signal originated from the flat portion of the sputter crater, thereby giving high depth resolution. The present ion gun further produces an optimum flatness of the eroded surface by a random rastering mechanism (Varian).

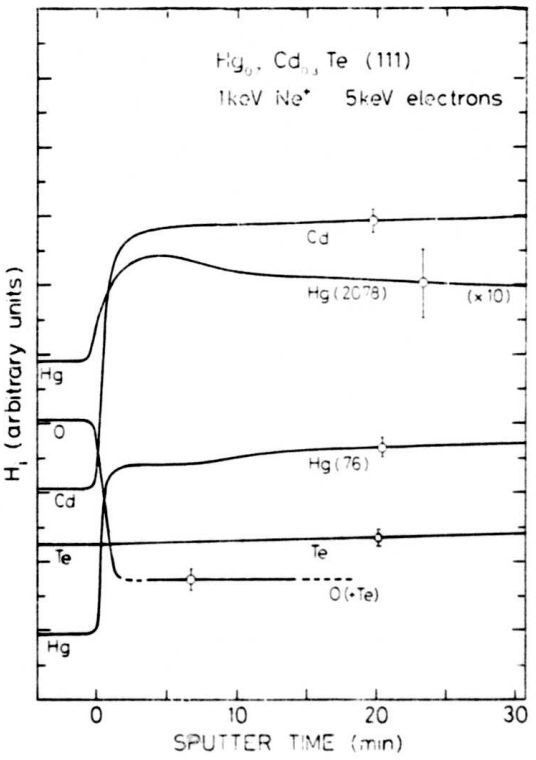

FIG. 2. AES signals during ion bombardment of a $Hg_{0.7}Cd_{0.3}Te$ wafer which had been etched in DMF prior to the measurements.

IV. DISCUSSION

Let us first examine the shapes of the concentration profiles as gauged by the AES signals (Figs. 1–2). The two sets of measurements were done under similar experimental conditions. Upon initial variation of the AES signals after starting the bombardment, the signals flatten to an approximately steady state. For the lightly oxidized sample (Fig. 2) they stay relatively flat, but for the oxide (Fig. 1) variation in the signals is observed as the substrate is approached by the erosion of the oxide. A reasonable assumption here is that this is indicative of flat profiles of the real concentrations for the bulk of the oxide. The oscillatory behavior of the AES signals at the surface and interface represents real concentration variations but also includes effects due to recoil implantation in combination with unequal sputtering rates of the constituents. A separate series of experiments is being devoted to study these effects during sputtering in the (Hg, Cd)Te system. This work is still in progress but we quote here the most relevant objectives. By varying the mass and energy of the ions, we can change the sputtering cross sections[6] and ranges of ions in the target. A comparison of profiles as the ones in Figs. 1 and 2 taken under such different conditions, and for different fluxes, is ultimately expected to permit the evaluation of preferential sputtering (different relative sputter yields) as separated from radiation induced diffusion and allow quantitative analysis of the transient signals observed at the surface and interface.

At present we limit ourselves to discuss results for the concentrations as obtained from the flat parts of the profile of Fig. 1. Using standard factors[7] to correct for escape depth, analyzer transmission, and Auger cross section, we find the oxide composition to be 4% Hg, 25% Cd, 19% Te, and 52% O. (The Hg concentration given is the average of that obtained using the 2078 and 76 eV transitions.) It has been suggested[3] that the sensitivity factors used[7] result in an overestimate of the Hg concentration and a Cd concentration which is too small. These values may also be altered from the true composition by effects of the sputtering process.

An important consideration in assessing the accuracy of the derived composition is the possibility that the composition will not be homogeneous throughout the volume sampled as a result of the ion interaction. The Hg Auger transition at 76 eV kinetic energy samples a region approximately 5-Å thick[8] while the higher energy transition (2078 eV) probes 25–30 Å into the sample. Inhomogeneity can therefore have a strong effect on the composition as determined by the two Auger lines or in comparing Auger and x-ray photoemission derived profiles.

V. CONCLUSIONS

Ion beam bombardment, as used for cleaning or depth profiling of (Hg, Cd)Te, is found to induce deviations of stoichiometry and changes in the spatial distribution of constituents near the surface. The derivation of details of the real concentration profiles, from XPS or AES signals, for oxides and other technologically important heterostructures could be hazardous without a basal knowledge of these effects. However, from the present results some unambiguous conclusions can be drawn: The oxide is Hg deficient and the interface is relatively sharp ($\sim$ 50-Å wide).

In this report we have presented data from an ongoing study which is meant to distinguish the effects of preferential sputtering, radiation induced diffusion, and recoil implantation in order to obtain accurate depth profiles.

VI. ACKNOWLEDGMENTS

This work is supported by DARPA, Contract No. MDA 903-80-C-0496. The Danish Natural Science Research Council supported one of the authors (PM). He also gratefully acknowledges the support and hospitality extended to him at Stanford.

[a]Permanent address: Odense University, Denmark.
[b]National Science Foundation predoctoral fellow.
[c]Stanford Ascherman Professor of Electrical Engineering.

[1]T. S. Sun, S. P. Buchner, and N. E. Byer, J. Vac. Sci. Technol. 17, 1067 (1980); G. D. Davis, T. S. Sun, S. P. Buchner, and N. E. Byer, J. Vac. Sci. Technol. 19, 472 (1981).
[2]U. Solzbach and H. J. Richter, Surf. Sci. 97, 191 (1980).
[3]H. M. Nitz, O. Ganschow, U. Kaiser, L. Wiedmann, and A. Benninghoven, Surf. Sci. 104, 365 (1981).
[4]P. Morgen, J. A. Silberman, I. Lindau, W. E. Spicer, and J. A. Wilson, presented at the Electronic Materials Conference, Santa Barbara, California June 24–26, 1981 (to be published).
[5]H. H. Andersen, in *The Physics of Ionized Gases*, edited by M. Matic (Boris Kidric Institute of Nuclear Sciences, Beograd, 1980).
[6]P. Sigmund, A. Oliva, and G. Falcone, presented at the Ninth International Conference on Atomic Collisions in Solids, Lyon, July 6–10, 1981 (unpublished).
[7]*Handbook of Auger Electron Spectroscopy*, 2nd ed., (Physical Electronics Industries, Eden Prairie, Montana 1976).
[8]I. Lindau and W. E. Spicer, J. Electron. Spectrosc. Relat. Phenom. 3, 409 (1974).

2.6

Room temperature stability of cleaved $Hg_{1-x}Cd_xTe$

J. A. Silberman,[a] P. Morgen,[b] I. Lindau, and W. E. Spicer[c]

Stanford Electronics Laboratories, Stanford University, Stanford, California 94305

J. A. Wilson

Santa Barbara Research Center, Goleta, California 93017

(Received 13 November 1981; accepted 10 February 1982)

X-ray and ultraviolet photoemission spectroscopy (XPS and UPS) at 21.2 eV have been used to determine the stability against Hg evaporation of cleaved (110) surfaces of p-$Hg_{1-x}Cd_xTe$ ($x = 0.2, 0.31, 0.39$) in vacuum at room temperature. No evidence of Hg loss was obtained for periods of observation from five to twenty hours. However, oxygen excited by an ionization gauge and Ne ion sputtering both produced preferential loss of Hg.

PACS numbers: 68.45.Da, 79.60.Eq, 81.40.Gh

I. INTRODUCTION

Because of the large difference in bonding energy of Hg and Cd in the alloy $Hg_{1-x}Cd_xTe$—the heat of atomization of HgTe is 30% less than that of CdTe—there has been considerable concern as to the stability of the alloy surface with respect to room temperature evaporation of mercury.[1-3] This question is of practical importance since $Hg_{1-x}Cd_xTe$ is emerging as the premier infrared detector material, and the electronic and optical properties of devices fabricated in this material depend strongly on alloy composition.[4] It is also of fundamental interest because the pseudobinary constituents, CdTe and HgTe, are believed to be miscible in all proportions despite the difference in cation bond energies.[4]

Preferential evaporation of Hg has been observed in dissociation,[5] vapor deposition,[6] and vapor–solid equilibrium[7] studies at moderate and high temperatures. Room temperature mercury out-diffusion and evaporation were mechanisms proposed to explain n- to p-type conversion observed in samples stored for periods of three to thirteen years in air.[1,2] Recently, Nitz *et al.*[3] measured the change in surface composition with time at room and elevated temperatures of $Hg_{0.8}Cd_{0.2}Te$ samples prepared by scraping the surface in vacuum or by ion bombardment. The concentration of Hg was reported to decrease by 25% in less than three hours at 290 °K.[3] For p-type alloy crystal surfaces prepared by cleaving in vacuum, however, we observed no evidence for loss of Hg at room temperature for periods of tens of hours. A loss of Hg was observed, however, from surfaces exposed to oxygen excited by an operating ionization gauge or bombarded by 3-keV Ne ions.[8] These results suggest that the structural imperfections in the lattice in the surface region are an important factor in the compositional stability of the alloy.

II. EXPERIMENTAL

To investigate the stability of $Hg_{1-x}Cd_xTe$ surfaces, XPS using Al$K\alpha$ x rays (1486.7 eV) and UPS with 21.2 eV photons from a synchrotron source were employed to determine and monitor the surface composition of p-type $Hg_{1-x}Cd_xTe$ single crystals with $x = 0.2, 0.31$, and 0.39. Atomically clean surfaces were prepared by cleaving along a (110) face in vacuum (10^{-10} Torr). The cleaved surfaces were highly reflecting and generally smooth, with regions of planar and contoured topology. The position of the Fermi level at the surface was determined from the high energy cutoff of emission (Fermi level) from a gold film evaporated onto a stainless steel substrate in electrical contact with the semiconductor samples.[9] All spectra were recorded using a double pass cylindrical mirror electron energy analyzer.

In a separate experiment, UPS and XPS were additionally used to examine the effects of two perturbations to the cleaved surface: exposure to oxygen in the presence of an operating ionization gauge and Ne ion sputtering.[8] The UPS measurements were on this occasion performed using 21.2 eV photons from a He discharge with monochromater. Operation of an ionization gauge has been found to greatly enhance oxygen uptake[8,10] and, in this case, exposure of $x = 0.31$ material to 3×10^6 L and 4×10^8 L (1 L = 10^{-6} Torr·s) was performed with 9 and 0.4 mA emission current at oxygen pressures of 2.5×10^{-3} and 0.35 Torr, respectively. Cleaved surfaces of $x = 0.31$ and 0.39 composition were sputtered for 15 min with 3-keV Ne ions at 15 μA/cm^2. Impurity gas pressure during sputtering was kept negligibly low by virtue of a cryopanel cooled to liquid nitrogen temperature.

III. RESULTS

UPS spectra of $Hg_{1-x}Cd_xTe$ taken at 21.2 eV are given in Fig. 1 for $x = 0.39, 0.31$, and 0.2. In each case, two spectra are presented for comparison: the solid line corresponds to emission measured within 25 min of cleaving, while the dotted spectrum represents the surface 5, 18, or 20 h later, as indicated in the figure. Because the two curves are virtually identical in each case, the dashed spectra have been displaced vertically to facilitate comparison with the solid curves. The position of the Fermi level at the surface is indicated above the valence band edge in the figure, and the valence band maximum has been taken as the onset of emission. While this method of locating the valence band maximum tends to reduce the measured Fermi energy, the Fermi level in many cases, such as those shown in Fig. 1, appears to be pinned above the expected bulk position. Further study is

 0022-5355/82/050154-03$01.00

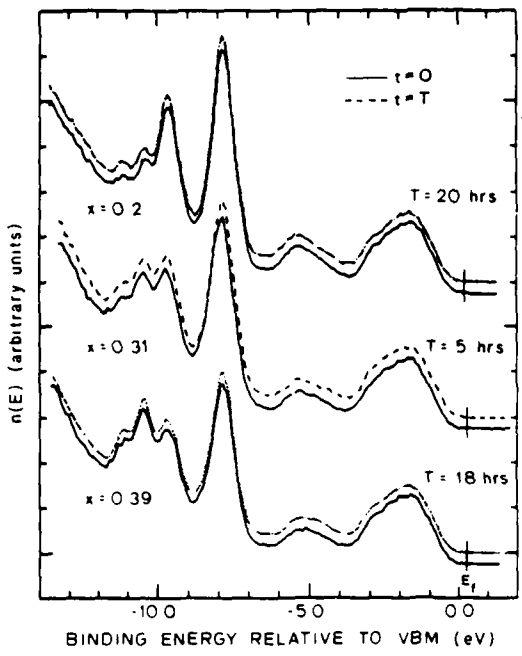

FIG. 1. Comparison of photoemission spectra (21.2 eV) taken immediately after cleaving (solid) and at a time T later (dashed) as indicated. The dashed spectra are virtually indistinguishable from the solid curves and so have been displaced to facilitate comparison. Compositions are $x = 0.2$, 0.31, and 0.39. $h\nu = 21.2$ eV.

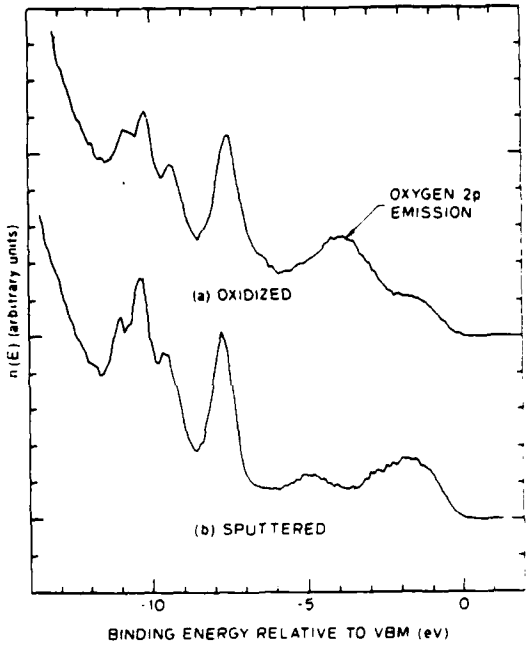

FIG. 2. Photoemission spectra of (a) $Hg_{0.69}Cd_{0.31}Te$ after exposure to 4×10^4 L O_2 in the presence of an operating ion gauge, and (b) an $x = 0.31$ surface after Ne ion sputtering. Note reduced Hg 5*d* emission relative to Cd 4*d* in comparison to the clean $x = 0.31$ surface in Fig. 1. $h\nu = 21.2$ eV.

required to fully understand the apparent *p*- to *n*-type conversion of the surface. Emission from the valence bands is clearly discernible to -6 eV. Details of a study of valence band structure as a function of composition and photon energy are reported separately.[11]

The sharp peaks below the valence bands in Fig. 1 are due to the spin-orbit split, atomic-like Hg 5*d* (-7.9 and -9.6 eV) and Cd 4*d* levels (-10.4 and -11.0 eV). The appearance of these features in the 21.2 eV spectra permits monitoring of relative changes in the Hg and Cd concentrations within 15 Å of the surface.[12] This is evident in Fig. 1 in the systematic decrease in intensity of the Hg 5*d* peaks relative to the Cd 4*d* lines as the CdTe mole fraction changes from $x = 0.2$ to $x = 0.39$. Such changes are not observed in the core line emission as a function of time for the curves of Fig. 1, indicating the compositional stability of the surface. A constant surface composition would result from a balance between Hg evaporation from the surface and readsorption. To maintain the core level intensity within 5% over the 20 h of observation for the sample of highest Hg content ($x = 0.2$), the equilibrium Hg vapor pressure would have to be 1×10^{-11} Torr, assuming a unity sticking coefficient for the readsorbing Hg. This figure thus represents an upper limit on the vapor pressure over a cleaved surface at room temperature. The actual vapor pressure is believed to be much lower. For comparison, the vapor pressure at room temperature extrapolated from measurements at higher temperatures range from 3×10^{-12}–2×10^{-9} Torr[6,7] for Te-saturated samples with $x = 0.2$.

To determine whether the surface composition had rapidly changed in the brief period between cleaving and the first measurements, the surface composition was determined using XPS after the periods indicated in the figure had elapsed. Elemental concentrations were obtained by correcting the areas under the Cd $3d_{5/2}$, Te $3d_{5/2}$, and Hg $4f_{7/2}$ peaks in XPS spectra for analyzer transmission, photoionization cross section,[13] and electron escape depth,[14] and setting the total to 100%. The $x = 0.39$ sample was found to be 27% Hg, 21% Cd, and 52% Te ($x = [Cd]/[Te] = 0.4$), while the $x = 0.2$ sample was composed of 35% Hg, 10% Cd, and 55% Te ($x = 0.18$). X-ray photoemission data were not obtained for the $x = 0.31$ sample. Due principally to the uncertainties associated with the correction factors, the concentrations derived are estimated accurate to 10–15%. The precision indicated by the results is better, however; doubling the nominal x value results in double the measured Cd concentration to within 5% with similar precision in the scaling of the Hg concentration with $1 - x$. Thus, within the experimental error, the composition of the surface region remains the same as that of the bulk.

The cleaved surface was found to be highly inert to ground state oxygen.[8] The effects of exposure to excited oxygen and ion sputtering on surface composition are illustrated in Fig. 2. Spectrum (a) was obtained from an $x = 0.31$ surface after exposure to 4×10^4 L of oxygen in the presence of an operating ionization gauge. The peak in the valence band around -4 eV arises from bound oxygen. A decrease in the emission of the Hg 5*d* lines relative to the Cd 4*d* emission for the

oxidized surface is evident by comparison to the clean spectrum of $x = 0.31$ material in Fig. 1. A similar loss of Hg is apparent in Fig. 2(b), the spectrum of an $x = 0.31$ surface after sputtering. Preferential sputtering of Hg has been reported by several investigators[3,15,16] and Cd[3,15,16] enrichment has been noted to accompany Hg loss for the sputtered surface and for scraped surfaces.[3] In the present experiments, XPS results confirm the loss of Hg observed in 21.2 eV spectra and document an increase in Cd concentration at the surface for both sputtered and oxidized surfaces. Perturbations to the surface such as oxidation and sputtering thus have a marked effect on surface composition.

IV. DISCUSSION

Based on the UPS data and the agreement between the measured surface region composition with the expected bulk valve, we find no evidence for loss of Hg from cleaved surfaces at room temperature for periods up to 20 h. Within 3 h, on the other hand, a loss of 25% of the Hg at the surfaces has been reported for scraped surfaces.[3] Stoichiometry may have some bearing on the stability of the cleaved surface reported here and the evaporation rate from a scraped sample observed by Nitz *et al.* The vapor pressure at elevated temperatures is greater over samples which are Hg-saturated than those which are Te-saturated.[7] The samples used in the UPS study were solid-state recrystalized, *p*-type bars and, owing to their large extent ($6 \times 6 \times 10$ mm), had not been post-growth annealed. It is likely that they were somewhat Te rich. Stoichiometry does not appear important, however, based on the results of Faurie,[17] who finds for molecular beam epitaxial $Hg_{1-x}Cd_xTe$ layers a low vapor pressure in agreement with our results but for *n*-type, presumably stoichiometric layers. The similarity of the results of the UPS study and that of Faurie[17] suggest that stoichiometry is not a significant factor determining the rate of Hg loss and supports a second possible contribution.

It is suggested that the more important factor influencing the stability of the alloy surface is sample preparation. Defects or dislocations introduced in preparing the surface or inherent in the material are likely to affect the electronic and mechanical properties of surfaces and interfaces.[18] The enhancement of Hg diffusion along a grain boundary has been recently observed.[19] Thus, lattice damage is perhaps the key difference in the evaporation rate observed for scraped[3] and powdered[5] samples and the stability found for cleaved bulk crystals and MBE layers.[17]

V. CONCLUSIONS

These experiments cannot be used to assert the stability of $Hg_{1-x}Cd_xTe$ for periods of years due to the comparatively short (20 h) period of observation. They do suggest, however, that the structural perfection of the surface region is, perhaps, the most important factor determining compositional stability. Additional study is necessary to understand this relationship in a detailed way.

ACKNOWLEDGMENTS

This project is supported by DARPA, Contract No. MDA-903-80-C-0496. One of the authors (P.M.) acknowledges financial support from the Danish Natural Science Research Council. He is grateful to Stanford University for support and hospitality. Part of this work was carried out at the Stanford Synchrotron Radiation Laboratory (SSRL), which is supported by the National Science Foundation through the Division of Materials Research in cooperation with the Department of Energy.

[a] National Science Foundation predoctoral fellow
[b] Permanent address: Fysisk Institute, Odense University, Campusvej 55, DK-5230, Odense M, Denmark
[c] Stanford W. Ascherman Professor of Engineering.

[1] W. F. H. Micklethwaite and R. F. Redden, Appl. Phys. Lett. **36**, 379 (1980).
[2] G. Nimtz, B. Schlicht, and R. Dornhaus, Appl. Phys. Lett. **34**, 490 (1979).
[3] H. M. Nitz, O. Ganschow, U. Kaiser, L. Wiedmann, and A. Benninghoven, Surf. Sci. **104**, 365 (1981).
[4] D. Long and J. L. Schmit, in *Semiconductors and Semimetals*, edited by R. K. Willardson and A. C. Beer (Academic, New York, 1970), Vol. 5. R. Dornhaus and G. Nimtz, in *Springer Tracts in Modern Physics*, (Springer, Berlin, 1976), Vol. 78.
[5] R. F. C. Farrow, G. R. Jones, G. M. Williams, D. W. Sullivan, W. J. O. Boyle, and J. T. M. Wotherspoon, J. Phys. D **12**, L117 (1979).
[6] D. K. Hohnke, H. Holloway, E. M. Logothetis, and R. C. Crawley, J. Appl. Phys. **42**, 2487 (1971).
[7] J. P. Schwartz, Tse Tung, and R. F. Brebrick, J. Electrochem. Soc. **128**, 438 (1981).
[8] P. Morgen, J. A. Silberman, I. Lindau, W. E. Spicer, and J. A. Wilson, presented at the Electronic Materials Conference, University of California, Santa Barbara, California (1981).
[9] W. E. Spicer, P. Skeath, C. Y. Su, and I. Lindau, J. Phys. Soc. Jpn. **49**, Suppl. A, 1079 (1980).
[10] P. Pianetta, I. Lindau, C. M. Garner, and W. E. Spicer, Phys. Rev. B **18**, 2792 (1978).
[11] J. A. Silberman, P. Morgen, I. Lindau, W. E. Spicer, and J. A. Wilson, these proceedings.
[12] I. Lindau and W. E. Spicer, J. Electron Spectrosc. Relat. Phenom. **3**, 409 (1974).
[13] J. H. Scofield, J. Electron Spectrosc. Relat. Phenom. **8**, 129 (1976).
[14] J. Szajman, R. C. G. Leckey, J. Liesegang, and J. G. Jenkin, J. Electron Spectrosc. Relat. Phenom. **20**, 323 (1980).
[15] U. Solzbach and H. J. Richter, Surf. Sci. **97**, 191 (1980).
[16] T. S. Sun, S. P. Buchner, and N. E. Byers, J. Vac. Sci. Technol. **17**, 1067 (1980).
[17] J. P. Faurie, these proceedings.
[18] W. E. Spicer, J. A. Silberman, P. Morgen, and I. Lindau, these proceedings.
[19] J. H. Tregilgas, these proceedings.

2.7

Summary Abstract: Cation bonds in $Hg_{1-x}Cd_xTe$[a]

J. A. Silberman,[b] P. Morgen,[c] I. Lindau, and W. E. Spicer[d]

Stanford Electronics Laboratories, Stanford University, Stanford, California 94305

A.-B. Chen

Department of Physics, Auburn University, Auburn, Alabama 36849

A. Sher

SRI International, Menlo Park, California 94025

J. A. Wilson

Santa Barbara Research Center, Goleta, California 93017

(Received 1 February 1982; accepted 18 March 1982)

PACS numbers: 73.20.Cw,79.60.Cn

The surface properties of the alloy $Hg_{1-x}Cd_xTe$, we believe, reflect differences in the chemistry of Hg and Cd. In an effort to understand these differences, an experimental and theoretical investigation of the electronic structure has been undertaken. Ultraviolet photoemission spectroscopy using photon energies between 7 and 30 eV from a synchrotron source were used to study cleaved (110) surfaces of $x = 0.2$, 0.31, and 0.39 alloys and CdTe.[1] These results can be compared to recent calculations[2] of the density of states of the alloy for these compositions. Using a tight binding approach and Gaussian orbitals, the theory was performed in two different ways: using the virtual crystal approximation (VCA), which treats the alloy as a periodic crystal with a cation potential which is a compositionally weighted average of the Hg and Cd potentials; and using the coherent potential approximation (CPA), which, unlike the VCA, accounts for the scattering induced by the aperiodic nature of the cation potential.[2]

The UPS results show emission from two groups of valence states. The upper bands (within about 3.5 eV of the

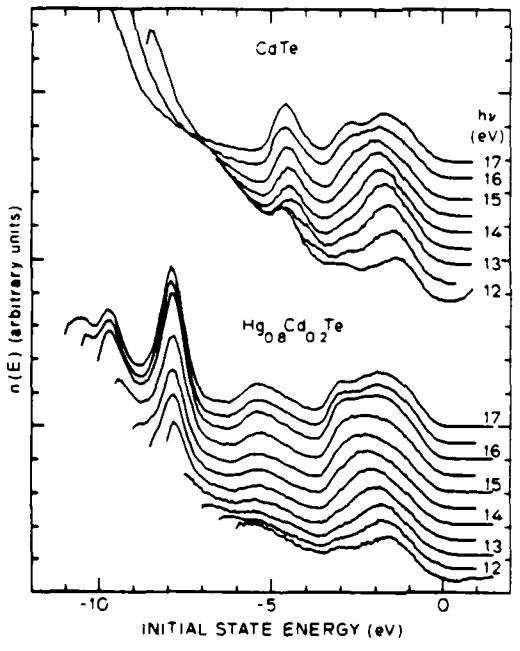

FIG. 1. Photon energy dependence of emission from CdTe and $Hg_{0.8}Cd_{0.2}Te$ for $12 < h\nu < 17$ eV. While structure in the upper valence bands above -3.5 eV shifts as a function of $h\nu$, the sharp peaks lower in the valence emission are essentially stationary.

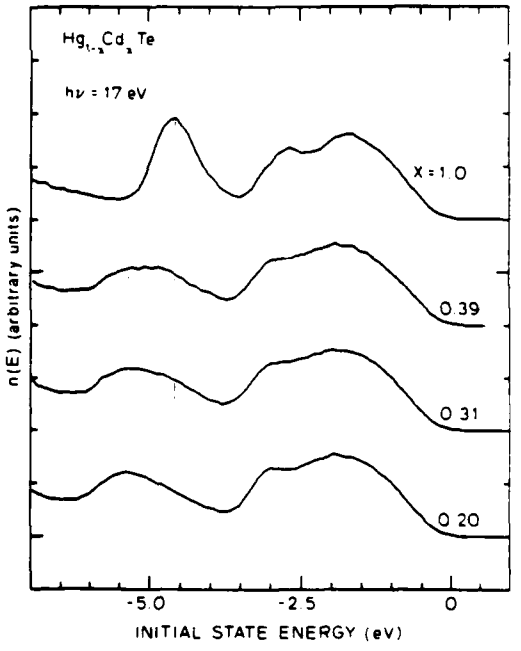

FIG. 2. Energy distribution curves at $h\nu = 17$ eV showing the compositional variation of structure of the lower, principally s-like group of states. The vertical line at -5.4 eV serves to highlight Hg-derived states; these states are absent in CdTe. As the Cd content (x) increases, the emission near -4.6 eV increases; this feature thus appears to be Cd derived.

 0022-5355/82/060467-02$01.00

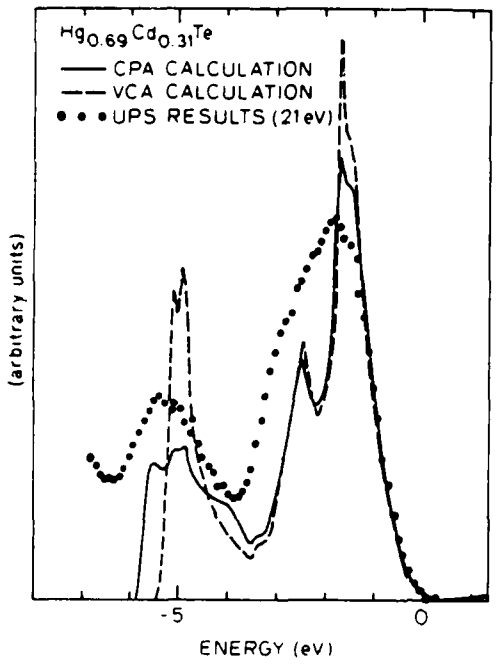

FIG. 3 Comparison of experimental results (dotted) with the density of states calculated under the VCA (dashed) and CPA (solid) methods. The peaks at -5.5 and -4 eV in the CPA calculation are of *s*-character and change in intensity with the Hg and Cd content, respectively; the peak at -5 eV is *p*-derived and shifts toward the VBM with increasing x.

valence band maximum) are mainly *p*-like and exhibit dispersion as a function of photon energy (Fig. 1) characteristic of *k*-conserving transitions in a periodic potential. Both the VCA and CPA approaches give highly similar densities of states in this energy range. The lower lying group of states (4 to 6 eV below the valence band maximum) on the other hand, does not show appreciable dispersion with $h\nu$. While emission from the upper, mainly *p*-like states is qualitatively similar for all compositions studied, the lower group, which is roughly 60% *s*-electron derived, exhibits features which correlate separately to Hg or Cd in their compositional dependence (Fig. 2). This behavior is predicted well by the CPA calculation, while the VCA results, which give a single peak in this region for all compositions which shifts monotonically with x, do not fit the data appreciably (Fig. 3).

The separation of Hg and Cd *s*-electron derived states in the alloy can be understood, at least qualitatively, by considering atomic Hg and Cd. While the (unoccupied) *p*-states occur at nearly the same energy, the valence *s*-electrons in Hg are bound 1.5 eV more strongly than in Cd, perhaps rendering Hg–Te bond formation more difficult relative to Cd–Te bonding. A shift to higher bonding energy of the Cd 4*d* lines relative to the valence band maximum upon a change of x from 1.0 (CdTe) to 0.39 observed in the UPS data[1] is consistent with this atomic description.

We suggest the breakdown of the virtual crystal model for the *s*-derived valence states indicates important differences in the cation–Te bonds. Such differences in the bulk bonding are of importance in fully understanding the surface properties of the alloy. For example, Hg loss observed from sputtered,[3,4] scraped,[4] and oxidized[5] surfaces is accompanied by at least partial replacement of the Hg by Cd, perhaps indicating that Cd–Te bonds are favored. In addition, it may not be possible to separate surface from bulk properties; dislocations and defects near the surface may have a first-order effect on surface stability.[6] The ease with which these lattice defects are formed may also be a consequence of the difference in cation bonds.

[a] Supported by DARPA Contract No. MDA 903-80-C496 and in part by AFOSR. A portion of this work was performed at the Stanford Synchrotron Radiation Laboratory which is supported by the National Science Foundation through the Division of Materials Research in cooperation with the Department of Energy.

[b] National Science Foundation predoctoral fellow.
[c] Permanent address: Odense University, Odense, Denmark.
[d] Stanford W. Ascherman Professor of Engineering.

[1] J. A. Silberman, P. Morgen, I. Lindau, W. E. Spicer, and J. A. Wilson, J. Vac. Sci. Technol. **21**, 142 (1982).
[2] A.-B. Chen and A. Sher, J. Vac. Sci. Technol. **21**, 138 (1982).
[3] U. Solzbach and H. J. Richter, Surface Science **97**, 191 (1980).
[4] H. M. Nitz, O. Ganshow, U. Kaiser, L. Wiedman, and A. Benninghoven, Surface Sci. **104**, 365 (1981).
[5] P. Morgen, J. A. Silberman, I. Lindau, W. E. Spicer, and J. A. Wilson, accepted, Journal of Electronic Materials (to be published).
[6] J. A. Silberman, P. Morgen, I. Lindau, W. E. Spicer, and J. H. Wilson, J. Vac. Sci. Technol. **21**, 154 (1982).

2.8

Dominance of Atomic States in a Solid: Selective Breakdown of the Virtual Crystal Approximation in a Semiconductor Alloy, $Hg_{1-x}Cd_xTe$

W. E. Spicer, J. A. Silberman, J. Morgen,[a] and I. Lindau

Stanford Electronics Laboratory, Stanford University, Stanford, California 94305

and

J. A. Wilson

Santa Barbara Research Center, Goleta, California 93017

and

An-Ban Chen

Physics Department, Auburn University, Auburn, Alabama 36830

and

A. Sher

SRI International, Menlo Park, California 94025

(Received 4 May 1982)

Ultraviolet-photoelectron-spectroscopy experiments and a coherent-potential-approximation calculation of the density of states of $Hg_{1-x}Cd_xTe$ show a clear deviation from virtual crystal behavior in bands ≥ 5 eV below the valence-band maximum where there is a 60% s-electron contribution. The large ($\simeq 1.4$ eV) atomic s-state shift between Hg and Cd is responsible for this deviation, as well as for the decrease of the band gap (1.5 to 0 eV) with composition, the high electron mobility (10^6 cm^2/V s), and difficulties experienced with growth and mechanical properties.

PACS numbers: 71.25.Tn, 79.60.Eq

Over ten years ago, it was firmly established[1] that metallic alloys such as NiCu required consideration of markedly different potentials for each atomic species. This forced the abandonment of the rigid-band model for metallic alloys (which had been widely accepted up to that time) and had enormous significance for fields extending from metallurgy to catalysis. In contrast, the relatively simple virtual crystal approximation (VCA), in which average potentials are assigned to each sublattice site, had been successful with semiconductors.

The objectives of this paper are to (1) show definitive experimental and theoretical evidence for the selective breakdown of VCA in a semiconductor alloy ($Hg_{1-x}Cd_xTe$), (2) establish that the coherent-potential approximation (CPA) works well where VCA fails, and (3) explain the physics underlying the shortcomings of the VCA in terms of the atomic orbitals involved.

$Hg_{1-x}Cd_xTe$ exhibits a number of properties that are both of fundamental interest and suitable for exploitation.[2] Because the lattice constants of HgTe and CdTe are nearly identical, the entire composition range can be made in the zinc-blend structure with a continuous change of band gap from 1.5 eV (CdTe) to 0, making these materials prime candidates for use in infrared photodetectors. Enormous electron mobilities ($>10^6$ cm^2/V s) are found for small band gaps, confirming the occurrence of extremely nonlocalized wave functions near the band edges.[3] As we will see, the breakdown of VCA occurs deep in the valence bands, where the states are more localized and have a large atomic "s" character.

Ultraviolet-photoelectron-spectroscopy measurements were made on samples cleaved along a (110) face in ultrahigh vacuum ($p < 10^{-10}$ Torr) with photon energies ranging from 7 to 30 eV on four compositions, $x = 0.2$, 0.31, 0.39, and 1. Figure 1 shows energy distribution curves (EDC's) for $12 \leq h\nu \leq 17$ eV (resolution < 0.2 eV) for an alloy sample and CdTe. The valence-band maximum (VBM) is taken as the zero of energy. Two major groups of valence-band features appear between -3.5 and 0 eV, and one between -6 and -4 eV. The upper feature exhibits dispersion characteristic of delocalized states.[4] The lower feature shows no dispersion (as would be expected for a more localized state), and it is here that breakdown of VCA is found. This same qualitative valence-band behavior was found in all $Hg_{1-x}Cd_xTe$ samples.

In Fig. 2, we examine the experimental struc-

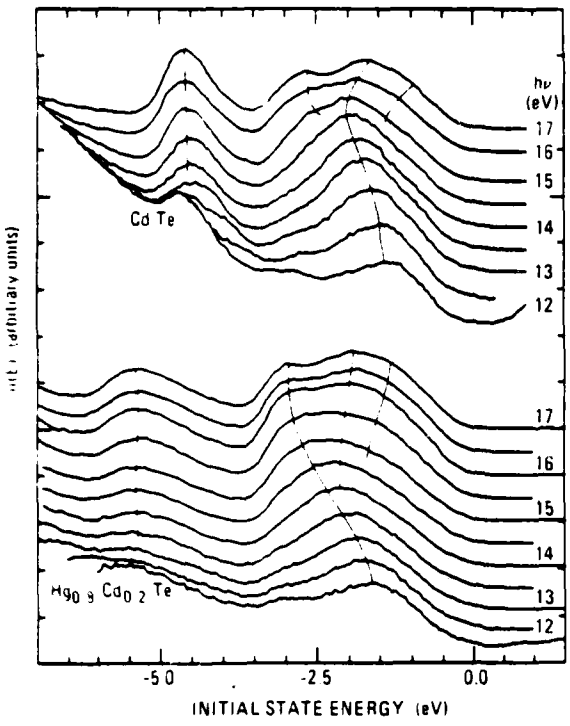

FIG. 1. Photoemission energy distribution curves for CdTe and the alloy $Hg_{0.8}Cd_{0.2}Te$. The number of electrons detected is plotted vs initial state energy with the origin set to the valence-band maximum. Contrast the relatively large dispersion and widths of the "p-like" bands within 3.5 eV of the valence-band maximum (VBM) with the small dispersion of the band centered about 5 eV below VBM. This band is relatively narrow in CdTe but broadened by the alloy effects in $Hg_{1-x}Cd_xTe$.

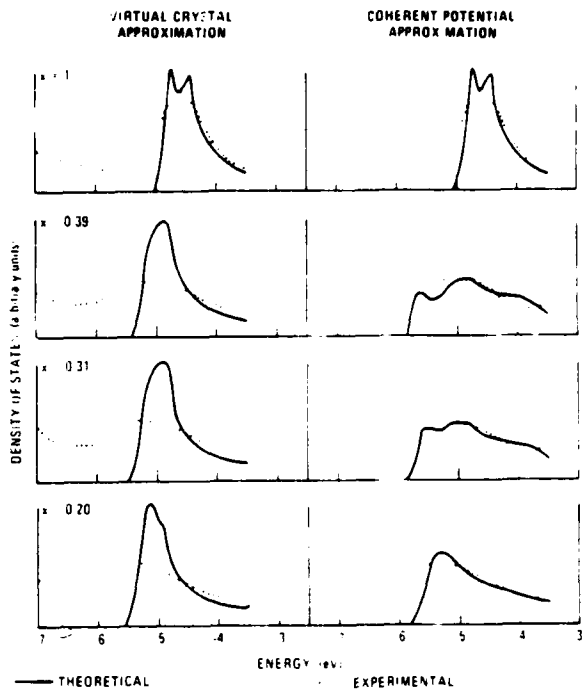

FIG. 2. Comparison of theory and experiment for $Hg_{1-x}Cd_xTe$ for the compositions indicated by the value of x in the figures. The virtual crystal approximation clearly does not agree with experiment for the alloys, whereas the agreement with coherent-potential theory is *surprisingly* good. No "experimental" broadening has been included in the theoretical curves, nor has background been subtracted from the experimental curves.

ture between − 3.5 and − 7 eV as a function of composition and compare it with the VCA and CPA calculations. The calculations give the density of states (DOS); because we found negligible dispersion for the features in this energy range, the EDC's should be closely related to the calculated DOS and can legitimately be compared. The experimental and theoretical curves were aligned in energy by superimposing the leading edge of the EDC's (i.e., experimental VBM) with the VBM given by the calculations. The structure in the calculated curves is sharp in comparison with the experimental curves. This results (at least in part) from the fact that no broadening has been put into the calculations to account for the finite (≈ 0.2 eV) experimental resolution or other broadening effects. Furthermore, the low-energy scattering-induced tail in the EDC has not been subtracted from the data.

Figure 2 shows that the general experimental features and trends in the alloys are predicted well by the CPA, but not by the VCA: The VCA predicts a peak with a relatively narrow total width (≃ 0.5 eV), which moves monotonically in energy from CdTe (− 4.6 eV—weighted average of the doublet) to that calculated for HgTe (−5.5 eV—not shown in curves, because no experimental data were available for HgTe). Most importantly, the width of the VCA-predicted peak(s) does not increase appreciably with energy. The CPA results (in agreement with experiment) increase in width as one moves from CdTe into the alloys. For $x = 0.39$ eV, both experiment and CPA give a width of ≃ 2 eV, roughly four times what would be predicted by VCA. More detailed examination of the $x = 0.39$ and $x = 0.31$ CPA curves indicates that peaks can be resolved near − 5.6 and − 5.0 eV and that there exists a weaker shoulder near − 4.2 eV. CPA calculations identify the origins of these three features: The

-5.6-eV peak and the shoulder are due to Hg- and Cd-derived s states, respectively; the intermediate peak is a "VCA-like" peak with p symmetry. Note that it lies at the same energy as the VCA peak (left panel of Fig. 2) and, insofar as can be seen, moves with energy, as does the VCA peak.

The theory proceeds in three steps: obtaining accurate band structures for HgTe and CdTe, characterizing the disorder of the potential in the alloys, and executing the CPA calculation.[5] The Hamiltonian matrix $H_0(\vec{k})$ for a given $\vec{k}$ is calculated in the manner described in Ref. 5 with use of published[6] local empirical pseudopotentials. A systematic orthogonalization and $\vec{k}$-integration procedure transforms the initial Gaussian orbital sp^3 set into a set of completely orthonormal atomiclike orbitals (OAO). The diagonalization of $H(\vec{k})$ then yields a band structure without the spin-orbit splittings. The spin-orbit interaction is incorporated as a simplified Animalu model.[7] The other relativistic corrections (the velocity term and the Darwin term) do not alter the symmetry of $H(\vec{k})$ and are partially taken into account in $H(\vec{k})$ by the choice of the parameters in the empirical pseudopotential.

Because of the limitations of local pseudopotentials and the truncated basis set, the net Hamiltonian $H(\vec{k}) - H_{\text{CPA}}(\vec{k})$ introduced thus far yields results differing from experiment by $\simeq 5\%$. The corrections needed to reach agreement with experiment are incorporated into the theory (as justified previously) by the addition of a localized perturbation Hamiltonian H_1.[5]

To facilitate the characterization of the local interactions and the CPA calculation, the OAO set is next transformed into completely orthonormal cell orbitals (OCO) with proper symmetries. The minimum basis then consists of two A_1 and six T_2 OCO's. When spin is included, each A_1 becomes two Γ_6 OCO's, and the six T_2's become four Γ_7 and eight Γ_8 OCO's. The crystal Hamiltonian matrix in the OCO basis for a given cell becomes block diagonal into eight 2×2 matrices: two in Γ_6, two in Γ_7, and four in Γ_8 representations. Because all the $2\cdot 2$ matrices for a given representation are the same, there are only nine independent single-cell interactions: six diagonal energies $\epsilon_\alpha(\Gamma_\eta)$, $\alpha = 1,2$, $\eta = 6,7,8$; and three off-diagonal interactions γ_η. These local energy parameters for HgTe and CdTe have been determined from parametrized band structures; their values are listed in Table I. Note that major differences between HgTe and CdTe are in the $\epsilon_1(\Gamma_6)$ and γ_6 terms; these terms are influenced strongly by the $5s^2$ and $6s^2$ valence orbitals of Cd and Hg, respectively. (The physical significance of this is discussed below.) The antibonding $\epsilon_2(\Gamma_6)$ and all the other states (which have T_2 or p-like symmetry) have small energy differences.

TABLE I. Intracell Hamiltonian matrix elements for HgTe and CdTe.

Local energy parameter	Intracell Hamiltonian matrix element (eV) HgTe	CdTe
$\epsilon_1(\Gamma_6)$	-12.96	-11.19
$\epsilon_2(\Gamma_6)$	-2.26	-2.27
γ_6	-2.52	-4.31
$\epsilon_1(\Gamma_7)$	-7.16	-6.58
$\epsilon_2(\Gamma_7)$	-1.45	-1.45
γ_7	-3.59	-3.43
$\epsilon_1(\Gamma_8)$	-7.08	-6.55
$\epsilon_2(\Gamma_8)$	-1.42	-1.43
γ_8	-3.61	-3.43

In the OCO basis, the alloy Hamiltonian can be written as $H = \bar{H} + \sum_l V_l$, where $\bar{H}$ is the average periodic VCA Hamiltonian and the random part V_l is the sum over nine terms of the form $|\psi_l{}^\alpha\rangle \times \delta\epsilon_{\alpha\beta}\langle\psi_l{}^\beta|$, where the $|\psi_l{}^\alpha\rangle$ are the OCO's of the lth cell, and $\delta\epsilon_{\alpha\beta}$ are the deviations from the mean for the nine intercell interactions. If only the diagonal terms in V_l are retained, then the CPA calculation reduces to the one reported before.[5]

Why has VCA worked so well in other semiconductors but performed poorly with $Hg_{1-x}Cd_xTe$? First, note that $Hg_{1-x}Cd_xTe$ is the first "covalent" semiconductor alloy studied containing "light" ($Z < 57$) and heavy ($Z > 78$) atoms. The explanation lies in the atomic orbitals of these atoms. The relative binding energies of the p and s orbitals of the cations in covalent semiconductors do not change appreciably as one moves through the periodic table until one moves from atomic numbers below 57 to those above 78. Above $Z = 78$, the s orbitals become markedly more tightly bound with respect to the p (or other higher-angular-momentum orbitals) as relativistic terms (which tend to decrease the orbital radius) become important. This is because the valence s orbitals, which penetrate the nucleus much more than do the orbitals with nonzero angular momentum, are more sensitive to these terms. We shall refer to this effect as the *s shift*. In the

present case, the ionization energy of the Hg $6s^2$ valence electrons is 1.4 eV higher than that of the Cd $5s^2$. It should further be noted that the work in the early 1960's showed[2] that both the decrease of E_g to zero and the high electron mobilities are associated with the metal s states of the conduction band decreasing in energy with increasing Hg content until they mix with the p states to form the valence-band maximum. We thus identify three phenomena (the breakdown of VCA, E_g going to zero, and high electron mobility) as resulting from the Hg $6s^2$ atomic levels being significantly below the Cd $5s^2$ levels.

$Hg_{1-x}Cd_xTe$ is perhaps the most promising material available for photodetection throughout the infrared, yet it has not been widely exploited. This may be because of difficulties in growing and handling the material[2]; we suggest that this also results from the "s shift" (i.e., selectivity increasing the bonding energy of the Hg valence s levels, which weakens the Hg-Te bond and leads to the difficulties mentioned above).

It is our hope that this paper will stimulate work to test our suggestions. Such work is greatly needed, both for fundamental understanding and to guide (and reduce the cost of) practical work.

This work was supported by U. S. Defense Advanced Research Projects Agency Contract No. MDA 903-80-C496 and U. S. Air Force Office of Scientific Research Contract No. F49620-81-K0012; work was performed at the Stanford Synchrotron Radiation Laboratory, which is supported by the National Science Foundation in cooperation with the U. S. Department of Defense One of us (J.A.S.) was the recipient of a National Science Foundation predoctoral fellowship.

[a]Permanent address: Fysisk Institut, Odense University, Capusvej 55, DK-5230, Odense M, Denmark.

[1]See, for example, *Band Structure Spectroscopy of Metal and Alloys*, edited by D. J. Fabian and L. M. Watson (Academic, London, 1973).

[2]See, for example, R. Dornhaus and G. Nimtz, in *Solid-State Physics*, Springer Tracts in Modern Physics Vol. 78 (Springer-Verlag, Berlin, 1976), p. 1 and references therein.

[3]P. Morgen, J. Silberman, I. Lindau, W. E. Spicer, and J. A. Wilson, J. Cryst. Growth 56, 493 (1982); P. Pianetta, I. Lindau, C. M. Garner, and W. E. Spicer, Phys. Rev. B 18, 2792 (1978); P. Pianetta, I. Lindau, P. E. Gregory, C. M. Garner, and W. E. Spicer, Surf. Sci. 72, 298 (1978).

[4]J. A. Silberman, P. Morgen, I. Lindau, W. E. Spicer, and J. A. Wilson, to be published; W. E. Spicer, in *Optical Properties of Solids—New Developments*, edited by B. O. Seraphin (North-Holland, Amsterdam, 1976).

[5]A.-B. Chen and A. Sher, Phys. Rev. B 23, 5360 (1981).

[6]D. J. Chadi, J. P. Walter, and M. L. Cohen, Phys. Rev. B 5, 3058 (1972).

[7]A. O. E. Animalu, Philos. Mag. 13, 53 (1966).

Physica 117B & 118B (1983) 60-62
North-Holland Publishing Company

UNUSUAL BEHAVIOR OF $Hg_{1-x}Cd_xTe$ AND ITS EXPLANATION*

W. E. Spicer, J. A. Silberman, P. Morgen, and I. Lindau
Stanford University, Stanford, CA 94305

J. A. Wilson, Santa Barbara Research Center

An-Ban Chen, Auburn University

A. Sher, SRI International

This paper involves an unusual semiconductor alloy, $Hg_{1-x}Cd_xTe$, a breakdown of the Virtual Crystal Approximation (VCA) in that alloy (the first such breakdown in a semiconductor alloy), the success of the Coherent Potential Approximation (CPA), the "first order" explanation of these results in terms of energies of atomic valence levels, and the qualitative explanation of the unusual properties of $Hg_{1-x}Cd_xTe$ in terms of the results reported above. The genesis of the work was the use of photoemission spectroscopy. Cd and Hg core shifts are detected as a function of alloy composition and related to bonding concepts developed here.

1. INTRODUCTION

$Hg_{1-x}Cd_xTe$ is a semiconductor alloy crystallizing in the zinc blende structure in which Hg and Cd randomly occupy sites on the cation sublattice. Until recently, the electronic structure of $Hg_{1-x}Cd_xTe$ and all other semiconductor alloys has been theoretically treated within the framework of the Virtual Crystal Approximation (VCA), in which the potential used is a compositionally weighted average of the potentials of Hg and Cd. This approach has been shown to be consistent with the nearly linear variation of the bandgap in this alloy from 1.5 eV to zero with increasing Hg content [1-5] and the large electron mobility (~10^6 cm^2/v-sec) found for narrow bandgap compositions. The volatility of Hg at slightly elevated temperature [6] and the relative ease of forming Hg vacancies, on the other hand, suggest that the bonding differs for Hg and Cd and that the electronic structure of the alloy should reflect the difference in potential of the Hg and Cd sites.

To investigate the electronic structure of $Hg_{1-x}Cd_xTe$, we have used Ultraviolet Photoemission Spectroscopy (UPS) with photon energies from 7 to 30 eV to examine single crystal alloys of three compositions and CdTe. The UPS results are compared to a recent calculation of the alloy density of states [7] computed using the Coherent Potential Approximation. CPA, unlike VCA, retains the aperiodic nature of the cation potential. In the UPS data, the upper, mainly p-like valence states within ~3.5 eV of the valence band maximum (VBM) were found to be band-like and qualitatively similar for all compositions studied in agreement with VCA calculations. In contrast, the lower lying states near 5 eV below the VBM, which are principally metal s-electron derived but contain 40% cation p-character, are more localized and reflect distinctly Hg or Cd parentage. Thus, the UPS data document differences in the contributions of the two cations to the electronic structure of the alloy and the selective breakdown of the VCA for the mainly metal s-electron band [8]. These observations are confirmed by comparison to the CPA calculation. The origin and consequences of the difference in cation bonding are discussed below.

2. EXPERIMENTAL

Clean surfaces of single crystal samples of $Hg_{1-x}Cd_xTe$ (x=0.2, 0.31, 0.39) grown by solid state crystallization (Santa Barbara Research Center) and a sample of CdTe (II-VI Inc.) were prepared by cleaving the samples along a (110) face in vacuum ($p < 10^{-10}$ torr). Light from a synchrotron source was incident on the cleaved surface at a 75° angle to the surface normal and largely p-polarized. A double pass cylindrical mirror electron spectrometer with symmetry axis along the sample normal performed the energy analysis of the emitted electrons. Electron Energy Distributions Curves were recorded for photon energies ranging from 7 to 30 eV. The energy resolution in the spectra obtained is believed to be better than 0.2 eV. In a separate experiment, a spectrum of cleaved (110) HgTe was recorded in a similar manner, but using a He discharge with monochromator as light source.

3. RESULTS

The selective breakdown of the VCA is apparent in the photon energy and compositional

* Supported by DARPA Contract No. MDA 903-80-C496 and in part by AFOSR. A portion of this work was performed at the Stanford Synchrotron Radition Laboratory which is supported by the National Science Foundation through the Division of Materials Research.

0 378-4363 83 0000 -0000 $03.00

dependence of the photoemission spectra. Peaks in the emission from the upper, mainly p-like valence states within ~3.5 eV of the VBM shift in binding energy as the photon energy is varied (Figure 1). Such dispersion with hν is characteristic of direct transitions between extended states [9]. As indicated in Figure 1, the emission from the upper portion of the valence bands shows similar features for all compositions.

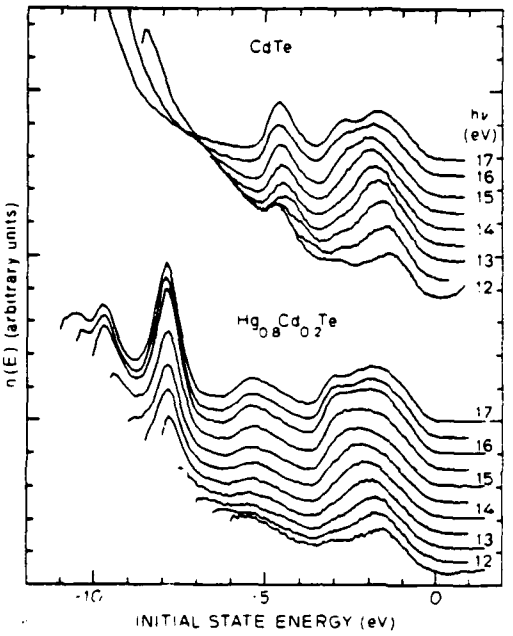

Fig. 1. Photon energy dependence of the valence band emission of $Hg_{1-x}Cd_xTe$

The mainly metal s-electron derived states in the region 4 to 6 eV below the VBM show little or no dispersion with photon energy but exhibit stronger compositional dependence then the upper, p-like bands [8]. The emission from this region is shown in Figure 2, where it is compared to the density of states in this energy range calculated in both the VCA and coherent potential schemes. The experimental and theoretical curves are aligned by superimposing the leading edge of the measured electron distribution with the VBM given by the calculations. Broadening has not been applied to the calculated curves nor background corrections made to the measured ones. As can be seen in the figure, the general experimental features and trends in the alloys are predicted well by the CPA but not by the VCA. In the virtual crystal case, a single sharp peak is predicted which remains sharp and shifts monotomically with decreasing Cd content. The UPS data show instead a broadening of the band as Hg is added and a

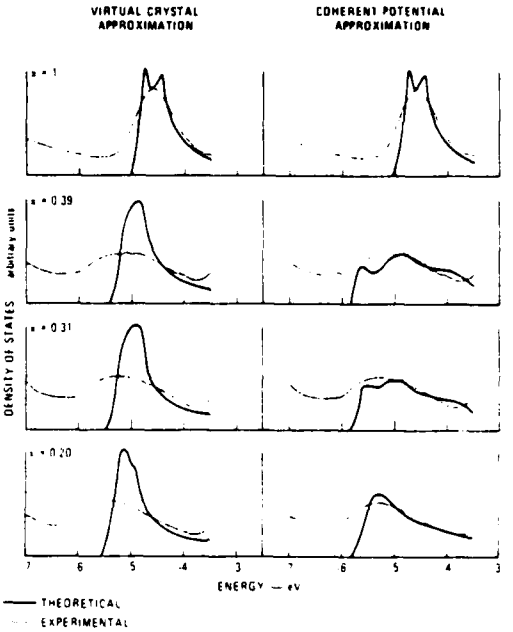

Fig. 2. Comparison of theory and experiment for $Hg_{1-x}Cd_xTe$

decrease in emission near -4.6 eV as the Cd content is reduced. This behavior is reproduced by the structure in the CPA density of states: The peaks at -5.6 and -4.2 eV in the x = 0.31 curve arise from Hg and Cd valence s-electrons, respectively, while the center peak near -5.0 eV is of cation p-character and exhibits VCA-like movement with x.

In addition to the separate contributions of Hg and Cd valence s-electrons to the electronic structure, the differences in Hg-Te and Cd-Te bonds are manifest in the change in binding energy relative to the valence band maximum of the Cd 4d and Hg 5d core levels. Figure 3, showing spectra recorded at 21 eV, details the location of these core levels relative to the VBM for the four samples studied. A spectrum obtained with hν = 21.2 eV from cleaved (110) HgTe is also shown. The peaks at -7.9 and -9.6 eV in the alloy arise from the spin-orbit split Hg 5d levels, while the Cd 4d lines appear around -10.4 eV and are split by 0.6 eV. Apparent in Figure 3 in a shift of 0.2 eV to higher binding energy of the Cd d-levels in going from CdTe to the x = 0.39 alloy and a smaller decrease in binding energy of the Hg 5d lines between HgTe and the alloys. The Cd and Hg contributions to the bonding, therefore, vary as the average composition changes.

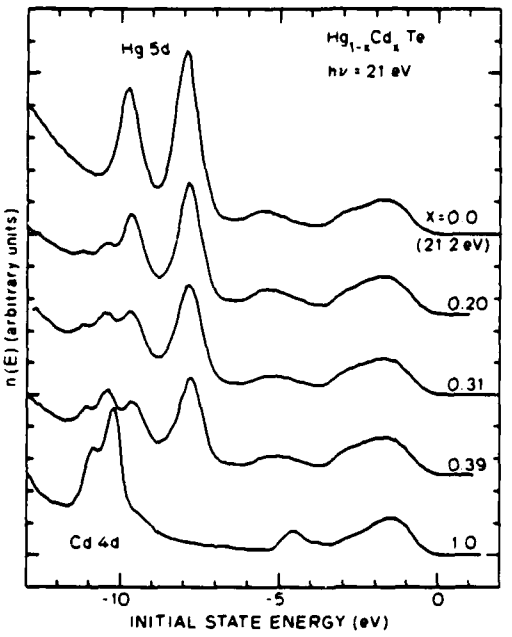

Fig. 3. Comparison of valence band and cation core level emission.

4. DISCUSSION

The breakdown of the VCA as well as the variation in the alloy bandgap are consequences of the difference in cation valence electron s-state energy and can be understood by considering atomic Cd and Hg. The Hg 6s electrons are bound 1.4 eV more strongly than the 5s electrons in Cd [10] while the p-state energies are nearly equal. The increase in binding energy arises from relativistic interactions which more strongly affect s- than p-orbitals and are greater in the higher Z Hg. The role of the cation s-electron in determining the bandgap in the alloy is illustrated by a model calculation of the band structure [1] performed within the VCA where the bands for HgTe were made to approximate those of CdTe by shifting the energy of the cation s-state. That this s-shift arise from relativistic interactions became clear by evaluating the contribution to the calculated energy of the states at the band edge from terms in a relativistic Hamiltonian used in a tight binding calculation of the alloy band structure [3]. Away from the band edges, the difference in cation s-state energy results in separate contributions to the elctronic structure and the breakdown of the VCA. Because the Hg valence electrons are more tightly bound, bond formation with Cd may be favored. The shift in energy of the Cd 4d and Hg 5d core lines as the Hg content increases is consistent with this view, with the Cd-Te bond becoming more ionic. A variation in the separation of Hg and Cd d-levels as a function of composition has been observed in HgCd alloys [11]; the explanation of this effect as due to d-band overlap is unlikely to apply to the case of $Hg_{1-x}Cd_xTe$, where the cations are second neighbors. Size effects may also contribute to the reduced Hg-Te bond strength [12].

The ease with which lattice defects are formed and the difficulty of growth of alloys with low Cd content may be a consequence of the increased difference in cation bonding. Because the variation in bandgap and breakdown of the VCA arise from the same feature, the large difference in cation valence electron binding energy, these difficulties will likely occur in other semiconductor alloy systems where the bandgap varies over such a large range.

References

[1] H. Overhof, Phys. Stat. Sol. B45 (1971) 315.
[2] Shin-ichi Katsuki and Makoyo Kunimune, J. Phys. Soc. Jap. 31 (1971) 415.
[3] A. Kisiel and P. M. Lee, J. Phys. F2 (1972) 395.
[4] D. J. Chadi and Marvin L. Cohen, Phys. Rev. B7 (1973) 692.
[5] M. Podgorny and M. T. Czyzyk, Sol. State Comm. 32 (1979) 413.
[6] R.F.C. Farrow, G. R. Jones, G. M. Williams, D. W. Sullivan, W.J.O. Boyle, and J.T.M. Wotherspoon, J. Phys. D12 (1979) L117.
[7] A.-B. Chen and A. Sher, J. Vac. Sci. Tech. 21 (1982) 138.
[8] J. A. Silberman, P. Morgen, I. Lindau, W. E. Spicer and J. A. Wilson, J. Vac. Sci. Tech. 21 (1982) 142.
[9] W. E. Spicer in B. O. Seraphin, Optical Properties of Solids--New Developments (North-Holland, Amsterdam, 1976).
[10] C. E. Moore, Atomic Energy Levles as Derived from analysis of Optical Spectra (U.S. Gov't Printing Office, Washington, D.C., 1958).
[11] J. A. Nicholson, R.C.G. Leckey, J. D. Riley, J. G. Jenkin, and J. Liesgang, J. Phys. F9 (1979) 393.
[12] J. C. Phillips and J. A. Van Vechten, Phys. Rev. B2 (1970) 2147.

2.10

Evidence of stress-mediated Hg migration in $Hg_{1-x}Cd_xTe$[a)]

P. M. Raccah and U. Lee
Department of Physics, University of Illinois at Chicago, Chicago, Illinois 60680

J. A. Silberman and W. E. Spicer
Stanford Electronics Laboratories, McCullough Building Number 228, Stanford University, Stanford, California 94305

J. A. Wilson
Santa Barbara Research Center, Goleta, California 93017

(Received 1 September 1982; accepted for publication 30 November 1982)

Photoemission results from some ⟨110⟩ cleaved surfaces of $Hg_{1-x}Cd_xTe$ indicate that the Fermi level is pinned suggesting that while the bulk of the material is p type the area stressed during cleavage has been converted to n type. Electrolyte electroreflectance (EER) measurement confirmed the n-type character of the cleaved surface and showed that the alloy composition x at the surface, after cleavage, is high ($x = 0.22$) compared to the bulk value ($x = 0.185$). The high x value associated with the n character indicates that under stress the Hg migrates, at least partially, via the formation of donor defects. The defect density is reflected in the EER linewidth.

PACS numbers: 78.50.Ge, 79.60.Eq

The treatment of $Hg_{1-x}Cd_xTe$ (MCT) surfaces is delicate because of the intrinsic fragility of the material. By coupling photoemission with electrolyte electroreflectance (EER) studies we have been able to analyze the response of MCT to mechanical shock, and conclude that under stress mercury tends to migrate, at least in part, via charged defects conferring an n character to the material.

In the photoemission experiments, the surface Fermi level position was measured[1] for ⟨110⟩ faces of MCT prepared by cleaving in vacuum.[2] In addition, the composition of the surface region was monitored for extended periods after cleaving[3] for comparison to surfaces prepared in vacuum in another way.[4] A cleavage surface was transported through air for EER analysis of both the cleavage face and the side of the crystal, which had been prepared by cutting, mechanical polishing, and etching prior to cleaving. Our objective in comparing the cleaved and polished faces as well as the vacuum prepared surfaces is to begin to gain insight into the critical problem of "damage" in MCT and its surface. Such knowledge is essential to economic utilization of the unique properties of MCT in infrared imaging and other possible electronic systems.

In Fig. 1, we present an energy distribution curve (EDC) obtained by cleaving and measuring a MCT crystal in ultrahigh vacuum (UHV). While this curve was obtained from a different sample than that examined by EER, the behavior is the same as that of the EER sample and representative of several cleaves. The material cleaved was p type; however, as can be seen from Fig. 1, the surface position of the Fermi level was well above the expected bulk position, indicating that the surface had been converted from p to n type by the mechanical shock due to the cleavage.

Using the intensities of the Cd and Hg core levels, the Hg loss due to the surface damage could be detected, if it occurred, after cleavage. No loss was observed after many hours.[3] In contrast, for a surface cleaned in UHV by a "spinning razor blade" a continuous loss of Hg over many hours and a depletion up to depths of 5 μ (at 330 K) has been reported.[4] Thus, the cleaving and "spinning razor blade" clearly appear to produce different degrees of damage.

The cleaved and polished surfaces also exhibit different amounts of damage. As we will see EER gives considerable detail about the surface region. Thus, the majority of this letter will concentrate on results obtained by that method.

We have conducted three sets of EER experiments on the E_1 interband transition of a cleaved MCT crystal. The experimental system has been described earlier[5] and need not be detailed here. It has been shown[6] that the EER line shape $L(E)$ can be represented by the expression

$$L(E) = \mathrm{Re}\left[ce^{i\theta}(E_g - E + i\Gamma)^{-n}\right],$$

where the magnitude c and the phase θ are parameters which vary very little with the incident light energy E and are usually considered constant in the fit of EER line shapes. The interband transition energy E_g and the broadening parameter are the two other parameters to fit. The exponent n

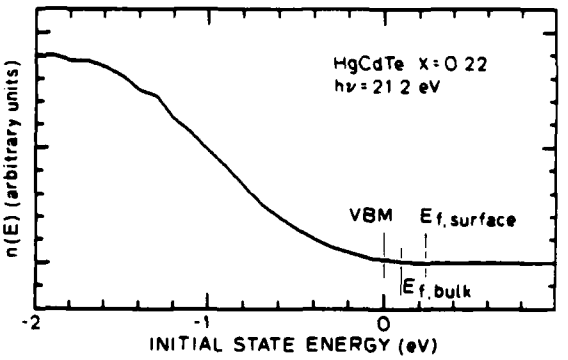

FIG. 1. Upper valence-band emission from $Hg_{0.78}Cd_{0.22}Te$; the number of electrons per second detected is plotted against the electron initial state energy with the origin set to the valence-band maximum. The expected bulk Fermi level position and measured Fermi level at the surface are shown.

[a)] This research was supported by the Defense Advanced Research Projects Agency under contract No. MDA-903-80-C-0090 and No. MDA-903-82-C-0506.

 0003-6951/83/040374-03$01.00

TABLE I. Summary of results obtained by fitting the EER line shapes in three cases: the case of the cleaved ⟨110⟩ face before damage removal: the case of the cleaved ⟨110⟩ face after damage removal; the case of a polished side surface of the same sample.

Results	θ	E_1 in eV	x	Γ in eV	Type
Before damage removal	0.5 ± 0.2	2.314 ± 0.004	0.220 ± 0.004	0.111 ± 0.005	n
After damage removal	0.2 ± 0.2	2.289 ± 0.004	0.188 ± 0.004	0.084 ± 0.005	p
From the polished side surface	2.2 ± 0.2	2.284 ± 0.004	0.181 ± 0.004	0.167 ± 0.005	p, n

is determined by the symmetry of the critical point in the Brillouin zone. We have found that the exponent fitting best all MCT results is $n = 2.5$ which corresponds to a tridimensional point. This is expected for the E_1 interband transition in most II-VI and III-V semiconductors.

The first set of experiments was carried out on the cleaved surface ($\sim 4 \times 4$ mm). Many spectra were taken at various points on the surface with a finely focused beam ($\sim 130 \mu$) and the line shapes fully analyzed. The results were very consistent, indicating a good uniformity of properties for the overall sample. The average values of the parameter are given, in the first line of the table, with their standard deviations. The alloy composition x was determined using the relationship E_1 vs x established earlier.[7]

The second set of experiments was carried out exactly in the same manner and within the same area. The only difference was the removal of $\sim 2 \mu$ of material by the standard 2% Br_2/methanol jet-etch. The topography of the sample under the metallographic microscope was unchanged. The purpose of the etch was to remove the cleavage damage. After anodization, carried out so as to form an oxide layer ~ 150 Å thick,[7] the results were very consistent. They are listed in the second line of Table I with their standard deviations.

Finally, since the sample was essentially a cube $4 \times 4 \times 4$ mm it was possible to carry out a third set of experiments on a side face of the sample which had been normally prepared by cutting, polishing, and etching. Here, we submitted the surface to a check of uniformity in depth as well as laterally through repeated jet-etching/anodization steps of the type used to remove the cleavage damage. Again, the results were very consistent and are summarized in the third line of Table I.

Representative runs from the first two sets of experiments are shown in Fig. 2. As can be seen, the line shapes are inverted one with respect to the other. Since it has already been shown[6] that, in the low field limit, the EER signal is given by

$$\Delta R / R = qNV_m L(E),$$

where q is the sign of the minority carriers, N the carrier concentration, V_m the modulation voltage, and $L(E)$ the EER line shape, this result clearly shows that the surface of the cleavage fracture is inverted and has an n character consistent with the photoemission results.

As can be seen in Table I the surface inversion observed after cleavage is associated with a high x value (~ 0.22) when compared to the value measured after removal of the cleavage damage (~ 0.188) or on the side surface, whether jet-etched or not (~ 0.181). The difference is well outside experimental error and indicates mercury impoverishment of the stressed volume. It is probable that mercury has actually migrated under stress and diffused out of the surface. Our results suggest that the mercury diffusion occurs, at least partially, via charged defects conferring an n character to the material.

The broadening parameter Γ is primarily affected by lattice defects such as disorder, vacancies, dislocation, etc.[5] and with a soft material such as MCT reflects very sensitively the response of the surface to treatment. As can be seen in Table I, the results are edifying. A surface developed by cleavage exhibits a value of $\Gamma \sim 0.111$ eV while a surface developed by cutting, polishing, and etching still exhibits treat-

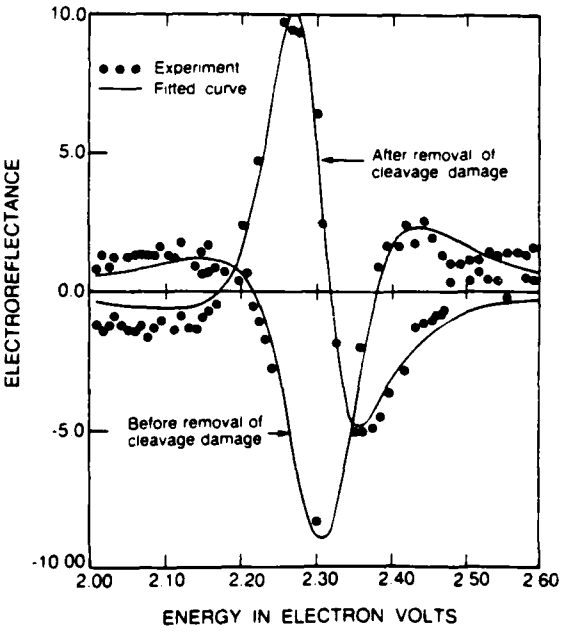

FIG. 2. EER data and fitted line shape. The traces presented here were obtained on the cleaved ⟨110⟩ face before and after removal of the damage. The line shapes are clearly inverted with respect to one another reflecting the change in the type of the minority carriers.

ment damage as shown by the large value of $\Gamma \sim 0.167$ eV. After removal of the cleavage damage Γ is of the order of 0.084 eV, a value not too different from that determined for defect-free GaAs surfaces[8] ($\Gamma \sim 0.060$ eV). Repeated jet-etching/anodization steps of the side surface to a depth of $\sim 17\,\mu$ (third set of experiments), however, failed to remove entirely the damage generated by the chemomechanical polish and while there was some decrease of Γ its value (~ 0.142 eV) remained much higher than 0.084 eV. In other words, conventional surface preparation of MCT seems to generate very deep damage which clearly affects electronic properties and is not easily removed. In our case the manner in which the sample was held during cleavage may have made an additional contribution to damage on the polished side face, but the value of Γ we observe here is not too different from the values we have observed on other samples which had not been cleaved.

Another interesting feature of the third set of experiments is the value of θ. The phase angle θ is a quantity related primarily to the strength of the electron-hole interaction and to the order of the critical point in the Brillouin zone contributing to the interband transition.[9] The value of θ yielded by the results obtained on the conventionally prepared side surface is $\theta \sim 2.2$; this value is quite consistent with the results we have obtained with a multitude of samples of different origins similarly prepared. However, it is very different from the value of 0.2 obtained from the cleaved surface.

This last result requires more study but one could suggest at least two possiblities. The first is a mixing of the M_1 and M_2 contributions as was concluded in an earlier thermoreflectance work.[10] The difficulty with this hypothesis is that this mixing would have to result from damage, since it is absent from the results obtained in the first and second sets of experiments (cleaved surface), and that seems unlikely. A more plausible hypothesis, one which would be consistent with all our results, is that the value of $\theta \sim 2.2$ results from superposed signals from primarily n and primarily p areas having different defect densities. In other words, damage seems associated with Hg migration and with the formation of n-type domains in the midst of the p-type bulk. This would not be observed in photoemission since the technique is applied to clean surfaces obtained by cleavage in ultrahigh vacuum and not to surface prepared conventionally.

Putting together the results reported here, considerable insight can be obtained into the type of surface (and perhaps bulk) damage which can be produced in MCT. The effect of cleavage in UHV is especially striking. The region within 2 μm or less of the surface is transformed to n type and has a higher Cd content when compared to the polished surface. The "pulsed" mechanical shock of the cleave results in electrically active defects (possibly Hg interstitials) and may produce a loss of Hg from the surface region. Relaxation of the lattice following the momentary cleavage shock is sufficient to yield a high degree of perfection, as indicated by the low value of Γ and lack of subsequent Hg out diffusion. The region 2 μ below the surface is surprisingly perfect ($\Gamma = 0.084 \pm 0.005$) and has a higher Hg content.

In contrast to the cleaved surfaces are those produced by polishing the same crystal. Here, no uniform type conversion takes place and a larger Hg content is observed than in the near surface region of the cleaved crystal. Rather, the θ value suggests that both n and p regions coexist with different defect densities. Thus, there may be a large degree of local damage and nonuniformity. This is also reflected by the large value of Γ (0.167 eV). It is important to note the linewidth is still large (0.142 eV) after 17 μ of MCT has been etched away.

This work emphasizes the large amount of damage which can be introduced into MCT by conventional techniques such as polishing. It also shows that other methods of surface preparation such as cleaving introduce much less and different types of damage. Perhaps the most significant conclusions in this work are those emphasizing the importance of "surface" and other damages in practical MCT applications. We hope that they will stimulate more extensive studies of damage mechanisms and structures.

[1] W. E. Spicer, P. Skeath, C. Y. Su, and I. Lindau, J. Phys. Soc. Jpn. **49**, Suppl. A 1079 (1980).
[2] P. Pianetta, I. Lindau, C. M. Garner, and W. E. Spicer, Phys. Rev. B **18**, 2792 (1978).
[3] J. A. Silberman, P. Morgen, I. Lindau, W. E. Spicer, and J. A. Wilson, J. Vac. Sci. Tech. **21**, 154 (1982).
[4] H. M. Nitz, O. Ganschow, U. Kaiser, L. Wiedmann, and A. Benninghoven, Surf. Sci. **104**, 365 (1981).
[5] R. L. Brown, L. Schoonveld, L. L. Abels, S. Sundaram, and P. M. Raccah, J. Appl. Phys **52**, 2950 (1981).
[6] D. E. Aspnes, Surf. Sci. **37**, 418 (1973).
[7] A. Lastras-Martinez, U. Lee, J. Zehnder, and P. M. Raccah, Proceedings of the First U.S. Workshop on the Physics and Chemistry of MCT, J. Vac. Sci. **21**, 157 (1982).
[8] S. Tachi, A. Moritani, and J. Nakai, J. Appl. Phys. **50**, 546 (1979).
[9] D. E. Aspnes, Phys. Rev. Lett. **28**, 913 (1972).
[10] Yu. F. Kavalyauskas and A. Yu. Shileika, Sov. Phys. Semicond. **13**, 671 (1979).

Section 3
CONCLUSION

The bulk property which makes $Hg_{1-x}Cd_xTe$ of such interest, the variation in bandgap as Hg is substituted for Cd, arises from the ~1.4 eV difference in binding energy of the valence s-electrons in atomic Hg and Cd. (The Hg 6s electrons are more tightly bound due to the importance of relativistic terms in the higher Z Hg.) The states at the conduction band minimum (CBM) are primarily cation s-states, and thus the CBM position is sensitive to x-value.[24] In order to obtain the large range of bandgap variation such as exhibited by HgCdTe, a large difference in valence electron energy for the randomly substituted elements is required. In $Hg_{1-x}Mn_xTe$, for example, the Mn ahd Hg valence electrons are even more widely separated than are those of Cd and Hg, with the result that the bandgap increases nearly twice as fast if Mn is substituted in HgTe than if Cd is used.[25]

The difference in electron energy in Hg and Cd results in differences in the bonding of HgTe and CdTe,[26] with weaker bond formation in the former case. Through the use of photoemission spectroscopy to probe the electronic structure of HgCdTe, we have observed that a difference in the bonding of Hg and Cd remains in the alloy, as evidenced by distinguishable Hg and Cd s-electron contributions to the valence bands of the solid.[27] This finding is at ods with previous theoretical treatments of the alloy electronic structure. Within the virtual crystal approximation (VCA), Hg-Te and Cd-Te bonds are rendered indistinguishable by calculating the band strtucture using a compositionally weighted average for the cation potential. Recent calculations [28-29] performed in the coherent potential approximately include the difference in Hg and Cd potential and correctly predict the behavior observed in the photoemission spectra.

The breakdown of the VCA in the s-electron contribution to the bonding of Hg and Cd has two important implications. It is likely the difficult materials problems associated with the alloy are a result of the weakness of the Hg-Te bond compared to that between Cd and Te.[30] The chemical shifts of the Hg 5d and Cd 4d core levels as a function of alloy composition observed in the photoemission data[31] as well as shifts in the NMR signals of Hg and Cd in the alloy[32] suggest the Cd-Te band becomes more ionic as Hg is added. This second neighbor effect is expected to further differentiate the bond strengths. A second,

related consequence of the breakdown of the VCA in the s-derived states deep in the valence band follows from the requirement of a large valence electron binding energy difference to produce a strong compositional dependence of the energy gap. Because the difficult materials properties have the same origin as the desired bandgap variation, any alloy system exhibiting an x-dependence of bandgap over a wide range may manifest similar difficulties in material growth.

One materials problem of special interest in HgCdTe is the high mobility of Hg in the lattice coupled with the ease of plastically deforming the alloy.[33-35] Samples of n-type $Hg_{0.8}Cd_{0.2}Te$ prepared by milling with a spinning razor blade in vacuum were reported to lose 25% of the Hg in the surface region in 3 hours at room temperature,[36] with Hg depletion occurring over a depth of 1000Å. Samples of p-type HgCdTe of the same composition prepared by cleaving in vacuum and monitored for tens of hours were found to be stable with regard to room temperature Hg loss.[37] To determine if subsurface microstructure introduced by the billing procedure could be responsible for the massive Hg loss, a p-type sample which had been cleaved was subsequently ground on a rotating diamond impregnated wheel in vacuum. The surface prepared in this way exhibited the same stability against Hg loss as was the one with simple cleavage. While damage to the material can enhance the Hg mobility as a result of the introduction of dislocations along which the Hg may rapidly migrate, the source of the Hg instability in one case and the lack of Hg loss in our measurements remains undetermined and an important issue in understanding the alloy properties.

As indicated above, the effects of damage to the alloy can be quite subtle. From direct measurement of the Fermi level position at the surface using photoemission techniques, it is usually observed that the surface produced by cleaving a p-type sample of solid state recrystallized HgCdTe is converted to n-type due to the mechanical chock of cleaving.[38-39] Type conversion is observed when p-HgCdTe is doped by ion bombardment; that this effect is due to some type of defect creation is evidenced by the fact that junction formation occurs independent of the implanted species and extends to a depth much greater than the range of the implant.[40]

Because of the high mobility of Hg in the lattice and the propagation of defects from the surface to some depth in the bulk, traditional surface properties must be considered in a broader context. One such property is the

reaction of the clean surface with oxygen. Like other II-VI compounds, HgCdTe is considerably more inert than group IV or III-V semiconductors as regards uptake of oxygen in the molecular ground state. The sticking coefficient for O_2 on the cleaved (110) surface is less than 10^{-13}.[41] In the case of oxidation stimulated by exposure of the clean surface to oxygen activated by operating a hot filament ionization gauge, a complex oxide containing Te and Cd is formed while Hg is released by the process. Continued study of native oxide formation is important to shed light on the chemistry of the alloy surface and communication of surface phenomena with the bulk.

ACKNOWLEDGMENTS

We gratefully acknowledge many helpful discussions with T.N. Casselman, D.R. Rhiger and R.E. Kvaas, and technical assistance with the DLTS experiments given by M.D. Jack, J.K. Henriksen and A. Toth of Hughes Aircraft Company, and to C.E. Jones and V.A. Cotton for aid in analysis of the DLTS and C-V data; and to R.A. Cole and C.R. Curtis who grew the crystals used in this study; and especially for the support and technical interaction from the Program Sponsor R.A. Reynolds of DARPA and the Technical Representative B.A. Sumner of NV&EOL.

We also appreciate greatly the opportunity to collaborate with Prof. P.M. Raccah, Prof. A.B. Chen, Dr. A. Sher, Dr. T. Magee and Prof. W.A. Harrison.

REFERENCES

1. W.E. Spicer, J.A. Silberman, P. Morgen, I. Lindau, J.A. Wilson, A.B. Chen and A. Sher, Phys. Rev. Lett. 49, 948 (1982)
2. A. Lastras-Martinez, V. Lec, P.M. Raccah and V. Zinder, J. Vac. Sci. Technol. 21, 157 (1982).
3. R.B. Schooler, B.K. Janousek, R.L. Ait, R.C. Carscallen, M.J. Daugherty, and A.A. Fote, J. Vac. Sci. Technol. 21, 164 (1982).
4. P. Morgen, J.A. Silberman, I. Lindau, W.E. Spicer and J.A. Wilson, J. Vac. Sci. Technol. 21, 161 (1982).
5. J.A. Wilson, C.E. Jones, V.A. Cotton, M.D. Jack, A.D. Toth and J.K. Henricksen, Paper C-12, Meeting of IRIS Specialty Group on Infrared Detectors, 27-29 July 1982, San Diego, CA.
6. D.R. Rhiger, J. A. Wilson, J.M. Myrosznyk, R.E. Starr, S.L. Price, K.A. Kormos, M. Ray, J.W. Peters, and N.H. Rogers. Paper D-8, Meeting of IRIS specialty group on Infrared Detectors, 27-29 July 1982, San Diego, CA.
7. J.A. Wilson, V.A. Cotton, J.A. Silberman, D. Laser, W.E. Spicer and P. Morgen. Presented at the second U.S. Workshop on the Physics and Chemistry of HgCdTe, Dallas, TX, 8-10 Feb. 1983.
8. D.K. Schroder and H.C. Nathanson, Solid-State Electronics 13, 577 (1970).
9. D.K. Schroder and J. Guldberg, Solid-State Electronics 14, 1285 (1971).
10. D.R. Rhiger and R.E. Kvaas, J. Vac. Sci. Technol. 21, 448 (1982).
11. P. Morgen, J. Silberman, I. Lindau, W.E. Spicer, and J.A. Wilson, J. Crystal Growth 56, 493 (1982).
12. S.A. Schwarz, C.R. Helmes, W.E. Spicer, and N.J. Taylor, NBS Publication 400-67 Series on Semi-Conductor Measurement Technology 1, Sept 1981.
13. Ibid.
14. R. Cartagne and A. Vapaille, Surf. Sci. 28, 157 (1971).
15. A. Lastras-Martinez, U. Lee, P.M. Raccah and V. Zender, J. Vac. Sci. Technol. 21, 157 (1982).
16. J.W. Peters and D.R. Rhiger, Paper I-3, Electronics Materials Conference, 24-27 June 1980, Ithaca, N.Y.
17. R.B. Schooler, B.K. Janousek, R.L. Ait, R.C. Carscallen, M.J. Daugherty and A.A. Fote, J. Vac. Sci. Technol. 21, 164 (1982).
18. Op. cit., Reference 6.
19. C.E. Jones, V. Nair, and D.L. Polla, Appl. Phys. Lett. 39, 248 (1981).
20. Op. cit., Reference 15.
21. J.A. Silberman, P. Morgen, I. Lindau, W.E. Spicer, and J.A. Wilson, J. Vac. Sci. Technol. 21, 142 (1982).
22. P. Morgen, J.A. Silberman, I. Lindau, W.E. Spicer and J.A. Wilson, J. Vac. Sci. Technol. 21, 161 (1982).
23. D.R. Rhiger and R.E. Kvaas, presented at the 1983 U.S. Workshop on HgCdTe, Dallas, TX, 8-10 February 1983.

24. H. Overhof, Phys. Stat. Sol. B 45, 315 (1971).

25. K.C. Hass and H. Ehrenreich, presented at the Second U.S. Workshop on the Physics and Chemistry of HgCdTe, Dallas, TX, 8-10 Feb 1983.

26. W.A. Harrison, presented at the Second U.S. Workshop on the Physics and Chemistry of HgCdTe, Dallas, TX, 8-10 Feb 1983.

27. W.E. Spicer, J.A. Silberman, P. Morgen, I. Lindau, J.A. Wilson, A.B. Chen, and A. Sher, Phys. Rev. Lett. 49, 948 (1982).

28. An-Ban Chen and A. Sher, J. Vac. Sci. Technol. 21, 138 (1982).

29. K.S. Hass, H. Ehrenreich, and B. Veliky, Phys. Rev. B 27, 1088 (1983).

30. W.E. Spicer, J.A. Silberman, I. Lindau, J.H. Wilson, A. Sher, A.B. Chen, presented at the Second U.S. Workshop on the Physics and Chemistry of HgCdTe, Dallas, TX, 8-10 Feb 1983.

31. Op. cit., Reference 27.

32. A. Willig, B. Sapoval, K. Leiber, and C. Verie, J. Phys. C 9, 1981 (1976).

33. H.M. Nitz, O. Ganschow, U. Kaiser, L. Wiedmann, and A. Benninghoven, Surf. Sci. 104, 365 (1981).

34. M. Brown, A.F.W. Willoughby, J. Cryst. Growth 59, 27 (1981).

35. S. Cole, A.F.W. Willoughby, and M. Brown, J. Cryst. Growth 59, 370 (1982).

36. Op. cit., Reference 33.

37. J.A. Silberman, P. Morgen, I. Lindau, W.E. Spicer, and J.A. Wilson, J. Vac. Technol. 21, 154 (1982).

38. P.M. Raccah, U. Lee, J.A. Silberman, W.E. Spicer, and J.A. Wilson, Appl. Phys. Lett. 42, 374 (1983).

39. P.R. Daniels, G. Margaritondo, G.P. Davis, and N.E. Byer, Appl. Phys. Lett. 42, 50 (1983).

40. L.O. Bubulac, W.E. Tennant, R.A. Riedel, and T.J. Magee, J. Vac. Sci. Technol. 21, 251 (1983).

41. P. Morgen, J.A. Silberman, I. Lindau, W.E. Spicer, and J.A. Wilson, J. Electr. Mater.